Mathematical and Theoretical Biology Institute at Cornell University

# Studies in Theoretical Biology: A Collection of Undergraduate Research

Interface between biology and the mathematical sciences

Research Efforts of the 1996 Cornell-SACNAS[1] Summer Program

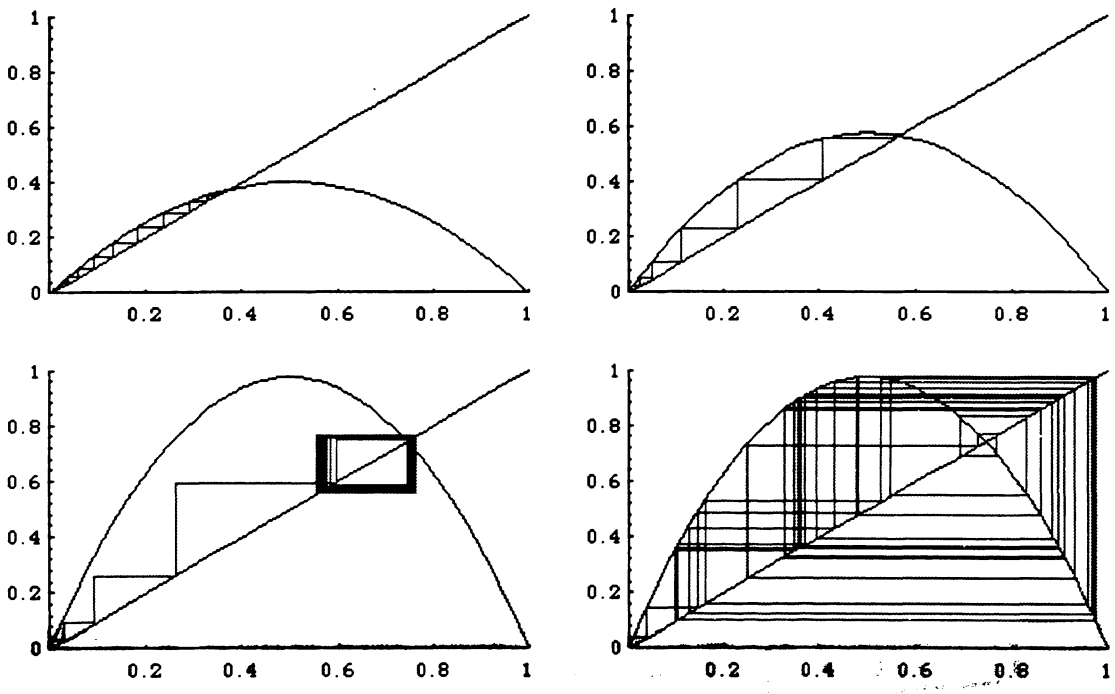


Biometrics Unit Technical Report
BU-1370-M

Prof. Carlos Castillo-Chavez
Director, MTBI
Biometrics Unit
435 Warren Hall
Cornell University
Ithaca, NY 14853
cc32@cornell.edu
biometrics@cornell.edu
http://www.cals.cornell.edu/dept/biometrics/MTBI/

**Funded by the National Security Agency, the National Science Foundation, the Office of the Provost, The College of Agricultural Sciences, and the Biometrics Unit at Cornell University.**

**The Society for the Advancement of Chicanos and Native Americans in Science (SACNAS) is a co-sponsor of the Cornell-SACNAS Summer Program.**

# Studies in Theoretical Biology: A Collection of Undergraduate Research

*Carlos Castillo-Chavez*

**Abstract.** In this introductory note, we describe the research from the work of thirty-five undergraduates and a high school student who participated in an intensive forty-five day program: the Cornell-SACNAS Mathematical Sciences Summer Institute (CU-SMSSI). Cornell-SMSSI is a program embedded in Cornell's Mathematical and Theoretical Biology Institute (MTBI) which is devoted to providing research opportunities to undergraduate college students across the nation, with the encouragement of the Society for the Advancement of Chicanos and Native Americans in Science. MTBI through the establishment of culturally sensitive environments, facilitates and instigates the active participation in the scientific enterprise of minority undergraduates. CU-SMSSI's environment was designed to meet the cultural needs of Chicanos, Latinos, and Native Americans (SACNAS). CU-SMSSI students learned about dynamical systems and probability models through the study of their applications to ecology, evolutionary biology, epidemiology and immunology during the first four weeks of the program. The last two-and-a-half weeks were devoted to the development of mathematical models from the students' efforts to answer specific scientific questions. The research of six interdisciplinary groups was–in part–motivated by recent theoretical advances in the fields of theoretical/mathematical epidemiology, immunology, ecology, demography, and sociology. The papers described in this note are part of the Biometrics Unit Technical Report Series. If a request for this note is made, it will send along with the six student reports.

BU-1370-M

## 1. Introduction: CU-SACNAS Mathematical Sciences Summer Institute.

The main objective of the Cornell-SACNAS Mathematical Sciences Summer Institute (CU-SMSSI) is to provide a first rate research experience in theoretical and mathematical biology to Chicano, Latino, and Native American students through a summer training program that includes participation in a series of small group research projects. CU-SMSSI's research training program in theoretical and mathematical biology is part of Cornell's Mathematical and Theoretical Biology Institute (MTBI) for undergraduate research. Cornell University's top-ranked programs in

biometry, statistics, ecology and evolutionary biology, applied mathematics, mathematics, and computer science and its NSF-supported supercomputing facility provide an ideal environment for MTBI. CU-SMSSI's research training program has been designed to provide an interdisciplinary research experience for undergraduates in mathematics, biology, and related disciplines who have completed at least a year of calculus. The research outlined in this report was completed by students who had mostly completed two years of college (albeit we had a student who had completed only his freshman year as well as a high school student). The program seeks students majoring in mathematics, biology, or related fields who have had a year of calculus and who are at least two years away from completing their college degree.

CU-SMSSI students learned about dynamical systems and probability models through the study of applications to ecology, evolutionary biology, epidemiology, and immunology during the first four weeks of the program. The last two-and-a-half weeks were devoted to the development of mathematical models from the students' efforts to answer specific scientific questions. The research of six interdisciplinary groups was–in part–motivated by recent theoretical advances in the fields of theoretical/mathematical epidemiology, immunology, ecology, demography, and sociology. The papers described in this brief note are part of the Biometrics Unit Technical Report Series.

Research topics given to the students emphasized questions associated with the evolution of virulence, coexistence of species, population dynamics of tropical diseases, immunology of tuberculosis, the dynamics of communicable diseases, the spatial spread of diseases, and the dynamics of sexually-transmitted diseases. The last two-and-a-half weeks were mostly dedicated to the research projects. Research was conducted in groups of six students (not all with the same college major) and focused on problems at the interface of biology and mathematics. Each of the six groups was required to write up a research technical report, as well as to present their findings to the group in a final series of presentations.

## 2. Research Projects

Biological questions can be studied at different spatial, temporal, or organizational scales. Two issues relevant to the the students research are: (i) how much organizational detail such as age structure, immune response, or genetic variability must be included in biological models? and (ii) how do we model relevant detail? In fact, by selecting a particular level of organization (immune system level or the population level) and a particular model, the investigator may have decided *a priori* what is and what is not relevant. This problem, although often discussed in the biological and social sciences, is not seriously addressed in the epidemiological/immunological literature.

The social consequences of epidemics such as the HIV/AIDS epidemic, the current rise of tuberculosis and the emergence of new diseases such as ebola provided

strong motivation to the students who could relate to the main culprit behind disease dynamics, poverty. The issue of scale resulted from students efforts to decide what question to address. Students interested in tuberculosis (TB) had to decide whether or not to study the dynamics of TB at the individual (immune system) or at the population level. Students interested in ebola were concerned with understanding outbreaks and estimating the basic reproductive number of ebola through the use of existing outbreak data. Students interested in HIV decided to focus on models that would help them estimate the life spans of free virions and infected T cells of HIV-infected patients. Another group was interested in the role of heterogeneity (core group dynamics) on the dynamics of sexually-transmitted diseases. Another group studied the dynamics of a tick population affected by Rocky Mountain Spotted Fever in order to understand how this disease affects other species. Finally, a group focussed on the study of the effects of spatial heterogeneity on disease dynamics. Hence, we had students looking at disease dynamics at various levels of aggregation as well as at different temporal and spatial scales.

Christian Herrera, Sharon K. Lima, Roberto Muñoz, Gloria Ramos, Ariel Rodríguez and Claudia Salzberg focus on a mathematical model that describe the dynamics of the immune system in the presence of the causative agent of tuberculosis, *Mycobacterium tuberculosis*. Their model takes into consideration the relations between the bacteria, T lymphocytes, and macrophages. The basic reproductive number is computed in order to determine under which conditions the immune system experiences no infection, latency, and active infection. The model can exhibit the dynamics of these three conditions of the disease for appropriate regions of parameter space. Two types of treatment are considered and the students analyze their effect on the dynamics of the system.

Jaime Astacio, Delmar Briere, Milton Guillén, Josué Martínez, Francisco Rodríguez, and Noe Valenzuela-Campos use S-I-R and S-E-I-R models to simulate and fit the data of two ebola outbreaks: the 1976 outbreak in Yambuku, Zaire and the 1995 outbreak in Kikwit, Zaire. The basic reproductive number, $R_0$, determines the likelihood and magnitude of an outbreak. Using available data, this group was able to estimate the basic reproductive number for ebola. They found it to be in the range $1.72R_05.32$.

Judit Camacho, Fernando Carreón, Derik Castillo-Guajardo, Hugo Jimnez-Pérez, Leticia Montoya-Gallardo, and Ricardo A. Sáenz consider a special case of the general spatial SIR (susceptible-infectious-removed) model. It is assumed that the population is distributed in separate cells and that there is no migration of individuals between cells. It is also assumed that disease can be transmitted with some probability within the cell by direct contact between an infected and a susceptible individual, but from cell to cell only through an external object capable of carrying the disease agent. The model was simulated in a $10x10$ grid of cells, and it was assumed that the disease can only be transmitted (via some external object) from a cell with infected individual to its immediate neighbors with some probability. The simulations showed typical spatial wave dynamics and dependance on initial conditions.

Michelle Arias, Erika Camacho, Rafael Castillo, Delmy Iñiguez, Eliel Melón, and Luz Parra begin with the observation that antiviral drugs may prolong the lives of HIV-infected patients although it is still uncertain if these drugs affect the rates of virion clearance, the loss of target cells, or both. A mathematical model was derived and applied to data to calculate the life spans of free virions and infected T cells. It was found that the antiviral drug decreased not only the number of free virions in the plasma but also the loss of infected target cells.

Marina Bobadilla, Sharon Lozano, Jessica Maia, Julio Villareal, Novaline Wilson and Roberta Winston (1996) examine a mathematical model for the dynamics of sexually-transmitted diseases where a vaccine (or an education program) capable of providing permanent protection (or permanent change in behavior) when *effective* is introduced into an infected population of highly-active individuals (the core group). The prevalence of the disease within the core group determines the recruitment rate into the core group. Oscillations of the disease over time were observed.

Mary Alderete, Carlos Castillo-Garsow, Guarionex Jordán Salivia, Carlos Lara-Moreno, Gina Ramírez, and Mónica Yichoy study the dynamics of the tick population affected by Rocky Mountain Spotted Fever in order to understand how this disease affects other species. The model proposed by Busenberg and Cooke [1993] for the tick population dynamics was modified to account for additional biological aspects. Numerical simulations are conducted to assess the effect of parameters on the dynamics of the model. It is observed that there is a region of parameter space where the population's behavior is found to be chaotic, and the boundaries for which chaos arises are computed numerically. It appears that additional biological detail affects the shape and location of the attractor.

# 3. Conclusions

I have edited the students' reports and this note tries to put their researh findings into a broader scientific context. It was tempting but impractical to encourage further development of research results, as it is difficult to mantaing good communication among group members, and undergraduate students are usually terribly busy during the academic year. Furthermore, I thought that it was important to see the truly *impressive* accomplishments of a diverse group of students who learned the basics of modeling, dynamical systems, probability, and stochastic processes while developing additional computational skills in four weeks. These four weeks of preparation were then followed by intense immersion in the biological literature needed to address their chosen biological questions, build a model, and carry out some preliminary analysis.

The titles of the six technical reports written by the students are listed in the references.

# Acknowledgements

The CU-SMSSI was supported through grants given by the National Science Foundation (NSF Grant DMS-9600027) and the National Security Agency (NSA Grant MDA 904-96-1-0032). Additional funding was granted by the Office of the Provost of Cornell University and Prof. Castillo-Chavez' Presidential Faculty Fellowship Award (DEB 925370). Partial support for international students came directly from CONACYT grants to Prof. Jorge X. Velasco-Hernández and Prof. E. Pérez (Universidad Nacional Autónoma de México, Ixtapalapa), Dr. Santiago López de Medrano (Facultad de Ciencias, Universidad Nacional Autónoma de México), Elena Pérez Alvarez-Buylla, ( Centro de Ecología, Universidad Nacional Autónoma de México), and to the Department of Mathematics (Facultad de Ciencias, Universidad Nacional Autónoma de México). Mexican students were recruited thanks to the efforts, support, and enthusiasm of Prof. Guillermo Gómez Alcaraz (Facultad de Ciencias, Universidad Nacional Autónoma de México). The research projects were carried out under the overal supervision of Professors Carlos Castillo-Chavez and Jorge X. Velasco-Hernández as well as with the collaboration of a wonderful research and writing staff. Each individual student report recognizes their support, assistance, and encouragement.

# References

[1] Herrera, C., Lima, S., Muñoz, R., Ramos, G., Rodríguez, A., and Salzberg, C. , A Model Describing the Response of the Immune System to *Micobacterium tuberculosis*. Biometrics Unit Technical Report, BU-1364-M, 1996.

[2] Astacio, J., Briere, D., Guillén, M., Martinez, J., Rodriguez, F., and Valenzuela-Campos, N., Mathematical Models to Study the Outbreaks of Ebola. Biometrics Unit Technical Report, BU-1365-M, 1996.

[3] Camacho, J., Carreon, F., Sáenz, R., Castillo-Guajardo, D., Jimnez-Pérez, H., and Montoya-Gallardo, L. , Stochastic Simulations of a Spatial SIR Model. Biometrics Unit Technical Report, BU-1366-M, 1996.

[4] Arias, M., Camacho, E., Castillo, R., Iñiguez, D., Meln, E., and Parra, L., HIV-1 Replication Rate. Biometrics Unit Technical Report, BU-1367-M, 1996.

[5] Bobadilla, M., Lozano, S.A., Maia, J., Villarreal, J., Wilson, N., and Winston, R, The effects of Vaccination in a Core Group. Biometrics Unit Technical Report, BU-1368-M, 1996.

[6] Alderete, M., Castillo-Garsow, C.W., Jordan-Salivia, G., Lara-Moreno, C., Ramirez, G., and Yichoy, M., A Mathematical Model of the Dynamics of Rickettsia rickettsii in Tick-Host Interactions. Biometrics Unit Technical Report, BU-1369-M, 1996.

[7] Busenberg, S., Cooke, K. "Vertically Transmitted Disease", *Biomathematics* **23**, Springer-Verlag, New York. 1993.

## Table of Contents

*Research funded by: NSF grant #29582; DMS-9600027 and NSA grant #26930; DMS-960002; 1996-1999*

# A Model Describing the Response of the Immune System to *Mycobacterium tuberculosis*

Christian Herrera
University of California at Los Angeles
Los Angeles, California 90024
cherrera@ucla.edu

Sharon Lima
Loyola Marymount University
Los Angelos, California 90045
sklima@stdntmail.lmu.edu

Roberto Muñoz
University of Puerto Rico at Humacao
Humacao, Puerto Rico 00791
rober5677@cuhac.upr.clu.edu

Gloria Ramos
University of California at Santa Cruz
Santa Cruz, California 95064
morla@cats.ucsc.edu

Ariel Rodríguez
University of Puerto Rico at Rio Piedras
Rio Piedras, Puerto Rico 00931
cn3r5041@upracd.upr.clu.edu

Claudia Salzberg
Brown University
Providence, Rhode Island 02912
st004333@brownvm.brown.edu

BU-1364-M

ABSTRACT

We present a mathematical model to describe the dynamics of the immune system in the presence of the causative agent of tuberculosis, *Mycobacterium tuberculosis*. We take into consideration the relations between the bacteria, $T$ lamphocytes, and macrophages. We compute the basic reproductive number to determine under which conditions we get certain disease states: no infection, latency, and infection. The behavior depicted by our model, under certain parameters, demonstrates the dynamics of these three conditions of the disease. We consider a treatment and analyze its effect on the dynamics of the system.

# 1 Introduction

During the 1800s, tuberculosis was an epidemic disease throughout the world. Due to improvements in living conditions and advances in medicine, the incidence of tuberculosis began to decline in the 1900s. However, it has remained a major cause of death in developing countries. It is transmitted through coughs and sneezes by a person with infectious (active) tuberculosis. Healthy persons who are infected have a high probability of being asymptomatic. There is a 10% risk of developing active tuberculosis after being infected [Hopewell 1994]. When tuberculosis is latent, it is incapable of being transmitted and does not cause any symptoms [Miller 1993].

Currently the number of cases of tuberculosis again is on the rise. Approximately one third of the global population is infected by *Mycobacterium tuberculosis* [Sudre *et al.* 1992], the causative agent of the disease. This makes tuberculosis one of the most common infectious diseases in the world. Some of the factors that have caused this increase of the disease are: immigration, overcrowded living conditions, substance abuse, and AIDS. Newly evolved strains that are resistant to one or more drugs used in treatment have developed with this new resurgence of tuberculosis.

An increase in awareness has motivated basic research on the pathogenesis of the bacteria and the mechanisms of the immune response. Our research is based on the microbiological perspective of tuberculosis and the immune system. The focus is on the immune system-pathogen interaction. Work using this approach has been done with Chagas' disease [Velasco-Hernández and Pérez-Chavela 1992] and the HIV virus.

In tuberculosis, the interaction among the causative agent, the macrophages, and the $T$ cell (CD4/CD8) populations establishes the state of the disease. The interaction between the bacteria and the immune system can be viewed as the combination of two ecological processes: predator-prey and pathogen-host interaction. Using this blended model, we analyze the potential outcomes resulting from human exposure to *Mycobacterium tuberculosis*. Three outcomes will be examined: no infection, a latent state of infection, and an infectious (active) state. The present paper seeks to model the dynamics between the *Mycobacterium tuberculosis* and the cells of the immune system by considering five separate populations: *Mycobacterium tuberculosis*, empty macrophages, inactivated macrophages, activated macrophages, and $T$ cells.

We seek to determine which initial states and which parameters lead to different outcomes in the health of the infected individual. From these findings we will have a better understanding of the immune system and its response to *Mycobacterium tuberculosis*. This may enable scientists to foresee and prevent the death of an infected individual.

# 2 Mathematical Model

A realistic model of the interactions between the immune system and *Mycobacterium tuberculosis* is required to elucidate the dynamics of these interactions. A notable limitation in the construction of this model has been the lack of understanding the mechanisms involving the immune response to *Mycobacterium tuberculosis*. To account for these limitations it is necessary to make some assumptions about the process and incorporate them into our model. There is still an ongoing debate as to the importance of the role of the humoral response, but in order to simplify the model we have assumed that it is negligible and have concentrated exclusively on the cell-mediated response.

The cell-mediated immune response includes the action of macrophages, or phagocytic cells able to digest foreign material, and $T$ cells which facilitate the activation of the response by secreting growth and cell-activating factors. The model discussed here includes effects of $CD4^+$ and $CD8^+$ $T$ cells. We do not distinguish between these two subpopulations. More explicitly, we have taken the liberty to consider their total effects as additive. Therefore we focused on a broader concept of a $T$ cell which combines the outcomes of both these subpopulations.

A very important note to consider is that our model presumes infection and concentrates on the possible outcomes of this infection. We consider infection only in the primary infection site. We do not consider spread of the bacteria via travel of the alveolar macrophages into other parts of the body nor do we consider systemic infection. We have considered three general outcomes which are summarized in Figure 1. All outcomes presume engulfment of bacilli by the alveolar macrophage. Once in the macrophage, the bacilli can restrain their growth and remain unnnoticed for years. The length of time which these bacilli can remain unnoticed inside macrophages depends on the individual. Genetic patterns have been observed with respect to the

length of this latent state (Rossman & Macgregor 1995). If the bacilli replicate once inside the macrophage, the stress of this activity will lead to an immune response involving the $T$ cells. From the latent state we can have reactivation of bacterial replication which will lead to a similar response. The mechanisms which activate this replication in latent-state bacilli remain unclear. Once an immune response is mounted we have two possible outcomes: defeat of the bacilli due to their destruction and elimination, and uncontrolled infection whereby the immune response was not strong enough to eliminate the pathogen, leading to symptomatic tuberculosis. Thus we consider the outcomes of infection as latency, infection progression, or infection elimination.

## 2.1 Macrophage growth and infection

In order to consider the relation of the macrophages to the system we have to consider the roles they play in the immune response mounted against the bacteria. We consider three states of the cell. The first is the free state before its encounter with a bacilli ($M$). In this state it simply remains prepared for an encounter with a foreign antigen. The next state is the inactive state from chance encounters with a tuberculosis bacilli ($M^*$). In the inactive state it now contains the bacilli within its cytoplasm (i.e., it is now full) yet remains inactivated. The third state consists of the activated full macrophage ($M^{**}$). Activation occurs from chance encounters of a $T$ cell which, after recognizing it, begins to mount an attack partly by activating the macrophage. The actual process of activation is also unclear, although there are some hypotheses, including the belief that when the $T$ cell activates the macrophage it enables it to produce nitrogenous compounds which the bacilli cannot resist. As a model for these three states we suggest the following:

$$dM/dt = \beta - \delta M - \epsilon MP, \tag{1}$$

$$dM^*/dt = \epsilon MP - \alpha TM^* - (\delta + g)M^*, \tag{2}$$

$$dM^{**}/dt = \alpha TM^* - \delta M^{**}, \tag{3}$$

where $\beta$ represents the birth rate of macrophages as seen in the bone marrow of a healthy adult; $\delta$ the natural cell death rate; $\epsilon$ the engulfing rate of a macrophage with respect to a bacillus; $\alpha$ the activation rate of a full macrophage with respect to its encounter with a $T$ cell; and $g$ the rate of

bursting of a macrophage as a result of the unbounded proliferation of bacilli inside its cytoplasm.

We have left out the possibility of a varying birth rate, although taking this possibility into account would make our model more realistic, since there is an increase in macrophages when a full one meets up with a $T$ cell.

## 2.2 $T$ cell proliferation

Immune response depends on chance encounters of $T$ cells with $M^*$ macrophages. The $T$ cell recognizes the $M^*$ macrophage and begins mounting an attack that not only activates the macrophage but also allows for the secretion of substances such as INF$\gamma$ (which kills free bacteria as well as destroys surrounding tissues). The $T$ cells also self-replicate in the process. Thus we consider the following equation to model the dynamics of the $T$ cells:

$$dT/dt = \Lambda + rTM^* - \delta_T T. \tag{4}$$

where $\Lambda$ is the birth rate for the formation of the $T$ lymphocyte in the bone marrow of a healthy adult; $\delta_T$ is the natural cell death rate of the $T$ cell; and $r$ is the rate of replication of the $T$ cell upon encountering a full macrophage. We have assumed that the birth rate is constant but we are aware that it should be represented as a function of $T$.

## 2.3 *M. tuberculosis* growth in an infected individual

The causative agent of tuberculosis is transmitted via the inhalation of infectious droplets emitted during an infected person's coughing, sneezing, or spitting. The contraction of the disease by a susceptible guinea pig or rabbit depends on the inhalation of droplets limited to the size of 1 to 3 bacilli in order to facilitate their engulfment by macrophages. Equivalent data is not found on humans so we have assumed a similar pattern of dependence in modeling the immune response for humans. As a model we propose:

$$dP/dt = bP - \delta_P P - \epsilon MP + (\delta N + gL)M^*, \tag{5}$$

where $P$ is the number of bacilli as would be measured in the blood; $\delta_P$ the natural cell death rate; $N$ the number of bacilli inside a macrophage when it dies a natural cell death; and $L$ the number of bacilli required in order to burst a macrophage.

# 3 Analysis and Simulations

## 3.1 Analysis

Our model consists of the following set of differential equations:

$$
\begin{aligned}
dM/dt &= \beta - \delta M - \epsilon MP && (6)\\
dM^*/dt &= \epsilon MP - \alpha T M^* - (\delta + g)M^* && (7)\\
dM^{**}/dt &= \alpha T M^* - \delta M^{**} && (8)\\
dT/dt &= \Lambda + rTM^* - \delta_T T && (9)\\
dP/dt &= bP - \delta_P P - \epsilon MP + (\delta N + gL)M^*. && (10)
\end{aligned}
$$

To begin the analysis of the system we compute the steady states for (6) – (10). For the disease-free equilibrium we take $P = 0$, $M^* = 0$, and $M^{**} = 0$, since in the absence of bacteria we would have no engulfing, hence no $M^*$ nor $M^{**}$ cells. From (1) and (4) we have

$$0 = \beta - \delta M \qquad \text{and} \qquad 0 = \Lambda - \delta_T T$$

so

$$E_0 = (M_0, M_0^*, M_0^{**}, T_0, P_0) = (\beta/\delta, 0, 0, \Lambda/\delta_T, 0).$$

The Jacobian matrix of the system at $E_0$ is

$$
J_{E_0} = \begin{pmatrix}
-\delta & 0 & 0 & 0 & -t\frac{\beta}{\delta} \\
0 & -\left(\delta + g + \alpha\frac{\Lambda}{\delta_r}\right) & 0 & 0 & t\frac{\beta}{\delta} \\
0 & \alpha\frac{\Lambda}{\delta_r} & -\delta & 0 & 0 \\
0 & 0 & 0 & -\delta & 0 \\
0 & \delta N + gL & 0 & 0 & b - \delta_p - \epsilon\frac{\beta}{\delta}
\end{pmatrix}.
$$

Let

$$
C = \begin{pmatrix}
-\left(\delta + g + a\frac{\Lambda}{\delta_r}\right) & t\frac{\beta}{\delta} \\
\delta N + gL & b - \delta_p - e\frac{\beta}{\delta}
\end{pmatrix}.
$$

For the stability of $E_0$, we can see that the real part of all eigenvalues of the matrix $J_{E_0}$ is negative if and only if both

$$det(C) = (\alpha\Lambda/\delta_T + \delta + g)(\epsilon\beta/\delta + \delta_P - b) - (\delta N + gL)(\epsilon\beta/\delta) > 0,$$

and

$$tr(C) = -(\alpha\Lambda/\delta_T + \delta + g) - (\epsilon\beta/\delta + \delta_P(b) < 0.$$

The condition in the determinant is equivalent to

$$\frac{(\epsilon\beta/\delta)(\delta N + gL)}{(\epsilon\beta/\delta + \delta_p - b)(\alpha\Lambda/\delta_T + \delta + g)} < 1.$$

We define the basic reproductive number as

$$\frac{(\epsilon\beta/\delta)(\delta N + gL)}{(\epsilon\beta/\delta + \delta_p - b)(\alpha\Lambda/\delta_T + \delta + g)}.$$

This parameter relates the average number of engulfings per lifetime of $M$ $(\epsilon\beta/\delta)$ per "true" lifetime of bacteria $(\epsilon\beta/\delta + \delta_p - b)$ with the average number of released bacteria $(\delta N + gL)$ per "true" lifetime of $M^*$ cells $(\alpha\Lambda/\delta_T + \delta + g)$. $R_0$ reflects the interplay of epidemiological, predator-prey, and population growth factors in our model. It relates epidemiological factors for the $M \rightarrow M^* \rightarrow M^{**}$ dynamics, predator-prey interactions between the $M$ and $P$ population, and the population dynamics of $P$.

For $R_0$ to make sense we should have $\epsilon\beta/\delta + \delta_P - b > 0$. If we consider the case when $\epsilon\beta/\delta + \delta_P - b < 0$, then bacteria will increase exponentially. To see why this happens, from (1) we can see that $M < \beta/\delta$. From (5) we have

$$dP/dt \geq (b - \delta_P - \epsilon\beta/\delta)P;$$

thus

$$P(t) \geq P(0)e^{(b-\delta_P-\epsilon\beta/\delta)t} \rightarrow \infty \text{ as } t \rightarrow \infty.$$

To determine endemic equilibria, we set equations (1) - (5) equal to zero. From (4) and (5) ,

$$T = \Lambda\delta_T - rM^* \quad \text{for} \quad M^* < \delta_T/r \qquad \text{and} \qquad P = \frac{(\delta N + gL)M^P*}{\delta_p + \epsilon M - b}.$$

Substituting these equations in (1) and (2), we have

$$0 = \beta - \delta M - \epsilon M \frac{(\delta N + gL)M^*}{\delta_p + \epsilon M - b}$$

and

$$0 = \epsilon M \frac{(\delta N + gL)M^*}{\delta_p + \epsilon M - b} - \alpha \frac{\Lambda}{\delta_T - rM^*} M^* - (\delta + g)M^*. \qquad (*)$$

Adding these two equations and solving for $M$ gives us

$$M = \frac{1}{\delta}\left[\beta - \frac{\alpha \Lambda M^*}{\delta_T - rM^*} - (\delta + g)M^*\right].$$

Let $x = M^*$, then let $g_1(x) = \delta_T - rx$, $g_2(x) = [\beta - \delta + g)x]g_1(x) - \alpha\Lambda x$. Then $M$ can be expressed as

$$M = \frac{g_2(x)}{\delta g_1(x)} \quad \text{with} \quad x = M^*.$$

Substituting $M$ in the second equation from (*) and considering $M^* > 0$ we define

$$F(x) = \frac{\epsilon(\delta N + gL)g_2(x)}{(\delta_p - b)\delta g_1(x) + \epsilon g_2(x)} - (\delta + g) = 0.$$

Take

$$e_1(x) = \frac{\epsilon(\delta N + gL)g_2(x)}{(\delta_p - b)\delta g_1(x) + \epsilon g_2(x)}, \quad e_2(x) = \frac{\alpha\Lambda}{g_1(x)} + (\delta + g).$$

Solving for $x$ $(= M^*)$ would be finding $x$ such that these two curves intersect: $e_1(x) - e_2(x) = 0$.

We show the existence of such an $x$, hence the existence of endemic equilibria. We restrict the analysis to the interval $[0, \delta_T/r)$. Note that $F(0) = e_2(0)(R_0 - 1)$. For $R_0 > 1$ we have $F(0) > 0$. Now consider $x* = \delta_T/r$. Note that

$$\lim_{x \to x*} e_1(x) = \delta N + gL, \quad \text{and} \quad \lim_{x \to x*} e_2(x) = \infty.$$

Then

$$\lim_{x \to x*} F(x) = -\infty.$$

Since $F(0) > 0$ and for some $h$, $F(\delta_T/r - h) < 0$, then $F(c) = 0$ for some $c \in (0, \delta_T/r)$. This shows the existence of an endemic equilibrium. We now show that for $\delta_p \geq b$ the endemic equilibrium is unique. Computing $F'(x)$,

$$F'(x) = \delta\epsilon(b - \delta_p)(\delta N + gL)[(\delta + g)g_1^2 + \alpha\Lambda g_1 + r\alpha\Lambda x] - \frac{\alpha\Lambda r}{g_1^2},$$

we can see that for $\delta_P \geq b$, $F'(x)$ is strictly negative. This shows that there is only one $c \in (0, \delta_T/r)$ such that $F(c) = 0$, when $R_0 > 1$.

## 3.2 Simulations

We complete our analysis through computer simulations. In the previous section, we determined analytically the conditions for stability of the disease-free equilibrium, the existence of endemic equilibria for $R_0 > 1$, and the uniqueness of an endemic equilibrium for the case where $\delta_P \geq b$, with $R_0 > 1$.

Through the simulations we corroborated our analytical results and extended them. The main purpose of the simulations was to find the three possible stages of tuberculosis: active, latent, and no TB. We identified the active stage with an exponential growth of the bacteria, the latent stage with an endemic equilibria, and the no-TB stage with the disappearance of bacteria.

While doing the simulations, we considered the cases where $R_0 < 1$ and $R_0 > 1$. This was done because of the lack of information on most of the parameters. We define

$$R_1 = \frac{\epsilon\beta/\delta}{\epsilon\beta/\delta + \delta_p - b} \quad \text{and} \quad R_2 = \frac{\delta N + gL}{\alpha\Lambda/\delta_T + \delta + g}.$$

For each of the cases, we considered three sub-cases, each a different combination of values for $R_1$ and $R_2$. For $R_0 < 1$ we considered: 1) $R_1 < 1$, $R_2 < 1$; 2) $R_1 > 1$, $R_2 < 1$; 3) $R_1 < 1$, $R_2 > 1$. For $R_0 > 1$ we considered the cases: 1) $R_1 > 1$, $R_2 > 1$; 2) $R_1 > 1$, $R_2 < 1$; 3) $R_1 < 1$, $R_2 > 1$. In each of these cases we paid most attention to the behavior of $P(t)$ (bacteria) and $M(t)$ (macrophages).

We obtained no TB ($P(t) \to 0, \quad M(t) \to \beta/\delta$) in the cases where $R_0 < 1$ and $R_1 < 1$. This can be interpreted as follows: $R_1 < 1$ is true only if $\delta_P > b$. Since bacteria is dying at a higher rate than their birth we would expect a settled growth of bacteria. With $R_0 < 1$ this behavior settles to the disease-free equilibrium.

Our model showed latency ($P(t) \to k_1$, $M(t) \to k_2$) in the case where $R_0 > 1$, with $R_1 < 1$ and $R_2 > 1$. $R_1 < 1$ means $\delta_P > b$, and $R_2 > 1$ means that there is a higher "release" rate of bacteria with respect to the removal of $M^*$ cells through activation. A latent stage is expected with high release rate and high death rate for bacteria since it is plausible to get a "balanced" system.

We found active TB ($P(t) \to \infty$, $M(t) \to 0$) in the case where $R_0 > 1$, $R_1 > 1$ and $R_2 > 1$. This can be interpreted as the consequence of $b > \delta_P$ ($R_1 > 1$) and a high release rate ($R_2 > 1$).

We also obtained interesting results for the cases where $R_1 > 1$ and $R_2 < 1$, both with $R_0 < 1$ and $R_0 > 1$. For some initial conditions, as the ratio $R_1/R_2$ increased we could observe a transition from a disease-free state to an active stage of exponential growth for $P(t)$. This was obtained for $R_0 > 1$ and $R_0 < 1$. The transition was sensitive to initial conditions. We do not give a biological interpretation because of the complex behavior. See Appendix for graphs.

### 3.3 Treatment

It is interesting to note the possible effect of treatment on the dynamics of the system. We consider a drug with an intracellular and an extracellular effect. Equations (2) and (5) would be modified in the following way:

$$dM^*/dt = \epsilon MP - \alpha TM^* - (\delta + g)M^* - \phi M^*,$$

and

$$dP/dt = (b - \delta_P)P - \epsilon MP + (\delta N + gL)M^* - \phi P.$$

The corresponding basic reproductive number is

$$R_0(\phi) = \frac{(\epsilon\beta/\delta)(\delta N + gL)}{(\epsilon\beta/\delta + \delta_P - b + \phi)(\alpha\Lambda/\delta_T + \delta + g)\phi)}.$$

From $R_0(\phi)$ we can note that the effect of treatment is an expansion of the domain of parameters that stay within the condition$R_0 < 1$, with $R_1 < 1$ and $R_2 < 1$.

## 4 Discussion

Our paper we proposes a system of differential equations to describe what happens when tuberculosis is in an infected individual. We found in our solution analysis the three possible results of TB after it attacks the body: latent or inactive TB, active TB, or a full recovery from the infection.

Our first important step in the analysis of our model was obtaining $R_0$, the basic reproductive number, which gave us the conditions of the three possible outcomes of TB when it attacks the individual. We also were able to find the stability condition in the disease-free state. In addition, we were able to prove the existence of an endemic state when $R_0 > 1$. In particular, if $\delta_b > b$ then we are guaranteed uniqueness of this endemic equilibrium with $R_0 > 1$.

In our analysis, we saw the importance of the engulfing mechanism. The macrophages served as a "reservoir" for the *Mycobacterium tuberculosis*. Either the bacteria are released into the immune system by explosion or the macrophages annihilate the bacteria. Through computer simulations, we were able to identify the important factors of the system that gave us different outcomes. These factors are: the birth of the bacteria, the death of the bacteria, the engulfment rate of the bacteria by the macrophages, the release of the bacteria by the macrophages, and the activation rate of the macrophages by the $T$-cells. Another important result was the interesting outcomes during the latent state of the disease. Latency was either permanent, temporary, or the person made a full recovery from the disease. From our system of differential equations, we found the three outcomes that we wanted to find, depending on the value of $R_0$ , $R_1$ ,and $R_2$.

However, our model did behave strangely; some of the analytical interpretations did not coincide with the computer analysis. There are special conditions in the model, such as a "gray area" where a slight change in the value of certain parameters changes the state of tuberculosis. A plausible explanation for the unusual behavior in the model is that many of the parameters in the model have not been found. For example, the engulfing rate of the bacteria is questionable. Also, we do not know the duration of the hibernation period of the bacteria in the macrophage. The lack of biological parameters limited our interpretation of our mathematical model.

The immunological model was further extended to include an intracellular and an extracellular treatment. This new parameter would be subtracted from the $P$ and $M^*$ equation. This would affect the $R_0$ because the new term would appear in the denominator of the basic reproductive number. Time did not permit us to do a complete analysis but from our interpretation of the model, we see that the likelihood of proper treatment raised the chances to a full recovery.

A possible area for further research is to extend the model to include another factor that is causing a weak immune system, such as HIV. Anyone infected with HIV is more likely to die of tuberculosis because HIV weakens the system, often allowing the tuberculosis to take over the immune system. Studies have shown that certain groups are more likely to become infected with tuberculosis than others, such as substance abusers, smokers, and the poor. We could accommodate the model to become specific to high-risk groups. We may be able to find similar patterns between each of these groups and be able to easily identify others who will fall in the defined high-risk group. Can a target treatment be designed for these high-risk groups? What happens if we consider resistant strains? We hope this project will lead others to study these important questions concerning the disease.

# 5 References


Hopewell, P.C., "Overview of Clinical Tuberculosis"in *Pathogenesis, Protection, and Control*, pp. 25-46, 1994.

Miller,Bess, "Preventive Therapy for Tuberculosis", *Medical Clinics of North America* **77**: 1263-1275, 1993.

Rossman and MacGregor, 1995.

Sudre, P., G. Dam, and A. Kochi, "Tuberculosis: A Global Overview of the Situation Today", *Bulletin of the World Health Organization* **70**: 149-159, 1992.

Velasco-Hernández, Jorge X. and Ernesto Pérez-Chavela, "A preliminary report on a model for the immune response to *Trypanosoma cruzi*", in *Differential Equations in Application to Biology and Industry*, Martelli *et al*, eds., World Scientific, New Jersey, pp. 521-530, 1992.


Additional References:


Barnes, Peter F. and William N. Rom, "Cytokine Production in Tuberculosis", in *Tuberculosis*, Little, Brown and Company, pp. 291-303, 1996.

Bell, George I., "Predator-Prey Equations Simulating an Immune Response", *Mathematical Biosciences* **16**: 291-314, 1973.

Castillo-Chavez, Carlos and Zhilan Feng, "Mathematical Models for the Disease Dynamics of Tuberculosis", BU-1321-M, Biometrics Unit, Cornell University, Ithaca, NY 14853, 1996.

Castillo-Chavez, Carlos and Zhilan Feng, "Optimal Vaccination Strategies for TB in Age-Structure Populations", BU-1323-M, Biometrics Unit, Cornell University, Ithaca, NY, 14853, 1996.

Castillo-Chavez, Carlos and Zhilan Feng, "To Treat or not to Treat: The Case of Tuberculosis". BU-1288-M, Biometrics Unit, Cornell University, Ithaca, NY, 14853, 1995.

Collins, Frank M., "Pathogenicity of *M. Tuberculosis* in Experimental Animals", in *Tuberculosis*, Little, Brown and Company, pp. 259-268, 1996.

Dannenburg, Arthur M. and Graham A.W. Rook, "Pathogenesis of Pulmonary Tuberculosis: An Interplay of Tissue-Damaging and Macrophage-Activating Immune Responses – Dual Mechanisms that Control Bacillary Multiplication", in *Tuberculosis: Pathogenesis, Protection, and Control*, pp. 459-483, 1994.

Dolin, P.J., M.C Raviglione and A. Kochi, *Bulletin of the World Health Organization* **72**: 213-220, 1994.

Ellner, Jerrold J., "Pathogenesis and Immunology", in *Tuberculosis*, McGraw Hill Inc,, pp. 19-34, 1995.

Hsieh, Ying-Hen and Jorge X. Velasco-Hernández, "Community Treatment of HIV- 1: Initial Stage and Asymptotic Dynamics", *Biosystems* **35**: 75-81, 1995.

Laal, Suman, "Humoral Response in Tuberculosis", in *Tuberculosis*, Little, Brown and Company, pp. 335-342, 1996.

Molloy, A. and G. Kaplan, "Cell Mediated Immune Response", in *Tuberculosis*, Little, Brown and Company, pp. 305-314, 1996.

Mortensen, J., P. Lange, H.K. Storm, and K. Viskum, "Childhood Tuberculosis in a Developed Country", Eur. Respir. J. **2**: 985-987, 1989.

Orme, Ian M. and David N. McMurray, "The Immune Response to Tuberculosis in Animal Models", in *Tuberculosis*, Little, Brown and Company, pp. 269-280, 1996.

Riley, Lee W., "Phagocytosis of *M. Tuberculosis*, in *Tuberculosis*, Little Brown and Company, pp. 281-289, 1996.

# 6 Appendix

**Acknowledgments**

The research in this manuscript has been partially supported by grants given by the National Science Foundation (NSF Grant DMS-9600027), the National Security Agency (NSA Grant MDA 904-96-1-0032) and Presidential Faculty Fellowship Award (NSF Grant DEB 925370) to Carlos Castillo-Chavez. Substantial financial and moral support was also provided by the Office of the Provost of Cornell University and by Cornell's College of Agricultural & Life Sciences (CALS) and its Biometrics Unit. The authors are solely responsible for the views and opinions expressed in this report. The research in this report does not necessarily reflect the views and/or opinions of the funding agencies and/or Cornell University.

We enthusiastically thank the following souls for their unwavering support and suggestions throughout the completion of this paper and project: Carlos Castillo-Chavez, Jorge Velasco-Hernández, Baojun Song, Wenzhang Huang, and Mercedes Franco. Our most heartfelt thanks to SACNAS and Cornell for making this experience possible.

## 6. Appendix

**Figure 1**
Visible dynamics of Tuberculosis and the Immune System

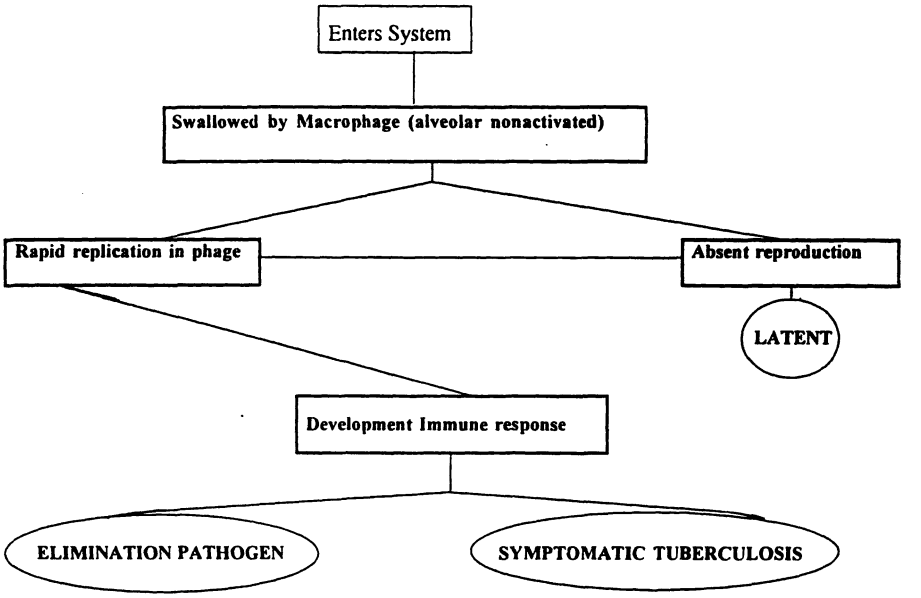


$R_0 < 1$:

**Figure 2**

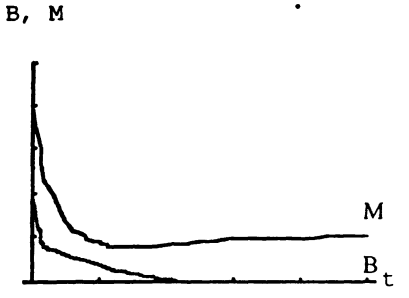


$R_1 < 1, R_2 < 1$

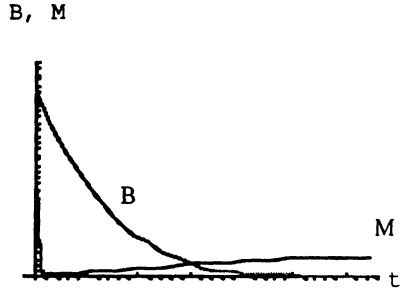


$R_1 < 1, R_2 > 1$

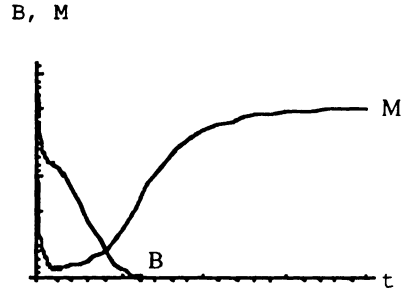


$R_1 > 1, R_2 < 1$

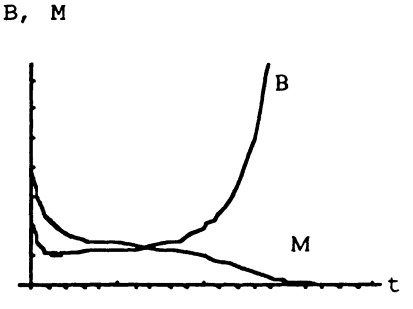


$R_1 > 1, R_2 < 1$

$R_0 > 1$

**Figure 3**

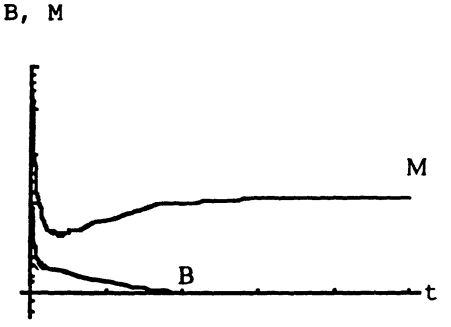


$R_1 > 1, R_2 < 1$

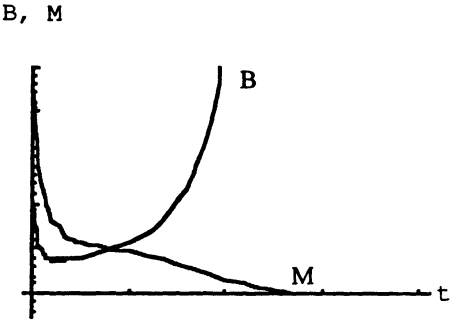


$R_1 > 1, R_2 < 1$

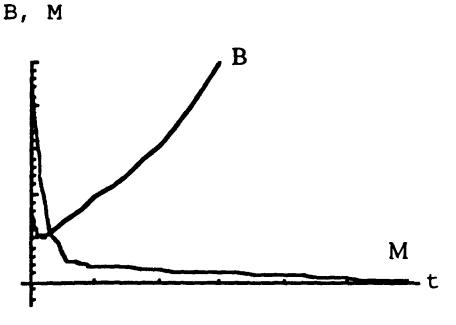


$R_1 > 1, R_2 > 1$

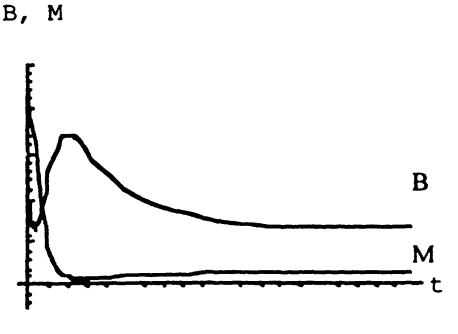


$R_1 < 1, R_2 > 1$

**Figure 4**

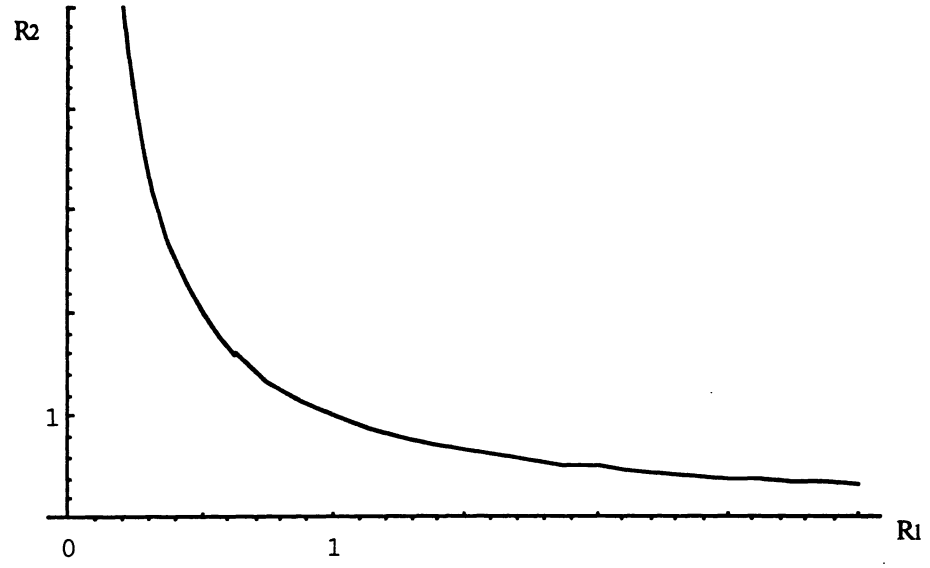


Outcomes after exposure: 1 - No TB, 2 - Latent TB, 3 - Active TB, depending on the values of parameters $R_1$ and $R_2$. The region under the curve is when $R_0 < 1$; over the curve we have $R_0 > 1$.

# MATHEMATICAL MODELS TO STUDY THE OUTBREAKS OF EBOLA

Jaime Astacio
University of Puerto Rico, Humacao

DelMar Briere
Blackfeet Community College

Milton Guillén
University of California, Santa Cruz

Josué Martínez
University of Texas, Austin

Francisco Rodríguez
California State University, Bakersfield

Noé Valenzuela-Campos
University of California, Davis

BU-1365-M

ABSTRACT

Using S-I-R and S-E-I-R models, it was possible to simulate two Ebola outbreaks: the 1976 outbreak in Yambuku, Zaire and the 1995 outbreak in Kikwit, Zaire. The dynamics of these models are determined by the per-capita death rate of infected individuals and the per-capita effective contact rate of an individual contracting the disease. The basic reproductive number, $\mathcal{R}$, determines the infectiousness of the disease. For Ebola, $1.72 \leq \mathcal{R}_0 \leq 8.60$, and this implies that Ebola is not as infectious as previously postulated. The results of these outbreak simulations will equip scientists in future outbreaks with information that may enable them to minimize potential deaths.

## Introduction

The origin of the Ebola virus is somewhat obscure. There have been only three major known outbreaks of the Ebola virus, and all have happened in West Central African countries. The latest major outbreak occurred in Kikwit, Zaire in 1995. The outbreak took the lives of 79 people.

Ebola is a unique member of the ribonucleic acid virus family that has no known natural reservoir. The incubation period of Ebola is 2–21 days, and the infectious period is 4–10 days. The onset of Ebola is characterized by severe headaches, malaise, fever, vomiting, bloody diarrhea, and rash. Severe bleeding and shock are usually followed by death. Diagnosis of Ebola can be difficult, because Ebola is frequently misdiagnosed as typhoid and malaria. Currently there is no treatment of Ebola [3]. The mortality rate of Ebola is anywhere from 50–90%. Ebola is transmitted through primary contact with health workers who are in direct contact with body fluids from the infected. Ebola can also be transmitted through secondary contact by family members caring for the infected. Finally, Ebola can be transmitted where infection control mechanisms are not in practice. These control mechanisms can be as simple as wearing gloves, or as complicated as level-four disease control. Airborne spread has not been proven as a means of transmission.

Our objective is to better understand the mathematical dynamics of a population infected by Ebola when an outbreak occurs. To model this outbreak, we are using systems of differential equations. Several distinct models will be used to study the known data; each model differs in the way the parameters are acquired. From these different models we will choose the model that best fits the data.

Inaccuracies in the model are to be expected since the parameters dictating the behavior of the model are obtained from only a few data points. There have been so few major outbreaks that the amount of data available is limited. The model's precision is dependent on this limitation.

## 1. Ebola outbreak of 1995 in Kikwit, Zaire.

The object of this part of the project is to model Zaire's 1995 Ebola epidemic, using the Susceptible-Infectious-Recovery (SIR) model (Brauer and Castillo-Chavez, 1994). The dynamics of this system happen in two stages: susceptible to infected, and infected to dead. This is a closed system where those that are susceptible could become infected at some point in time. This

model assumes that the initial population is equal to the population that will eventually be infected. The parameters are $\mu$, the per-capita death rate; and $\beta$, the probability that a susceptible host will become infected. The parameter $\beta$ can vary from a constant function to an exponential function of decay with respect to the number of infected at time $t$. Once the parameters are found, the system modeling the data is solved using Mathematica 2.22. Mathematica uses the Runge-Kutta method to solve these differential equations.

The population studied is divided into three classes: $S(t)$, the number of susceptible individuals; $I(t)$, the number of individuals infected; and $R(t)$, the number of dead individuals at time $t$. We will assume that the population studied will be a constant population during the outbreak, meaning there are no deaths due to outside factors and the number of births that occurred are so small that we can essentially ignore them. (This is a valid assumption since the lengths of the Ebola epidemics are not longer than three to four months.) We will denote our total population at time $t$ by $N$, so at any time $t$, $N = S(t) + I(t) + R(t)$.

Following a model proposed by Kermack and MacKendrik (1927) to explain the frequent rapid rise and fall of cases observed frequently in epidemics such as the Great Plague in London (1665-1666), the cholera epidemic in London (1865) and the plague in Bombay (1906), we are able to propose a model that approximates the outbreak reasonably well:

$$\begin{aligned} \frac{dS}{dt} &= -\beta SI/N, \\ \frac{dI}{dt} &= \beta SI/N - \mu I, \\ \frac{dR}{dt} &= \mu I. \end{aligned}$$

This model takes into consideration the number of people infected due to direct contact with an infected individual at time $t$: $\beta SI/N$, where $\beta = pc$; $p$ is the probability of successfully getting infected when coming into contact with an infected individual, and $c$ is the per-capita contact rate. The death rate is denoted by $\mu I$, where $\mu$ is the per-capita death rate. Even though recoveries do occur, we will not return these individuals to the susceptible class since there has never been a person who has recovered from Ebola and contracted the disease again in the same epidemic.

The data which we are studying is of the number of people that died each day during the outbreak in Kikwit, Zaire in 1995 [4]. See Figures 1 and 2. The second data set is the total number of dead individuals at time $t$, which can also be interpreted as the integral of the daily death data. From this relation we will be able to estimate the parameter $\beta$ by solving the second differential equation for small values of $t$ and relating it to the number of dead at time $t$. Since $dI/dt = \beta SI/N - \mu I$, for small $t$, $dI/dt \approx \beta I - \mu I$; solving this equation, $I(t) = I(0)\ Exp[(\beta - \mu)t]$, where $I(0) = 1$. Under these conditions, we can assume that $I(t) \propto R(t + 1/\mu)$, because $1/\mu$ is the average *time* for an infected individual to die. So $Exp[(\beta - \mu)t] = kR(t + 1/\mu)$, where $k = 1/0.77$ and 77% of infected people eventually die.

We have data that represents the total number of dead people at time $t$, cumulative of $R(t)$, so we fit the data with the curve. We take the natural log of the data so that our fit will be a linear fit:

$$(\beta - \mu)t = Ln[1/0.77] + Ln[R'(t + 1/\mu)].$$

The slope of the line which best fits the data is 0.14. By substitution,

$$\begin{aligned} (\beta - \mu)t &= Ln[R(t + 1/\mu)], \\ 0.14t &= Ln[R(t + 1/\mu)], \\ (\beta - \mu)t &= 0.14t, \\ \text{so } \beta &= 0.14 + \mu. \end{aligned}$$

Since the slope of this graph is so sensitive to the number of data points used in the fit, an average of these slopes is used to solve for $\beta$. This average slope was taken for fits for 10–20 data points. The average slope is 0.113. With this information we are able to calculate a range for the basic reproductive number $\mathcal{R}_0$, where $\mathcal{R}_0 = \beta/\mu$. For our range of $\mu$ between 1/6 and 1/31, $\mathcal{R}_0$ ranges from 1.57 to 5.03. We are now ready to look at the solution of the system of differential equations:

$$\begin{aligned} \frac{dS}{dt} &= -\beta SI/N, \\ \frac{dI}{dt} &= \beta SI/N - \mu I, \\ \frac{dR}{dt} &= \mu I. \end{aligned}$$

Since we only have numerical solutions, we can only view the graph of the solutions of each of these equations [see Figure 3]. The solutions plotted there contain the number of susceptible at time $t$, $S(t)$, the number of dead at time $t$, $R(t)$, and the number of infected at time $t$, $I(t)$.

We want to use the relation between $I(t)$ and $R'(t)$ to plot $I(t)$ to fit $R'(t)$ the best. Recall that $R'(t) = \mu I$, so the data being considered is fitted by $\mu I$ plus a shift of $1/\mu$ to account for the average time from infection to death. We first consider how $\mu$ varies: $1/31 < \mu < 1/6$. For the graphs of Figure 4, we have taken $\mu = 1/22$, $1/5$, and $1/30$, and $N(0) = 900$. The respective graphs show exactly what one expects, since by increasing the period that an infected individual lives, $1/\mu$, there is an increase in the number of dead which the model predicts.

The next variable that we have to take into account is $N(0)$. The range for this variable is attained by taking an educated guess as to who the true susceptible individuals are in the population. These individuals are the family members and medical staff that care for the sick. This is a reasonable assumption since the only individuals who are at risk are those that have personal contact with the infected individuals. The lowest possible value of $N(0)$ would be about 250 individuals since only 244 died in this outbreak. A possible top limit for the greatest value of $N(0)$ could be around 900–1000, taking into consideration only the population size of families, health-care workers, and others involved in close and personal contact with infected individuals [refer to Figure 5].

The model, for larger values of $N(0)$, overestimates the number of expected individuals that will die. This observation may give the impression that the model badly represents the data, but in reality this overestimation could be of use to health-care workers who plan for how bad an outbreak may become by knowing statistics about the first 10–20 days of the outbreak.

## 2. Ebola outbreak of 1976 in Yambuku, Zaire.

We will now model the 1976 outbreak of Ebola in Yambuku, Zaire. The data that we will use for this outbreak was obtained from the Center for Disease Control (CDC) in Atlanta, GA. We will model the total infections that occurred during the outbreak using a modification to the S-I-R model. In this model, we will differentiate between the incubation period and the infectious period of the disease. As before, the number of susceptible indi-

viduals at time $t$ will be denoted as $S(t)$. We will refer to the incubation period of the disease as the latent stage. The number of latent individuals at time $t$ will be denoted by $E(t)$. Individuals that are infected with the disease and are suffering the symptoms of Ebola will be classified as infectious individuals. The number of infectious individuals at time $t$ will be denoted by $I(t)$. Similarly, the number of dead individuals at time $t$ will be denoted by $R(t)$.

The population studied will be a constant population during the outbreak; i.e., the total population at time $t$ will be denoted by $N$ where $N = S(t) + E(t) + I(t) + R(t)$. Our model is:

$$\begin{aligned}
\frac{dS}{dt} &= -\beta S(I + qE)/N \\
\frac{dE}{dt} &= \beta S(I + qE)/N - \delta E \\
\frac{dI}{dt} &= \delta E - \gamma I \\
\frac{dR}{dt} &= \gamma I.
\end{aligned}$$

This model takes into consideration the number of people infected due to direct contact with an infected individual and the number of people infected due to direct contact with a latent individual: $\beta S(I+qE)/N$. In this model, $\beta = pc$ where $p$ is the probability of successfully getting infected when coming into contact with an infected individual, and $c$ is the per-capita contact rate. The parameter $q$ $(0 \leq q \leq 1)$ is a weight factor added to the model since it is known that a susceptible individual has a higher chance of getting infected from an infectious individual than from a latent individual [3]).

The individuals in the latent stage eventually show the symptoms of the disease, and pass on to the infectious stage. This is denoted by $\delta E$, where $\delta$ is the per-capita infectious rate. Then $1/\delta$ becomes the average time for a latent individual to become infectious. This will be denoted by $\gamma I$, where $\gamma$ is the per-capita death rate. Then, $1/\gamma$ becomes the average time it takes an individual to die once he/she has entered the infectious stage. As before, death and recovery are taken to be the same, since there has not been a case in which a person who survived Ebola contracts the disease again.

Figure 6 shows the number of people who became infected each day during the outbreak in Yambuku, Zaire in 1976. From this data we can now estimate $\beta$ using a similar method to the one in the previous model. To do this, we first make three assumptions:

**Assumption 1**: In the beginning of the epidemic, $N(t) = S(t)$.

**Assumption 2**: Initially, there is a constant number of individuals infected. Those individuals infect other individuals who become latent. It takes $1/\delta$ days for the latent individuals to become infectious. Therefore, for the first $1/\delta$ days, the rate of change of the infectious individuals is 0 (i.e., $dI/dt = 0$.)

**Assumption 3**: In order for an individual to become infectious, they must pass through the latent stage. Thus, the data for the latent stage is the same as the data for the infectious stage, the only difference being that the latent stage data occurred $1/\delta$ days before. Since $1/\delta$ is the average time it takes for a latent individual to become infectious, and the latent stage ranges from 2 to 21 days, we choose $1/\delta = 12$. Similarly, since $1/\gamma$ is the average time it takes for an infectious individual to die, and of the infectious stage ranges 4 to 10 days, $1/\gamma = 7$. Thus, we then look at the following equation to estimate $\beta$:

$$\begin{aligned} & \frac{dE}{dt} = \beta S(I + qE)/N - \delta E \\ \Rightarrow \quad & \frac{dE}{dt} = \beta(I + qE) - \delta E \qquad (*) \\ & \text{by the first assumption;} \\ \Rightarrow \quad & \frac{dI}{dt} = \delta E - \gamma I = 0 \Rightarrow \delta E = \gamma I \Rightarrow I = \delta E/\gamma \\ & \text{by the second assumption.} \end{aligned}$$

If we substitute $I$ into $*$, then $dE/dt = [\beta(\delta/\gamma - \delta)]E$.

The information for $dE/dt$ is given by the daily infection data; the information for $E$ is the cumulative of the daily infection data. Thus, we have a linear relationship, and we can estimate the slope by doing a linear fit. Using Mathematica and the data for the first 12 days, we obtain the fit shown in Figure 7 where equation of the line is $0.3893t$. Thus, we now have the slope of the best fit line, and $\beta = (0.3893 + \delta)/(\delta/\gamma + q) = 0.567114$, if we take

$q = 0.25$ and the values of $\delta$ and $\gamma$ given above. The choice for $q$ is arbitrary and is picked so that the model best fits the supplied data.

Another important number that needs to be computed is the basic reproductive number, $\mathcal{R}_0$. This number tells us how fast the disease will spread at the beginning of the epidemic. To calculate the value for $\mathcal{R}_0$ , we need to find the Jacobian matrix of the system of equations. We then evaluate it at the disease-free state. Since the four- dimensional system can be reduced to a three-dimensional system, only the first three equations need to be considered. It is easy to show that the disease-free state is $(S, E, I, R) = (N, 0, 0, 0)$. Once the Jacobian is evaluated at this point, the determinant and the trace must both be greater than zero to insure that the disease-free state is an unstable fixed point. Once all of this is accomplished, we obtain a value for $\mathcal{R}_0$:

$$\mathcal{R}_0 = (\beta/\gamma)(1 + q\gamma/\delta) = 5.67.$$

All the parameter values are known, and thus we can solve our system of differential equations. The system of differential equations cannot be solved explicitly, so Mathematica is used to solve the system numerically. Figure 8 shows two numerical solutions to the system plotted with the initial infectious data. Note the label of the axes. It reads "Positive Part of $dI/dt$" because the given data only takes into account the recruitment rate of infectious people. The data does not reflect the infectious individuals that die; therefore, only the positive part of $dI/dt$ is plotted. As can be seen in the plots, the numerical solutions are very good in the first part of the epidemic. After the peak is reached, the model is not very accurate.

### 3. Ideas for Future Research.

Both of the models that were presented in this research project used a constant effective contact rate, $\beta$. This is probably not the best model for $\beta$ since the probability of contracting the Ebola virus varies as the disease becomes more widespread. People are more careful with whom they have contact, and thus the number of contacts decreases as time elapses or as the number of infected increases. Therefore, it makes sense to have $\beta$ decrease. Another idea for enhancing the model is to consider quarantine. When infected people are isolated, the number of contacts that can transmit the disease decreases. This is something that could be taken into account in future work with these models.

More research needs to be conducted to estimate $N$, the total population. A good number for $N$ is very important, since as it varies, the accuracy of the model also varies, as was seen in the numerical solutions of the models. Information that may prove helpful in estimating $N$ includes the number of staff members in hospitals, family size, and other data that may help determine the total susceptible population at the beginning of an Ebola outbreak.

Research on $q$ is also essential. It is intuitively clear that individuals showing symptoms of the Ebola disease are more infectious than latent individuals who show no symptoms. Therefore, a better value for $q$ would make the model more accurate in predicting the dynamics of a future Ebola outbreak.

## 4. Conclusions.

The calculated $\mathcal{R}_0$ values ranged from 2.6 to 8.6 for the Yambuku, Zaire outbreak in 1976; meanwhile the range for $\mathcal{R}_0$ for the 1995 epidemic in Kikwit, Zaire was slightly lower: $1.57 \leq \mathcal{R}_0 \leq 5.03$. This makes sense since it shows that Ebola patients were infected more during the first epidemic due to misunderstanding and misdiagnosis of the Ebola virus. The values calculated for the basic reproductive number were lower than one may expect for Ebola, and were lower than for other diseases. For example, $\mathcal{R}_0$ ranged from 16–18 for the measles in England and Wales between 1950-68; and $\mathcal{R}_0$ for HIV in Hampara, Uganda for heterosexuals between 1985-7 was 10–11 (Anderson and May, 1991). This may be due to Ebola's method of transmission and the fear people have of contracting Ebola.

These models are very important because they can put an upper bound on the number of deaths, and thus can help health officials plan for the latter part of an outbreak by calculating the parameters from the data at the start of the epidemic. The number of deaths can also be minimized by altering the environment; i.e., lowering $\beta$ (the effective contact rate). This can be accomplished by implementing quarantine.

**Acknowledgments**

The research in this manuscript has been partially supported by grants given by the National Science Foundation (NSF Grant DMS-9600027), the National Security Agency (NSA Grant MDA 904-96-1-0032) and Presidential Faculty Fellowship Award (NSF Grant DEB 925370) to Carlos Castillo-Chavez. Substantial financial and moral support was also provided by the Office of the Provost of Cornell University and by Cornell's College of Agricultural & Life Sciences (CALS) and the Biometrics Unit. The authors are solely responsible for the views and opinions expressed in this report. The research in this report does not necessarily reflect the views and/or opinions of the funding agencies and/or Cornell University.

Thanks to: Carlos Castillo-Chávez, Bonnie Delgado, Carlos Hernández-Suárez, Elion Mboussa, Tamara Parker, Julie M. Seda, Jorge X. Velasco-Hernández, and the Centers for Disease Control (CDC). We would like to specially thank Herbert A. Medina, "El Bañao Número Siete."

**References**

Anderson, R.M and May, R.M., "Infectious Diseases of Humans," Oxford University Press, 1991.

Brauer, F. and Castillo-Chávez, C., "Basic Epidemiology Models," in *Ecological Time Series*, eds. T.M. Powell and J.H. Steele, Chapman & Hall, New York, pp. 410-447, 1994.

Centers for Disease Control, Atlanta, GA, World Wide Web Page, http:www.cdc.gov/ncidod/diseases/virlfvr/ebolainf.htm.

Kermack, W.O. and McKendrick, A.G., "A contribution to the mathematical theory of epidemics, in *Proceedings of the Royal Society of London, Series A* **115**: 700-721, 1927.

World Health Organization, World-Wide Web Page, http:www.who.ch/programmes/cds/ebupdate.html.

List of Figure Captions

Data of Daily Deaths in Kikwit, Zaire in 1995 Outbreak.
Figure 1

Data of Total Deaths in Kikwit, Zaire in 1995 Outbreak.
Figure 2

Plots of Solutions to the System of Differential Equations with Parameter Values: $\mu = 1/22$, $\beta = 0.113$, $N = 900$.
Figure 3

Graphs of $\mu I(t)$ Compared to Actual Data for $N = 900$, $\beta = 0.113$, and $= 1/22, 1/5, 1/30$, respectively.
Figure 4

Figure 5 (no caption)

Data of Daily Deaths in Yambuku, Zaire in 1976 Outbreak.
Figure 6

Linear Fit to Data to Approximate $\beta$.
Figure 7

Figure 8 (no caption).

## Data of Daily Deaths in Kikwit, Zaire in 1995 Outbreak

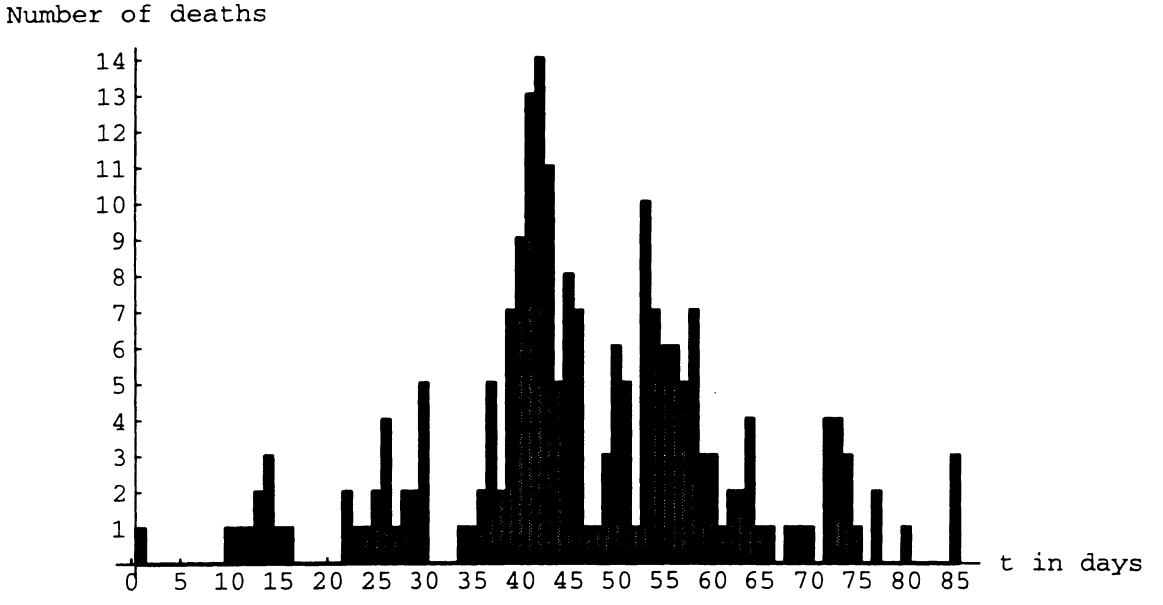


**Figure 1**

## Data of Total Deaths in Kikwit, Zaire in 1995 Outbreak

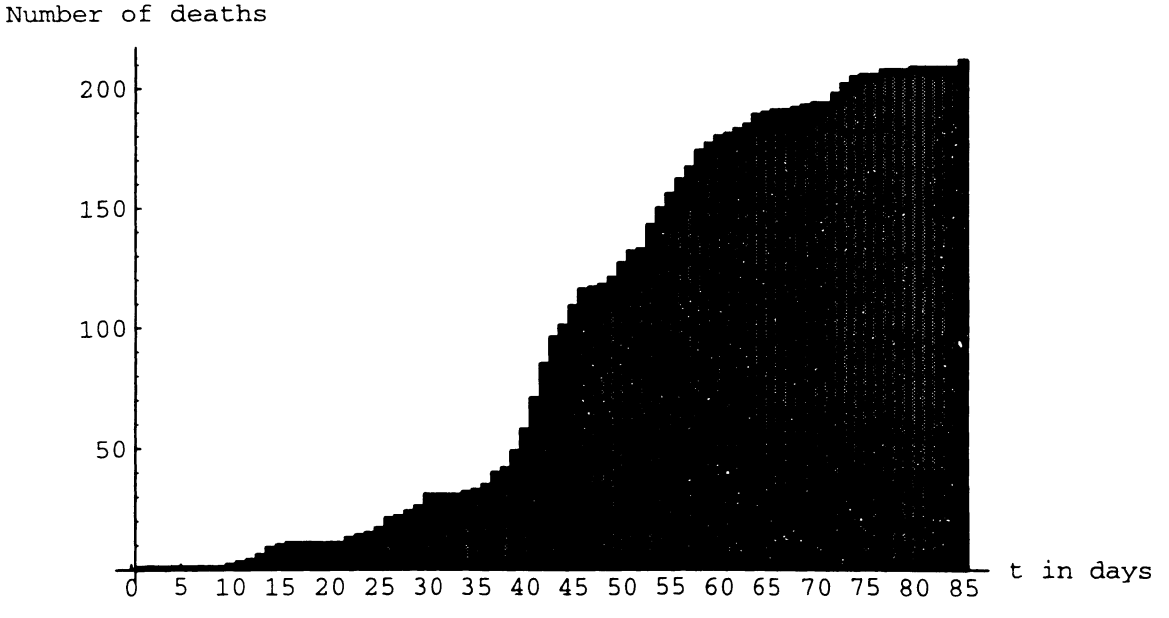


**Figure 2**

**Plots of Solutions to the System of Differential Equations with Parameter Values:** $\mu = 1/22$, $ß = 0.113$, $N = 900$

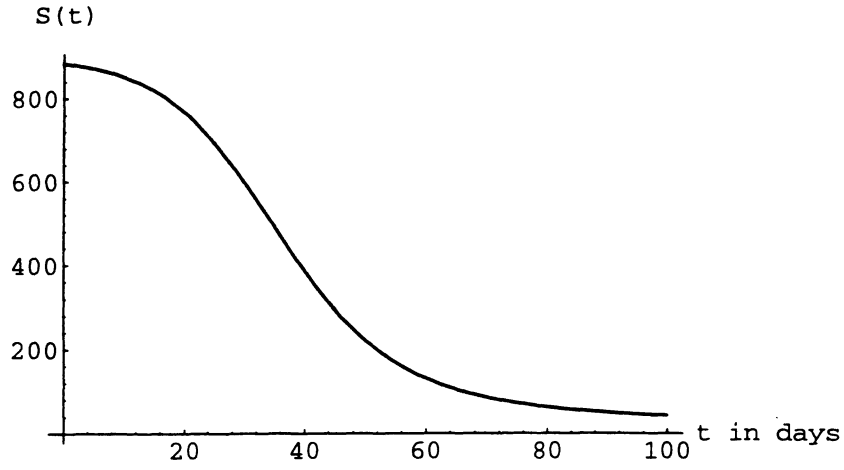


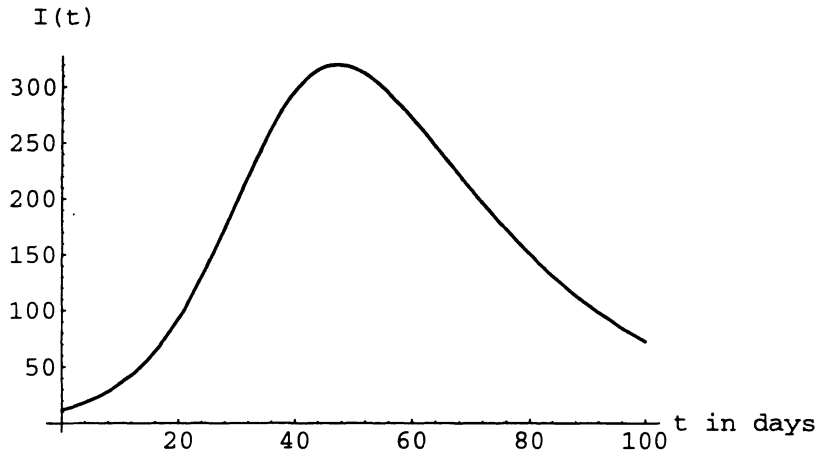


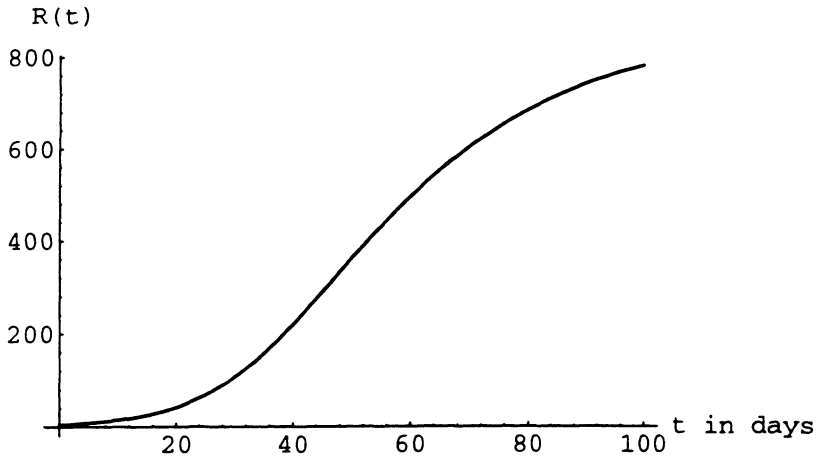


**Figure 3**

**Graphs of μ I(t) Compared to Actual Data for**

N = 900, ß = 0.113, **and** μ = 1/22, 1/5, 1/30 respectively

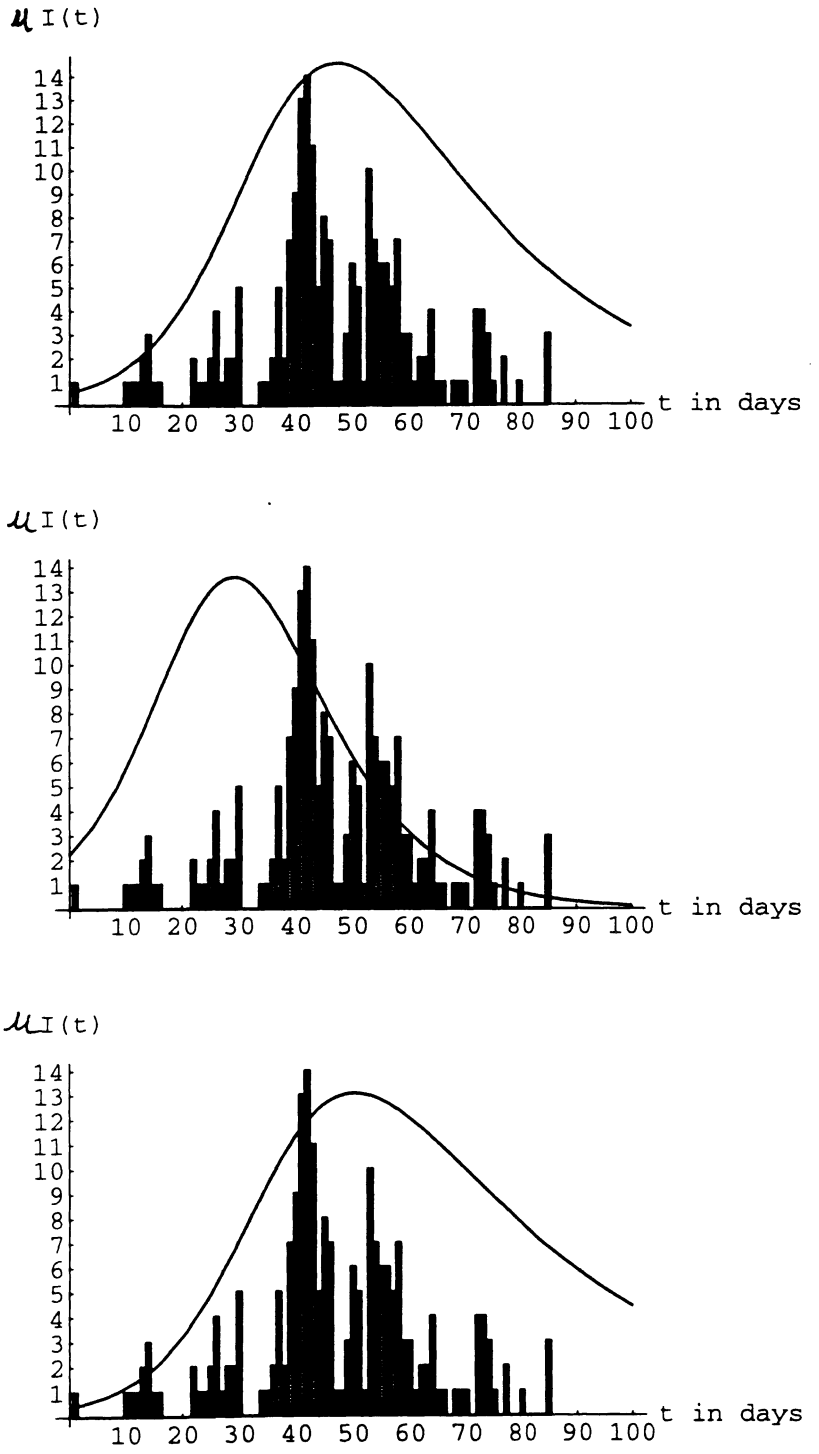


**Figure 4**

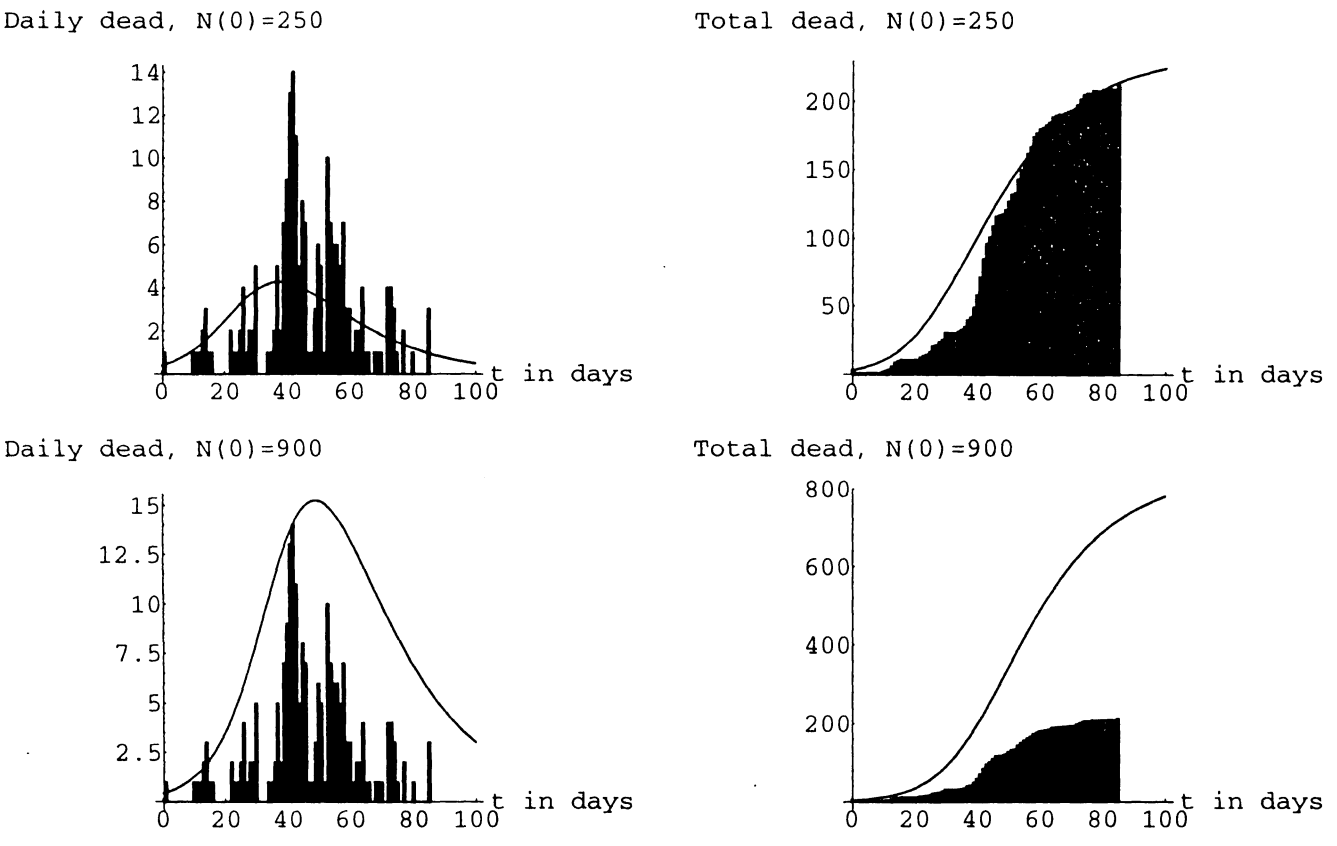
Daily dead, N(0)=250
14
12
10
8
6
4
2
0 20 40 60 80 100
t in days
Total dead, N(0)=250
200
150
100
50
0 20 40 60 80 100
t in days
Daily dead, N(0)=900
15
12.5
10
7.5
5
2.5
0 20 40 60 80 100
t in days
Total dead, N(0)=900
800
600
400
200
0 20 40 60 80 100
t in days

**Figure 5**

## Data of Daily Deaths in Yambuku, Zaire in 1976 Outbreak

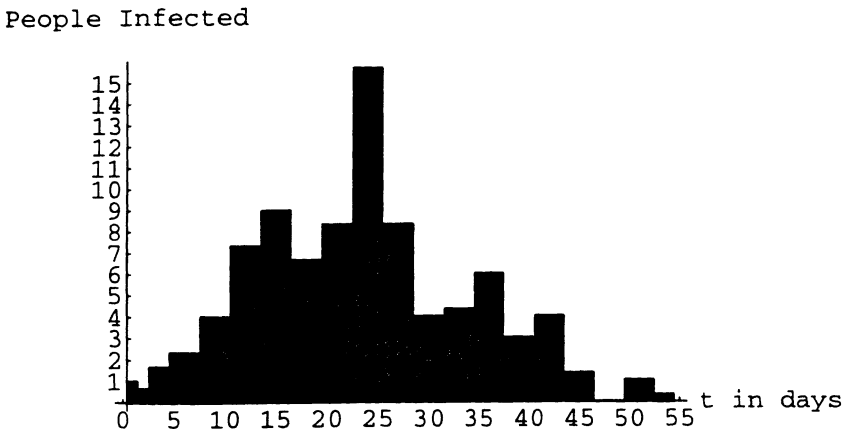


**Figure 6**

## Linear Fit to Data to Approximate $\beta$

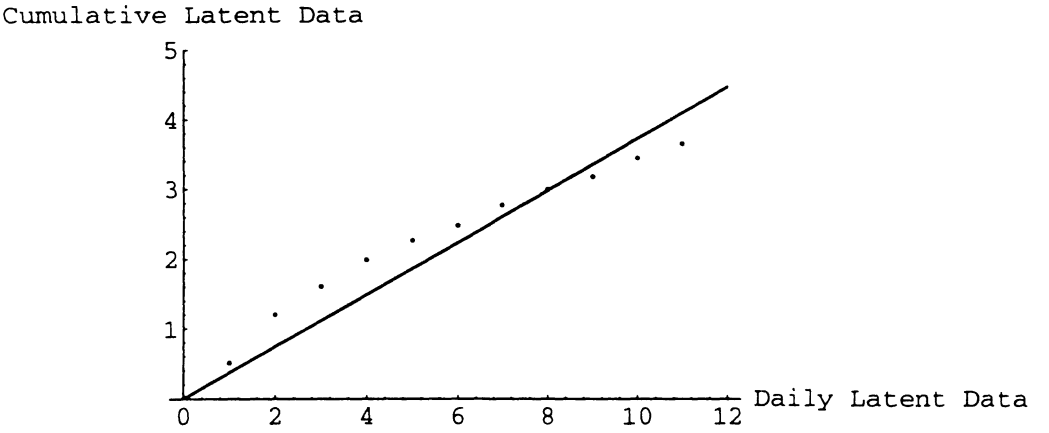


**Figure 7**

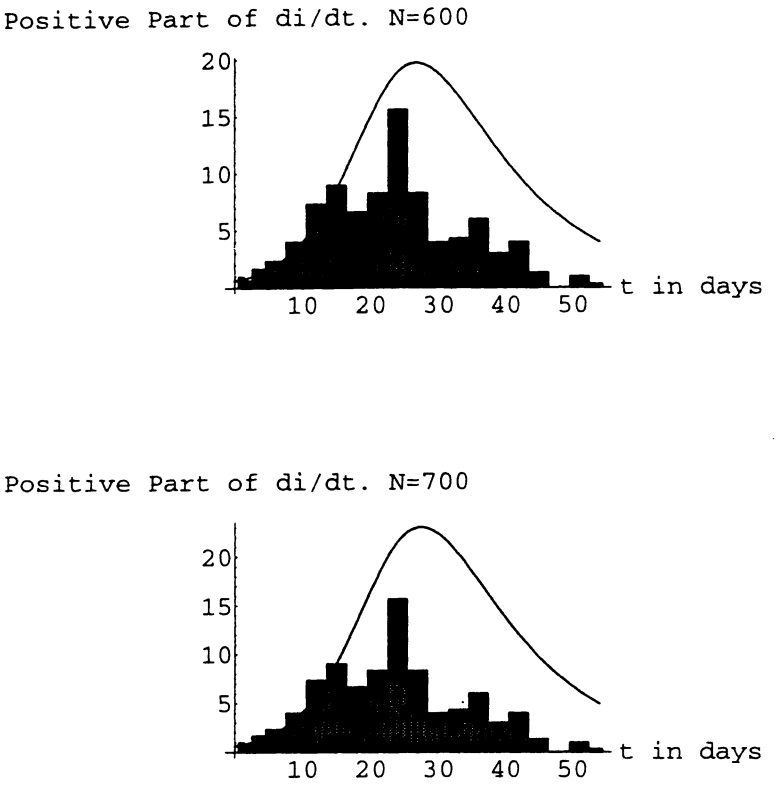
Positive Part of di/dt. N=600
20
15
10
5
10 20 30 40 50
t in days
Positive Part of di/dt. N=700
20
15
10
5
10 20 30 40 50
t in days

**Figure 8**

# Stochastic Simulations of a Spatial SIR Model

Judit Camacho
Uiversity of California, Santa Cruz
sacnas.cats.ucsc.edu

Fernando Carreon
University of Texas at El Paso
fcarreon@mail.utep.edu

Derik Castillo-Guajardo
Universidad Autonoma Metropolitana Unidad Xochimilco
aesquiv@cueyatl.uam.mx

Hugo Jiménez-Pérez
Universidad Nacional Autonoma de Mexico
hugo@barajas.fciencias.unam.mx

Leticia Montoya-Gallardo
Universidad Nacional Autonoma de Mexico
mjordan@matem.unam.mx

and Ricardo A. Sáenz
University of Texas at El Paso
saenz@math.utep.edu

BU-1366-M

ABSTRACT. In this paper we consider a stochastic spatial SIR (Susceptible-Infectious-Recovered) model. We assume that the population is distributed in separate cells. The disease is transmitted within the cell by direct contact, and from cell to cell through an external object (vector or vehicle) capable of carrying the disease. We simulate this model in a $10 \times 10$ grid of cells, and investigate the effects of the relative rates of transmission within and between cells on the predictability and progression of the disease. Results of simulation indicate that as the rate of intercellular transmission increases relative to intracellular transmission, the mean number becoming effected within each cell increases but so does the spatial variability. We also found that the time for the epidemic to run its course reaches a maximum average value at intermediate relative rates as does the spatial variability.

## 1. Introduction

The common mathematical models for diseases are the SIS (Susceptible-Infectious-Recovered) models, developed by Kermack and McKendrick (see discussion in [2], [5] and [6]). In the case when infective individuals recover and again become susceptible to the disease, the model used is the SIS. In the case when infective individuals recover and attain permanent immunity, we use an SIR model. The classical models do not consider how the population is distributed in space, only the number of individuals in each class.

In this paper we describe a spatially discrete model, and simulate this model in a $10 \times 10$ grid of cells. The effects of the relative rates of transmission within and between cells on the predictability and progression of the disease are investigated.

## 2. The Spatial Model

The classical SIS and SIR models do not take into account how the individuals are distributed in space. However, spatial models have been studied. For instance, D. G. Kendall (see discussion in [1] and [2]) formulated the following model: assuming that the individuals are continuously distributed on a region of the plane with density $\sigma$ individuals per unit area, $S(x, y, t)$, $I(x, y, t)$, and $R(x, y, t)$ being the density of susceptible, infectious and recovered individuals, respectively, at point $(x, y)$ and at time $t$, we have the equations

$$\begin{aligned} \frac{\partial S(x,y,t)}{\partial t} &= -\beta S(x,y,t)\,\overline{I}(x,y,t) \\ \frac{\partial I(x,y,t)}{\partial t} &= \beta S(x,y,t)\,\overline{I}(x,y,t) - \gamma I(x,y,t) \\ \frac{\partial R(x,y,t)}{\partial t} &= \gamma I(x,y,t) \end{aligned}$$

where $\beta$ is the infection rate, $\gamma$ is the recovery rate, and $\overline{(I)}$ is a spatially weighted average of $I$ given by

$$\overline{(I)}(x,y,t) = \int\int W\left[(x'-x),(y'-y)\right] I(x',y',t)\,dx'dy',$$

$W$ being an appropriate nonnegative weighting coefficient satisfying

$$\int\int W\left[(x'-x),(y'-y)\right]\,dx'dy' = 1.$$

The model above assumes a continuous distributed population. In this paper, however, we will consider the case in which the population is distributed in separate cells.

We assume that the population is distributed in a grid of cells. The individuals inside each cell are free to move within their cell, but there is no direct contact (contagion) among the individuals of different cells. The infection is transmitted within cells at rate $\beta$, and between cells by a vector or vehicle at transmission rate $\alpha$. Individuals recover with a rate $\gamma$ and become immune to the disease. We also assume that the dynamics of the disease are on a fast time scale compared to the birth and death rates of the population so that the population can be considered fixed. Then we have the following deterministic version of the model describing this system:

$$\begin{aligned}
\frac{dS_{x,y}}{dt} &= -\left(\beta I_{x,y} + \alpha \sum_{k,m} W(k,m) I_{x+k,y+m}\right) \frac{S_{x,y}}{N_{x,y}} \\
\frac{dI_{x,y}}{dt} &= \left(\beta I_{x,y} + \alpha \sum_{k,m} W(k,m) I_{x+k,y+m}\right) \frac{S_{x,y}}{N_{x,y}} - \gamma I_{x,y} \\
\frac{dR_{x,y}}{dt} &= \gamma I_{x,y},
\end{aligned}$$

where $N_{x,y} = S_{x,y} + I_{x,y} + R_{x,y}$ (the total number of individuals in cell $(x, y)$), $S_{x,y}$, $I_{x,y}$, and $R_{x,y}$ are the number of susceptible, infectious and recovered individuals, respectively, and $W$ is a nonnegative weighting function satisfying $\sum_{k,m} W(k,m) = 1$.

The above model is quite general for most spatial processes where populatins are confined locally or migration is on a longer time scale than that of the disease. Examples are diseases in breeding farms, where the affected animals are confined but transmission can take place by pests or vehicles such as maintenance tools or feed. This model could also be applied to hospitals, where a disease could be transmitted between wards by staff or visitors.

## 3. Simulations

The stochastic version of the above model is too complicated to be studied analytically. Computer simulations are an alternative of studying complicated systems such as this. In our model $\alpha$, $\beta$ and $\gamma$ are as above, and

we assume that a cell can only be infected by its four immediate neighbors (nondiagonal), as the next diagram shows:

In the diagram we represent the process inside each cell $(x, y)$ as susceptibles becoming infected, and after a time recovering and then becoming immune to the disease. The dotted lines represent indirect transmission of the disease from the neighboring cells. This particular case is then described by the set of equations

$$\begin{aligned}
\frac{dS_{x,y}}{dt} &= -\left(\beta I_{x,y} + \frac{\alpha}{4}\sum I_{k,m}\right)\frac{S_{x,y}}{N} \\
\frac{dI_{x,y}}{dt} &= \left(\beta I_{x,y} + \frac{\alpha}{4}\sum I_{k,m}\right)\frac{S_{x,y}}{N} - \gamma I_{x,y} \\
\frac{dR_{x,y}}{dt} &= \gamma I_{x,y},
\end{aligned}$$

where the sum is taken over the four immediate neighbors of cell $(x, y)$. Note that here

$$W(k,m) = \begin{cases} \frac{1}{4} & k = \pm 1 \qquad m = 0 \\ \frac{1}{4} & k = 0 \qquad m = \pm 1 \\ 0 & otherwise \end{cases}$$

since we are assuming that all contiguous cells have equal weight with respect to direction in the external transmission of the disease. The grid size was $10 \times 10$ on a torus. To simulate the stochastic process, then, we define the following:

Call the rate of infection $B$. Then

$$B_{x,y} = \left(\beta I_{x,y} + \frac{\alpha}{4}\sum I_{k,m}\right)\frac{S_{x,y}}{N}$$

and call the rate of recovery $D$. Then $D_{x,y} = \gamma I_{x,y}$. The total event rate is then $\sum B_{x,y} + D_{x,y}$ or equivalently the mean time between events is

$$\tau = \left(\sum_{x,y} B_{x,y} + D_{x,y}\right)^{-1}.$$

The time between events (the inter-event times) can be simulated as an exponential with $S = -\tau ln(U_1)$ where $U_1$ is a uniform (0,1) random variable.

The event occurs in a particular cell $(i, j)$ if a second unform random variable $(U_2)$ is

$$\frac{\sum_{x,y}^{i-1,j-1}(B_{x,y}+D_{x,y})}{\sum_{x,y}^{n,n}(B_{x,y}+D_{x,y})} < U_2 \leq \frac{\sum_{x,y}^{i,j}(B_{x,y}+D_{x,y})}{\sum_{x,y}^{n,n}(B_{x,y}+D_{x,y})}.$$

The probability of an infection given that an event has occurred $= B_{i,j}\tau$ and the probability of a recovery given that an event has occurred $= D_{i,j}\tau$. Then to decide if the event is an infection or a recovery we pick a third uniform random variable $(U_3)$ and if

$$0 \leq U_3 < \frac{B_{i,j}}{B_{i,j}+D_{i,j}},$$

then $S_{i,j} \rightarrow Si, j-1$, $I_{i,j} \rightarrow Ii, j+1$, and $R_{i,j} \rightarrow Ri, j$ (an infection occurs) and if

$$\frac{B_{i,j}}{B_{i,j}+D_{i,j}} \leq U_3 \leq 1,$$

then $S_{i,j} \rightarrow Si, j$, $I_{i,j} \rightarrow Ii, j-1$, and $R_{i,j} \rightarrow Ri, j+1$ (a recovery occurs).

We simulated the system with initial conditions $I_{5,5} = I$ and $I_{x,y} = 0$ for all other $(x, y)$, and $R_{x,y} = 0$ for all $x$ and $y$. Figure 1 represents the results after 100 simulations for several pairs $(\alpha, \beta)$ with $\gamma = 1$ and $N = 10$. Setting $\gamma = 1$ changes our time units to the mean recovery period. The surfaces represent the average number of survivors (individuals who remained susceptible during the whole development of the epidemic), the average times for the epidemic to finish, the average maximum of infectious individuals at a certain time and the average time when this maximum occurs. The colors represent the variance of the results.

Figure 1 shows the effects that the parameters $\alpha$ and $\beta$ have on the system. Our choice of parameter values was severely limited by computer time for large values of $\alpha$ and $\beta$. In order to better understand the effect of the parameters on the model we established the following relationship. The basic reproduction number for the development of the infection inside an isolated cell is given by $\mathcal{R}_0 = \beta/\gamma$. The spatial aspect of the problem leads to $\mathcal{R}_0' = (\beta + \alpha)/\gamma$.

We define the *spatial infection number* $S_0$ by

$$S_0 = \frac{\alpha}{\beta},$$

the quotient between the transmission rates inside and outside the cells, which can be interpreted as the ability of the disease to spread throughout the cells. We can then write $\mathcal{R}_0' = (1 + S_0)\,\beta/\gamma = (1 + S_0)\mathcal{R}_0$.

Figures 2, 3, 4 and 5 show the results after 100 simulations with $\gamma = 1$ and $N = 10$, for the values of $\mathcal{R}_0 = 1$, 2, 4 and 8 (since $\gamma = 1$ these correspond to the values of $\beta = 1$, 2, 4 and 8), and the values of $S_0 = 1/100$, $1/200$, $1/400$, $1/800$ and $1/1600$. The points plotted are the values of $\alpha$ that correspond to the values of $S_0$ mentioned above and the average results after the set of simulations, where the calculations correspond to the same calculations as in Figure 1. The vertical lines represent one standard deviation of the data.

Note that for $\mathcal{R}_0 = 1$ (Figure 2) the average times for the disease to die out are around 1, since we just need to wait for the infected individual to recover. As we increase $\mathcal{R}_0$, we see that an epidemic develops, and that as we increase $S_0$ the number of survivors (those that never contract the disease) decreases, since the disease attacks more cells. Note that for $\mathcal{R}_0 = 8$ (Figure 5), as we increase the value of $S_0$, the time for the epidemic to finish decreases, assuming a maximum of around 15 at $S_0 = 1/400$. This means that $S_0$ also tells us the speed of the development of the epidemic. Note that the epidemic finishes with maximum average time of 15 recovery periods.

Simulations of the stochastic process lead to two interesting conclusions. First, even though the spatial aspect of the infection leads to lower numbers of survivors as the spatial infection number increases (the result one would expect from the deterministic process), the variability of the number of survivors increases even more dramatically. And second, the time for the infection to run its course reaches a maximum of variability at intermediate values of the spatial infection number.

## Acknowledgments

The research in this manuscript has been partially supported by grants given by the National Science Foundation (NSF Grant DMS-9600027), the National Security Agency (NSA Grant MDA 904-96-1-0032), Presidential Faculty Fellowship Award (NSF Grant DEB 925370) to Carlos Castillo-Chávez. Substantial financial and moral support was also provided by the Office of the Provost of Cornell University and by Cornell's College of Agricultural and Life Sciences (CALS) and its Biometrics Unit, CONACYT (Grant 400200-5-3551 E to Jorge Velasco-Hernández), Universidad Autónoma de México and The University of Texas at El Paso, with special thanks to Santiago López de Medrano, Guillermo Gómez Alcaraz, Jorge Velasco-Hernández and Javier Rojo. The authors are solely responsible for the views and opinions expressed in this report. The research in this report does not necessarily reflect the views and/or opinions of the funding agencies and/or Cornell University. The authors would specially like to thank Carlos M. Hernández-Suárez and Harold T. Figueroa for the time they spent in the completion of this work, for their ideas, their patience and their friendship. Also we want to thank Estelle Tarica and Tamara Parker for their proof reading and suggestions.

## REFERENCES


Bailey, N.T.J. The Simulation of Stochastic Epidemics in Two Dimensions. *Proc. 5th Berkeley Symp. Math. Stat. and Prob.* **4** (1967) pp. 237-257.

Bailey, N.T.J. *The Mathematical Theory of Infectious Diseases.* Griffin, 1975.

Bass, J. *Elements of Probability Theory.* Academic Press, 1966.

Chiang, C.L. *Introduction to Stochastic Processes in Biostatistics.* Wiley, 1968.

Estava, L. *et al.* Matemáticas y Epidemiolog'a. *Ciencias*, **24** (Oct. 1991), pp. 57-63.

Hethcote, H.W. Three Basic Epidemiological Models. *Applied Mathematical Ecology*, ed. S. Levin and T. Hallow. Springer-Verlag, pp. 119-144.

Renshaw, E. *Modelling Biological Populations in Space and Time.* Cambridge Studies in Mathematical Biology: 11. Cambridge University Press, 1991.

Ross, S.M. *Introduction to Probability Models*, 5th Ed. Academic Press, 1993.

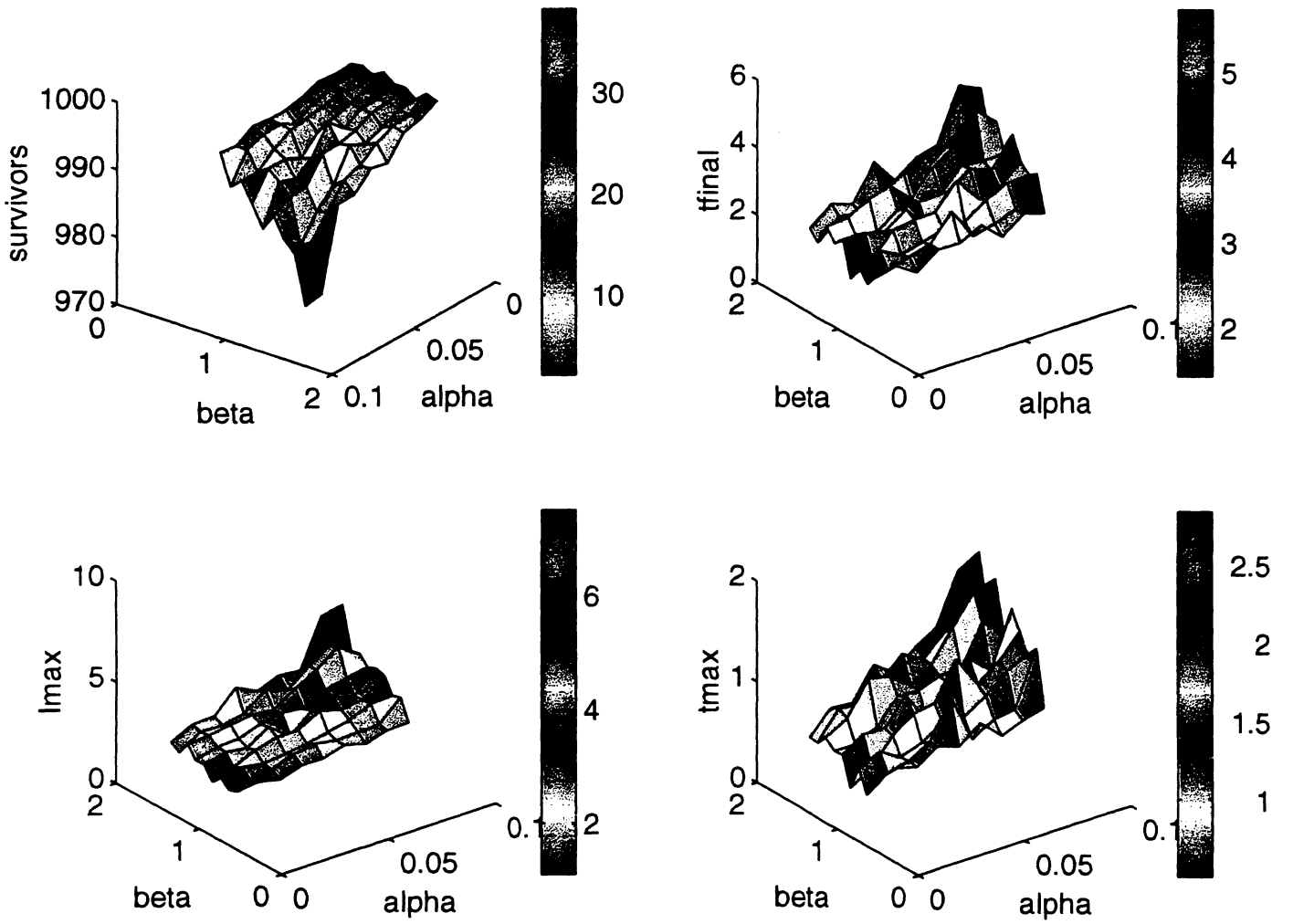
survivors
1000
990
980
970
0
1
2
beta
0
0.05
0.1
alpha
30
20
10
tfinal
6
4
2
0
2
1
beta
0
0
0.05
alpha
5
4
3
2
Imax
10
5
0
2
1
beta
0
0
0.05
alpha
6
4
2
tmax
2
1
0
2
1
beta
0
0
0.05
alpha
2.5
2
1.5
1

Figure 1.

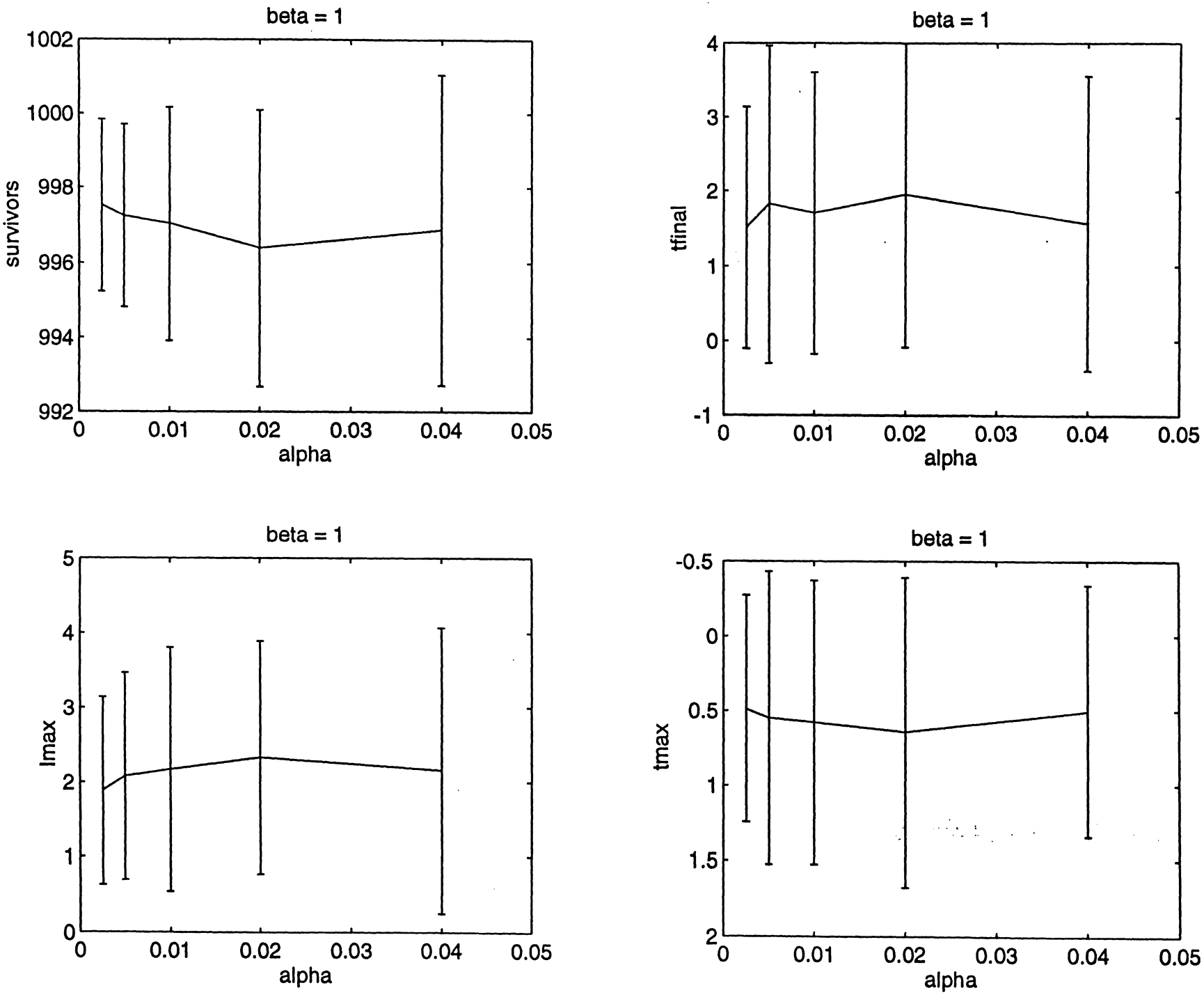
beta = 1
survivors
1002
1000
998
996
994
992
0
0.01
0.02
0.03
0.04
0.05
alpha
beta = 1
tfinal
4
3
2
1
0
-1
0
0.01
0.02
0.03
0.04
0.05
alpha
beta = 1
Imax
5
4
3
2
1
0
0
0.01
0.02
0.03
0.04
0.05
alpha
beta = 1
tmax
-0.5
0
0.5
1
1.5
2
0
0.01
0.02
0.03
0.04
0.05
alpha

Figure 2.

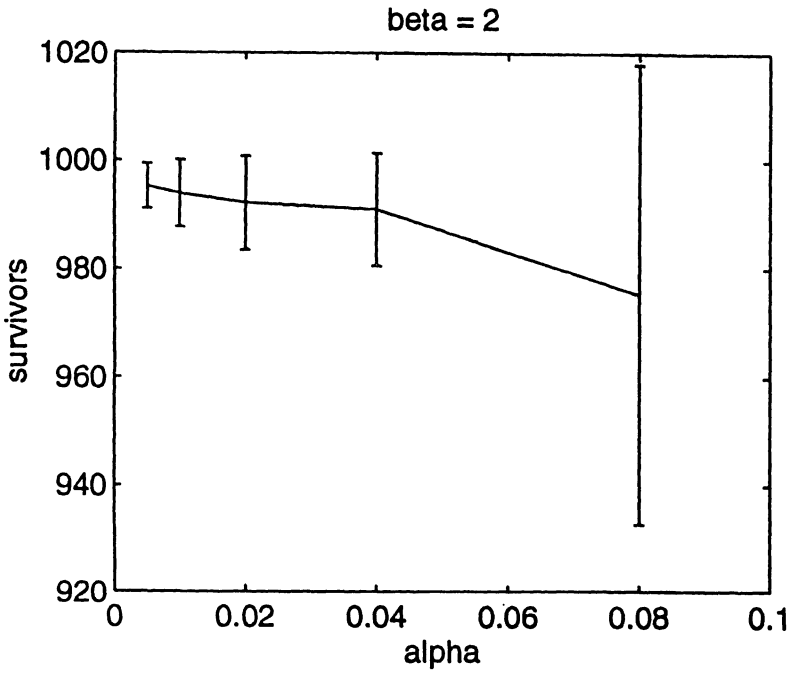
beta = 2
survivors
alpha
1020
1000
980
960
940
920
0
0.02
0.04
0.06
0.08
0.1

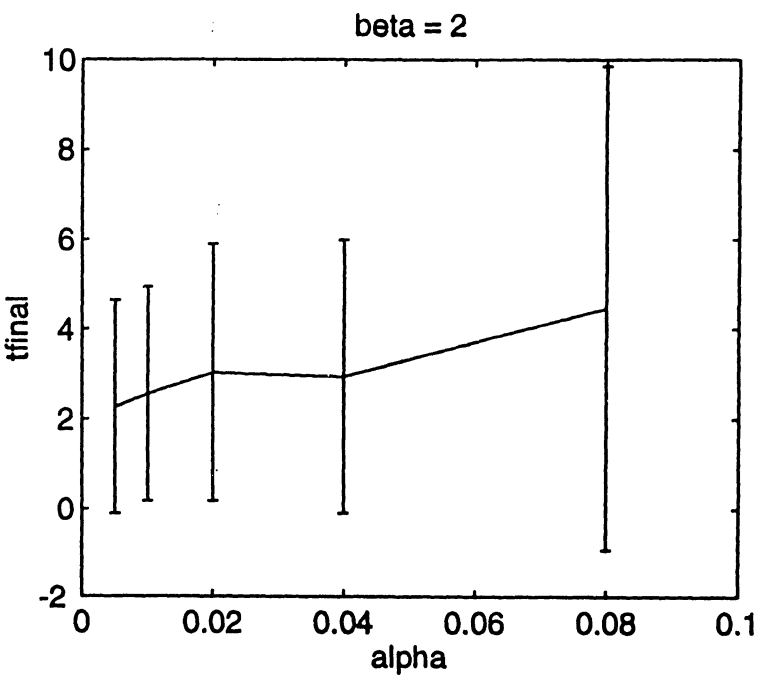
beta = 2
tfinal
alpha
10
8
6
4
2
0
-2
0
0.02
0.04
0.06
0.08
0.1

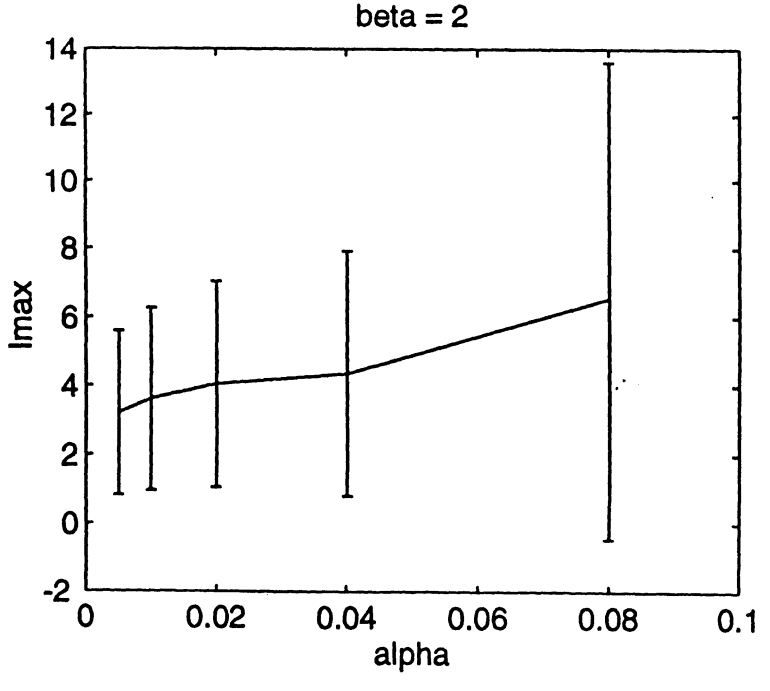
beta = 2
Imax
alpha
14
12
10
8
6
4
2
0
-2
0
0.02
0.04
0.06
0.08
0.1

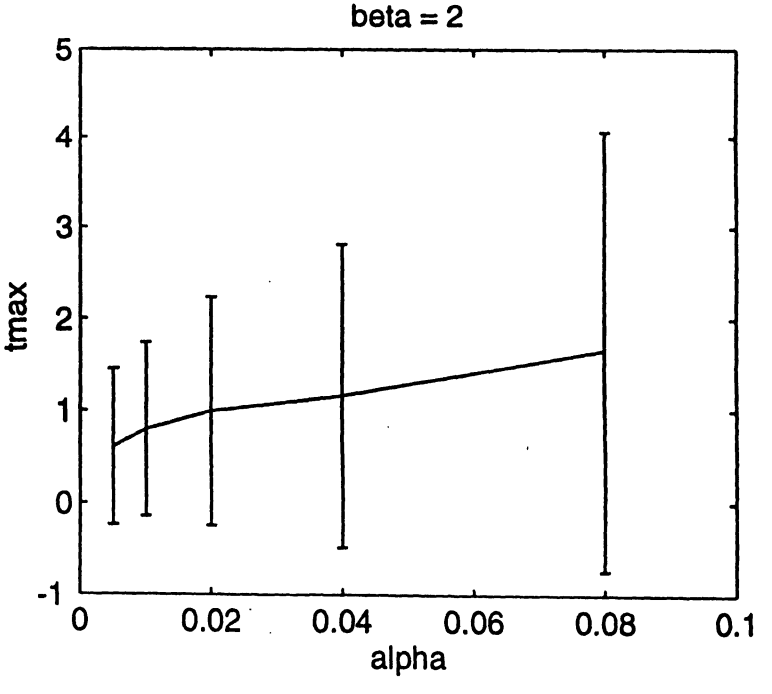
beta = 2
tmax
alpha
5
4
3
2
1
0
-1
0
0.02
0.04
0.06
0.08
0.1

Figure 3.

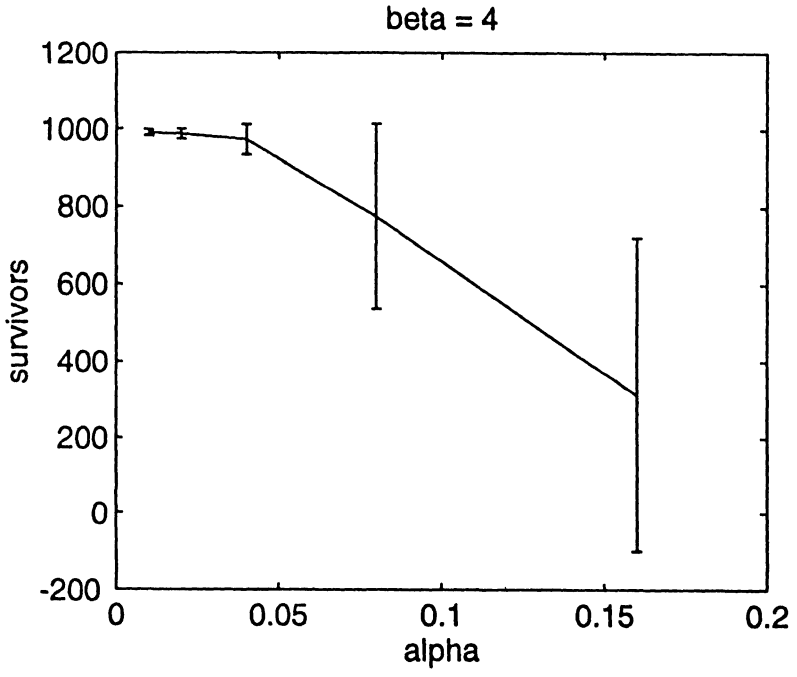
beta = 4
survivors
alpha
1200
1000
800
600
400
200
0
-200
0
0.05
0.1
0.15
0.2

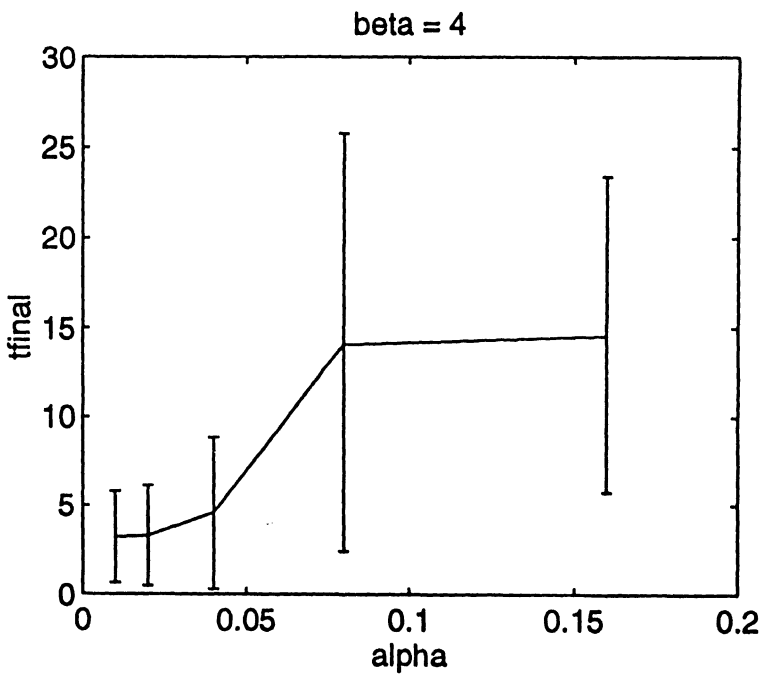
beta = 4
tfinal
alpha
30
25
20
15
10
5
0
0
0.05
0.1
0.15
0.2

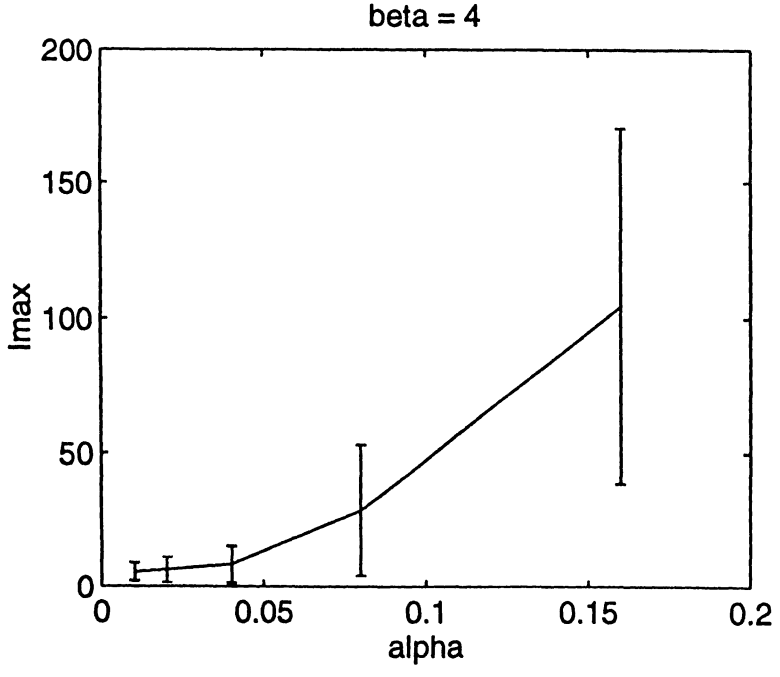
beta = 4
lmax
alpha
200
150
100
50
0
0
0.05
0.1
0.15
0.2

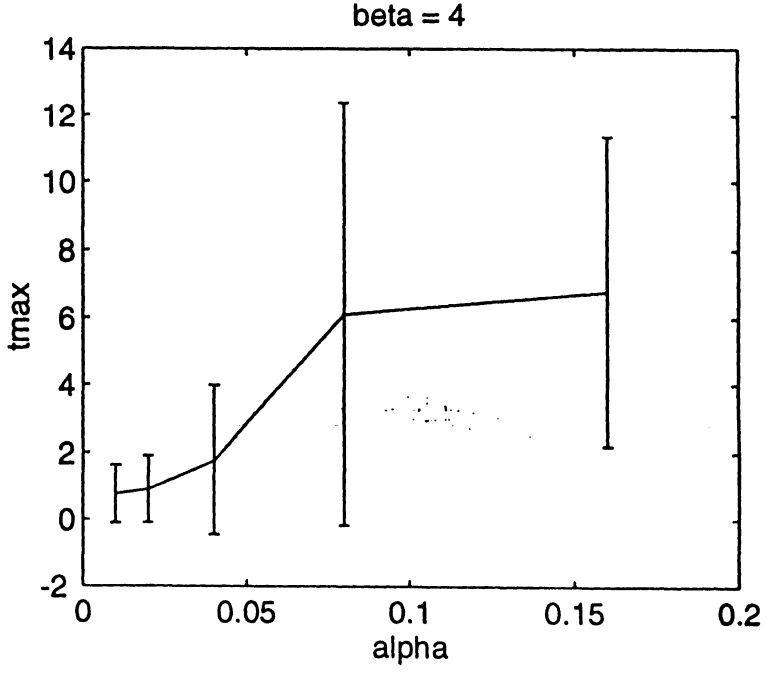
beta = 4
tmax
alpha
14
12
10
8
6
4
2
0
-2
0
0.05
0.1
0.15
0.2

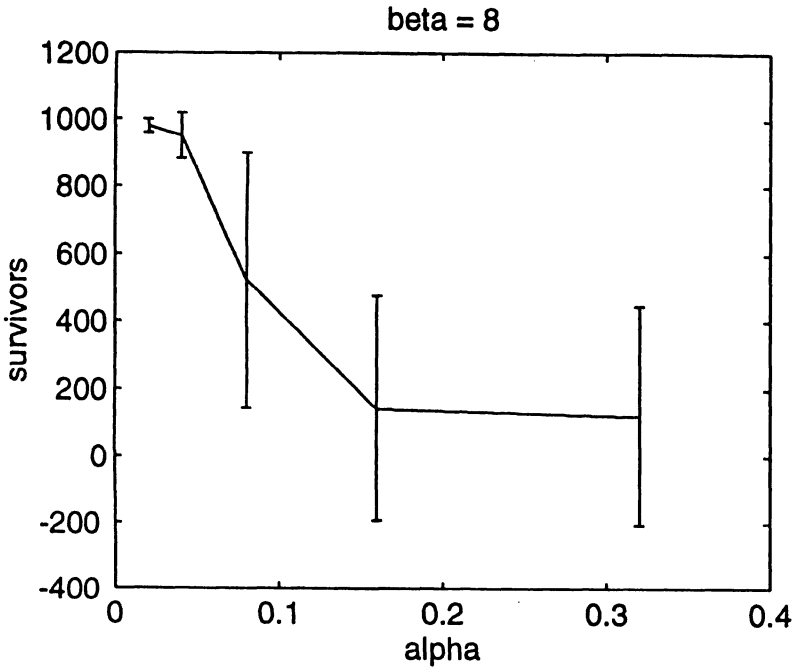
beta = 8
survivors
alpha
1200
1000
800
600
400
200
0
-200
-400
0
0.1
0.2
0.3
0.4

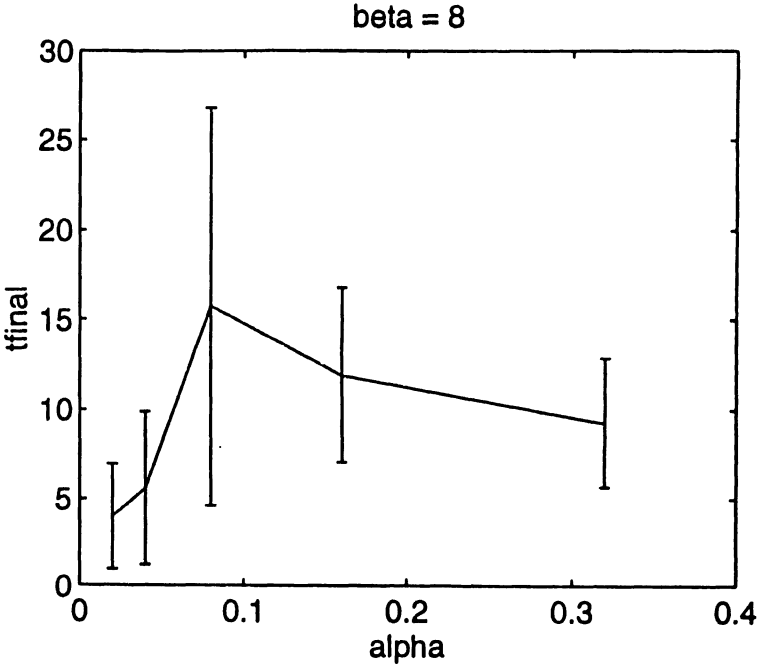
beta = 8
tfinal
alpha
30
25
20
15
10
5
0
0
0.1
0.2
0.3
0.4

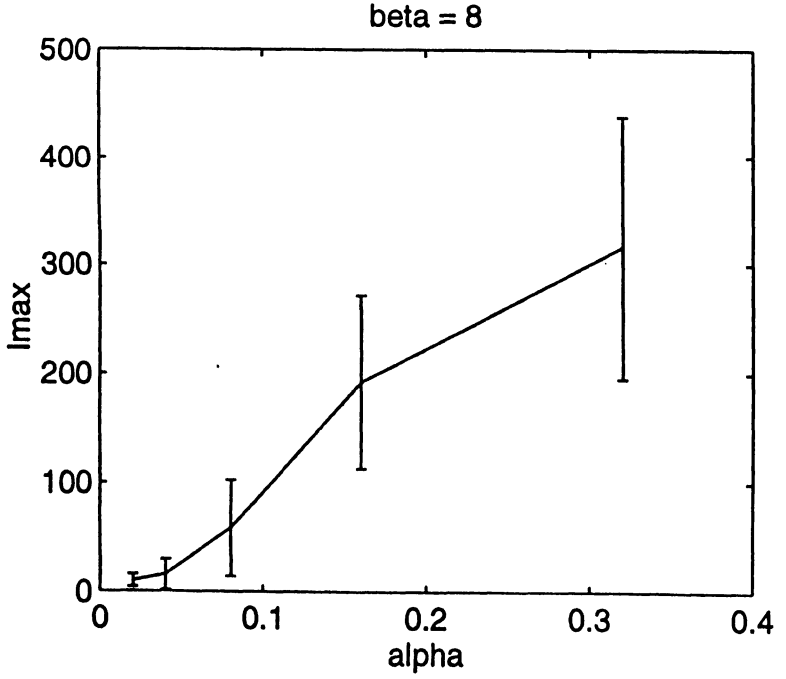
beta = 8
Imax
alpha
500
400
300
200
100
0
0
0.1
0.2
0.3
0.4

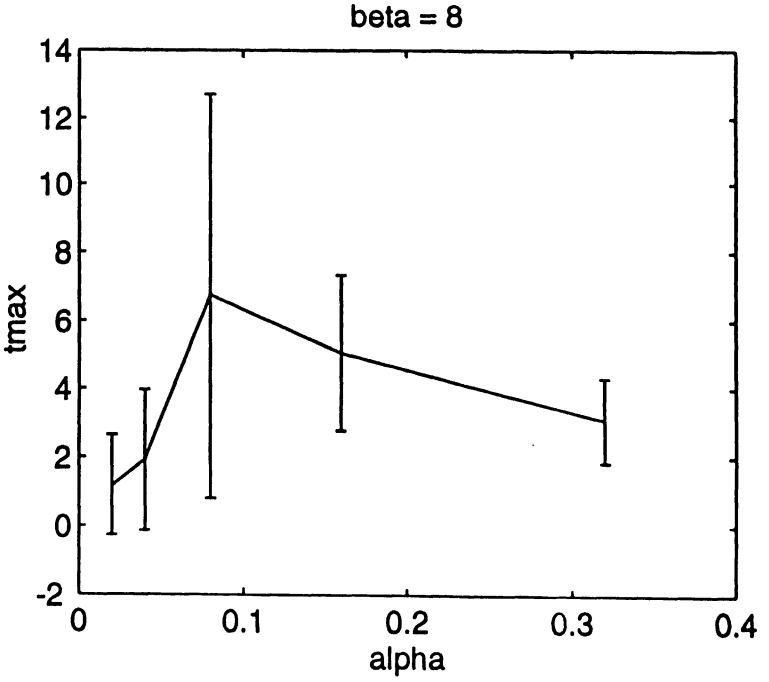
beta = 8
tmax
alpha
14
12
10
8
6
4
2
0
-2
0
0.1
0.2
0.3
0.4

Figure 5.

# HIV-1 Replication Rate

Michelle J. Arias and Delmy Iñguez
University of California, Riverside

Erika T. Camacho
Wellesley College

Rafael B. Castillo
State University of New York at Stony Brook

Eliel Melón
University of Puerto Rico, Humacao

Luz E. Parra
Northern Arizona University

Abstract

Antiviral drugs have been known to prolong the lives of HIV infected patients. However, it is still uncertain if antiviral drugs affect the rate of virion clearance, the loss of target cells, or both. In this study, we used mathematical models to measure the effects of a protease inhibitor on three infected patients. After analysis of this data, we were able to calculate the lifespans of free virions and infected cells. We found that the antiviral drug decreased not only the number of free virions in the plasma but also the loss of infected target cells. Although this antiviral drug is not a cure for this disease, it can provide insight into creating an effective treatment program for HIV patients.

BU-1367-M

# 1 Introduction

Researchers have been trying to understand why the *human immunodeficiency virus* (HIV) leads to the collapse of the immune system. One hypothesis is that HIV destroys target cells that have CD4 receptors. These target cells, or white blood cells, are crucial to the immune system. Once infected, a target cell becomes a virus-producing cell. After about seven hours, the target cell releases free virions into the plasma either by budding or erupting.

In a recent study, plasma levels of HIV-1 were shown to decrease exponentially after an antiviral drug was administered to five patients (Ho *et al.* 1996). The antiviral drug, known as Ritonavir, is a protease inhibitor that prevents the virus from producing core proteins necessary for viral infection. These core proteins include RNA, gag, and pol proteins (Schupbach 1990). Ritonavir has only been on the market since 1996. Since Ritonavir's lifespan is only 8-10 hours, HIV patients need to take the drug consistently; the recommended dosage is 600mg twice a day (Ad).

Our project initially studied the dynamics of HIV-1 replication rate using what we will refer to as the P-Model (Ho *et al.* 1996). Our main purpose was to estimate the clearance rate and the lifespan of free virions and infected $T$ cells on simulated data from three patients over a ten-day period. By analyzing the derivation of the P-Model, we were able to determine its efficiency for explaining the behavior of HIV replication. We realized that the P-Model's efficiency depends upon many unrealistic assumptions, and decided to take our research further. We came up with a model that takes into account the drug's efficiency, the fact that $T$ cells replicate, and that there is an immune response.

What we call the L-Model is

$$\begin{aligned}
& & dT/dt &= \Lambda - kVT/P - \mu T + qkVT/P & (1)\\
\text{Before treatment} & & dT^*/dt &= (1-q)kVT/P - \delta T^* & (2)\\
& & dV/dt &= N\delta T^* - cV - qNkVT/P & (3)\\
\\
& & dT/dt &= \Lambda - kV_1T/P - \mu T + qkV_1T/P & (4)\\
\text{After treatment} & & dT^*/dt &= (1-q)kV_1T/P - (r+\delta)T^* & (5)\\
& & dV_1/dt &= \phi N\delta T^* - cV_1 - q\tilde{N}kV_1T/P & (6)
\end{aligned}$$

$$dV_{NI}/dt = (1-\phi)N\delta T^* - cV_{NI}, \quad (7)$$

where the total concentration of virions in the plasma is $V(t) = V_I(t)+V_{NI}(t)$. $V_I(t)$ is the plasma concentration of virions in the infectious pool and $V_{NI}(t)$ is the concentration of virions in the noninfected pool. At the beginning of the treatment, when time is zero, $V_I(0) = V_0$ and $V_{NI}(0) = 0$.

**Variables**

$V(t)$ = the concentration of viral particles in plasma at time $t$.
$V_1(t)$ = the plasma concentrations of virions in the infectious pool. produced before the drug's application, $V_i(0) = V_0$.
$V_{NI}(t)$ = the concentration of viral particles in the noninfectious pool. produced after the drug's application, $V_{ni}(0) = 0$.
$T$ = target cells.
$T^*$ = virus-producing cells.

**Unknown**

$N$ = number of new virions produced per infected cell during its lifetime.
$\tilde{N}$ = virions killed by each $T$,

**Parameters**

$q$ = proportion of successful attacks by the $T$ cells.
$T/P$ = probability of $T$ cell infection.
$\Lambda$ = constant recruitment rate.
$\mu$ = per capita death rate.
$\phi$ = drug efficiency.
$P$ = total population of $T$ cells.
$k$ = the rate at which HIV infects target cells.
$c$ = the viral clearance rate.
$\delta$ = the loss rate of infected cells.

In this paper we find a solution in terms of $V_0$, $c$, and $\delta$ for the total concentration of virions in the plasma at time $t$. We then use this solution

and the data to estimate $c$ and $\delta$. Next, we compute the half life of free virions and interpret the average lifespan of a virion, an infected cell, and the average generation time of the virus. In the following section we estimate parameters and compare the predictions of a different model with results from the average lifespan of a virion, an infected cell, and the average generation time. We conclude with remarks on the biological implications of our results.

# 2 Interpretation of the L-Model

What we have named the L-Model is an extension of our initial project. It takes into account the $T$ cells' dynamics and the immune system's defense reaction; therefore, it includes such factors as the rate of change of $T$ cells, the recruitment rate, the mortality rate of $T$ cells, and the number of successful attacks by $T$ cells on the virions. These important elements, omitted in the P-Model, are now taken into account to provide a more accurate analysis. Like the P-Model, the L-Model contains two parts: before and after treatment. As we analyze the change of $T$ cells with respect to time, before treatment we see that there is a recruitment rate as well as a result of the interaction between the virions and the T cells. There is also a mortality rate, reducing the number of $T$ cells. Successful attacks by the immune system on the virus reduce the number of infected $T$ cells. Changes in the number of infected $T$ cells relative to time are also affected by the loss rate of infected $T$ cells. As the number of infected $T$ cells increases, so does the number of virions, but as the population of virions grows there is a portion of virions being eliminated by the clearance rate and by the immune system's successful attacks. Similarly, the "after-treatment" portion of the L-Model includes an analysis of changes in the number of $T$ cells with respect to time. This change is almost identical to the one before treatment, except that this time only the infectious virions affect the normal $T$ cells. This is because the only virions that the $T$ cells recognize are the initial ones. Likewise, the change in the number of infected $T$ cells after treatment is similar to that of before treatment except that the mortality rate of $T$ cells influences the number of infected $T$ cells. There are two types of virions, the infectious and the noninfectious. The change in the number of infectious virions relative to time is related to the drug's effectiveness since the drug is not 100% effective. The term $\phi N \delta T^*$ represents infectious virions that the $T$ cells continue to

attack after treatment. The number of noninfectious $T$ cells is related to the drug's effectiveness and the clearance rate.

In comparison to the P-Model, the L-Model is a better fit for reality because it relaxes most of the assumptions made in the P-Model. The L-Model makes only three assumptions: it assumes that the drug is administered once and that its effectiveness is a constant function of time; it also assumes low initial estimates for the number of new virions produced per infected $T$ cell during its lifetime, and for the number of virions killed by one $T$ cell.

# 3 Solving for the Concentration of Virions

By simplifying the L-Model and utilizing a few mathematical methods of approximation, we were able to find appropriate estimates for the viral clearance rate, denoted by $c$, and the loss rate of infected $T$ cells, denoted by $\delta$. In order to simplify the L-Model, we considered the situation when we have a 100% effective drug (i.e., $\phi = 0$) and when the $T$ cells are unable to attack the virus (i.e., $q = 0$). In addition, we must also make the following assumption for simplification purposes: $T$ cells are initially at a quasi-steady state. This implies that the replication rate of $T$ cells relative to time, in comparison to the replication rate of HIV-1 relative to time, is negligible (i.e., $dT/dt = 0$). Thus the number of $T$ cells is considered to be constant throughout the steady period. In dealing with such a small-time interval ($T_0$), we can also neglect the mortality rate of normally producing $T$ cells (i.e., $\mu T = 0$).

Given these assumptions, we can eliminate equations (1) and (4) from the system, as well as any component containing $\phi$ or $q$ to obtain:

$$\begin{aligned}
\text{Before treatment} \quad dT^*/dt &= kVT - \delta T^* && (8)\\
dV/dt &= N\delta T^* - cV && (9)\\
\\
dT^*/dt &= kV_I T - \delta T^* && (10)\\
\text{After treatment} \quad dV_I/dt &= -cV_I && (11)\\
dV_{NI}/dt &= N\delta T^* - cV_{NI}, && (12)
\end{aligned}$$

As a result of this elimination process, we are able to derive the P-Model from the L-Model. With this system of five nonlinear differential equations

and a few assumptions, we can derive a solution for the number of virions in the plasma at time $t$.

Several assumptions are included in this model to simplify the analysis of HIV's behavior under drug treatment. First of all, we assume that the HIV-1 virus infects a target cell at a constant rate $k$, at which time it takes on the role of a productively infected cell, $T^*$. Second, we assume the drug is 100% effective and that the number of target cells remains constant. Furthermore, we assume infected cells do not recover during the treatment period, to reduce the complications on the estimation of $c$ and $d$. We also assume that the system describing the dynamics of HIV-1's reproduction rate is at a quasi-steady state, that is, that $dT^*/dt = 0$ and $dV/dt = 0$ before the drug treatment. This assumption may be reasonable if the uninfected cell concentration stays at its steady state level for approximately a week after the administration of Ritonavir. Given these assumptions, the model becomes simple enough that an interpretation of the dynamics of the virus is possible (a caricature).

Using the P-Model, we were able to derive a mathematical expression for the total concentration of virions at time $t$ that depends only on the initial number of virions, $V_0$, the rate of virion clearance, $c$, and the loss rate of infected cells $\delta$. To analyze the replication rate of HIV-1 under drug treatment, we assume that (at the moment we start the treatment) the replication rate of infected $T$ cells and of virions is zero. Thus $dT/dt = 0$ and $dV/dt = 0$. We also assume that the level, $T_0$, remains constant for the first week after the drug is administered. In other words, we assume that $T$ remains at a steady state for one week after the drug is administered.

Then we obtain the number of infectious virions $V(t)$ by using separation of variables to integrate equation (11):

$$\begin{aligned}
\int_{V_0}^{V_I(t)} \frac{dV_I}{V_I} &= \int_0^t -c\,dt \\
\ln|V_I|\Big|_{V_0}^{V_I(t)} &= -ct\Big|_0^t \\
\Rightarrow \quad \ln|V_I(t)| - \ln|V_0| &= -ct \\
\ln\left|\frac{V_I(t)}{V_0}\right| &= -ct \qquad (13) \\
e^{\ln\left|\frac{V_I(t)}{V_0}\right|} &= e^{ct}
\end{aligned}$$

$$\begin{aligned}\left|\frac{V_I(t)}{V_0}\right| &= e^{ct} \\ V_I(t) &= V_0 e^{-ct}.\end{aligned}$$

Next, in order to find the number of noninfectious virions in the plasma, we solve equations (10) and (12). First we solve for $T^*$ after we substitute our last result for $V_I(t)$ into equation (10)

$$\frac{dT^*}{dt} = kV_0 e^{-ct} T - \delta T,$$

and since $T$ is constant then

$$\frac{dT^*}{dt} = kV_0 e^{-ct} T_0 - \delta T^*.$$

Using the integrating factor technique yields

$$e^{\delta t}\frac{dT^*}{dt} + \delta e^{\delta t} T^* = kV_0 e^{\delta - ct} T_0.$$

This expression can be written

$$\Rightarrow \quad \frac{d}{dt}(T^* e^{\delta t}) = kV_0 T_0 e^{\delta - ct}.$$

Changing the variable of integration we get

$$\begin{aligned}\int_0^t \frac{d}{ds}(T^* e^{\delta t})ds &= \int_0^t kV_0 T_0 e^{(\delta - c)s} ds \\ T^*(t)e^{\delta t} - T^*(0) &= \frac{kV_0 T_0}{\delta - c}\left(e^{t(\delta - c)} - 1\right) \\ T^*(t)e^{\delta t} &= \frac{kV_0 T_0}{\delta - c}\left(e^{t(\delta - c)} - 1\right) + T^*(0) \\ T^*(t) &= \left[\frac{kV_0 T_0}{\delta - c}\left(e^{t(\delta - c)} - 1\right) + T_0^*\right] e^{-\delta t} \qquad (14) \\ T^*(t) &= \left[\frac{kV_0 T_0\left(e^{t(\delta - c)} - 1\right) + (\delta - c)T_0^*}{\delta - c}\right] e^{\delta t},\end{aligned}$$

where $T_0^*$ is the initial value of $T^*(t)$.

Assuming that we are in a quasi steady-state so that $dT^*/dt = 0$, it follows from equation (8) that if $T_0^*$, $V_0$, and $T_0$ are the initial conditions of $T^*$, $V$, and $T$, respectively, then $kdV_0T_0 = \delta T_0^*$. Making this substitution, equation (14) becomes

$$\begin{aligned} T^*(t) &= \left[\frac{[T_0^*\delta\left(e^{t(\delta-c)}-1\right)+(\delta-c)T_0^*)}{\delta-c}\right]e^{-\delta t}, \qquad (15)\\ &= \frac{T_0^*\delta e^{-ct}-T_0^*ce^{-\delta t}}{\delta-c}\\ &= \frac{T_0^*}{\delta-c}\left(\delta e^{-ct}-ce^{-\delta t}\right). \end{aligned}$$

Next we substitute this expression for $T^*(t)$ into equation (12) and solve for $V_{NI}(t)$, obtaining the number of noninfectious virions in the plasma:

$$\begin{aligned} \frac{dV_{NI}}{dt} &= N\delta\left(\frac{T_0^*}{\delta-c}(\delta e^{-\delta t}-ce^{-\delta t})\right)-cV_{NI}\\ &= \frac{N\delta T_0^*}{\delta-c}(\delta e^{-ct})-\frac{N\delta T_0^*}{\delta-c}(ce^{-\delta t})-cV_{NI}\\ \frac{dV_{NI}}{dt}+cV_{NI} &= \frac{N\delta T_0^*}{\delta-c}(\delta e^{-ct})-\frac{N\delta T_0^*}{\delta-c}(ce^{-\delta t}). \end{aligned}$$

Using the integrating factor technique yields

$$\begin{aligned} e^{ct}\frac{dV_{NI}}{dt}+ce^{ct}V_{NI} &= \frac{N\delta^2T_0^*}{\delta-c}-\frac{N\delta^2T_0^*}{\delta-c}ce^{ct}e^{-\delta t}\\ \int_0^t\frac{d}{ds}(e^{cs}V_{NI}) &= \int_0^t\frac{N\delta^2T_0^*}{\delta-c}ds-\int_0^t\frac{N\delta T_0^*}{\delta-c}ce^{(c-\delta)t}ds \qquad (16) \end{aligned}$$

$V_{NI}e^{ct} = \frac{N\delta^2T_0^*t}{\delta-c}\left(\frac{1}{c-\delta}\right)e^{(c-\delta)t}$,since $V_{NI}(0)=0$.

Now equation (9) and $dV/dt = 0$ implies $N\delta T_0^* = cV_0$, and with this substitution equation (16) can be rewritten as

$$\Rightarrow \quad V_{NI}(t) = \frac{N\delta T_0^*}{\delta-c}\left(\delta te^{-ct}-\frac{ce^{-\delta t}}{\delta-c}+\frac{ce^{-ct}}{c-\delta}\right)$$

$$= \frac{N\delta T_0^*}{\delta - c}\left(\delta t e^{-ct} - \frac{c}{\delta - c}\left(e^{-\delta t}e^{-ct}\right)\right) \qquad (17)$$

$$= \frac{N\delta T_0^*}{c - \delta}\left(\frac{c}{\delta - c}(e^{-\delta t} - e^{-ct}\right) - \delta t e^{ct}$$

$$V_{NI}(t) = \frac{cV_0}{c - \delta}\left(\frac{c}{c - \delta}(e^{-\delta t} - e^{-ct}\right) - \delta t e^{-ct}.$$

Hence, using equations (13) and (17) the total number of virions in the plasma at time $t$

$$V(t) = V_I(t) + V_{NI}(t)$$

can be expressed as

$$V(t) = V_0 e^{-ct} + \frac{cV_0}{c - \delta}\left(\frac{c}{c - \delta}(e^{-ct} - \delta t e^{-ct}\right).$$

Given this solution, we can obtain appropriate values for the parameters for $c$ and $\delta$ using various mathematical techniques. This work is described below.

# 4 Estimation of $c$ and $\delta$

We estimated the clearance rate of virions and the loss rate of infected cells by using the *Mathematica*'s packages NonlinearFit, Statistica Nonlinear Regression Analysis, Least Squares Method, and Find Minimum Program.

The *Mathematica* NonlinearFit Package applies internally to Quasi Newton's Method, which gives the best approximations for the parameters of nonlinear multivariable equations. Here we entered the data of virions produced for all three patients. For each patient, we found estimates for $V_0$, $c$, and $\delta$, using the solution of $V(t)$ and giving initial estimates to these parameters. We then computed the average estimates for $V_0$, $c$, and $\delta$. These approximations enabled us to graph the P-Model by plotting the average predicted values. Finally, we used Mathematica to compute the relative error of the P-Model with respect to the data observed, applying the relative error formula to the data of each patient. Thus, we obtained converging values for every parameter with a minimum error. Similarly, the Statistica Nonlinear Regression analysis package provided these minimum estimates, but for a more complicated case. The Regression Analysis Package, unlike the

NonlinearFit, applied the Quasi Newton's Method to the observed data for all patients simultaneously. As a result, it yielded the average estimates of the parameters. The FindMinimum program, unlike the two aforementioned methods, takes much longer and incorporates more steps to compute the best parameter approximations.

# 5 Graphical Analysis of the Latino and Perelsom Models

The decline that occurs in the number of virions in the plasma after the drug is administered to the three patients can be interpreted graphically. By graphing the solution to the P-Model $V(t)$ and using the obtained average parameter values of $c$, $\delta$, and the initial number of virions, $V_0$, we observe an exponential decay in the number of virons as time progresses (see Figure 1).

Initially we see a delay in the decline of virions, followed by a rapid, then a slower, decline. The delay that occurs in the first few hours is due to the amount of time needed for the drug's absorption, distribution, and penetration. The slow rate of decay in the number of virions during the last hours of the treatment period results from the dissipation of the drug's concentration.

By comparing the predicted data with the observed data we can conclude that the P-Model, under the assumptions made, accurately describes the replication dynamics of HIV-1. This model provides a well-fitting curve for the observed data of each of the patients (Figures 2a-2c). The deviation from the curve to the observed data is almost insignificant, yet as we approach the end of the 10-day trial period this deviation increases. The efficiency of this model for all three cases under study is reflected in the relative error rate of each patient. As time goes by, the relative error for each patient increases (Table 1).

We used *Matlab* to simulate our model. We created a program to find the best number of parameters for $k$, $\phi$, and $q$, then we graphed the functions of $V_I$, $T$, $T^*$, and $V_{NI}$ to see the behavior of the graphs. Finally, we analyzed the graphs to see if these behaviors are consistent with biological behavior.

# 6 Comparison of the P-Model to the Wei *et al.* Model

$$V(t;c,\delta) = [V_0/(c-\delta)]\left(ce^{-\delta t} - \delta e^{-ct}\right) \qquad (18)$$

This model was introduced by Wei *et al.* (1995) and its symmetrical formulation does not allow us to distinguish between the viral clearance rate and the loss rate of infected $T$ cells. In addition to this ambiguity involved in finding parametric values for $c$ and $\delta$, we find that the nonlinear regression analysis utilized in finding estimates for $c$ and $d$ in the P-Model is not suitable for this model. Consequently, use of this data-fitting procedure in the Wei *et al.* (1995) model only establishes the fact that it is sensitive to the initial conditions chosen; that is, a slight alteration of the initial conditions for $c$ and $\delta$ yields entirely different results for their minimum values as processed by the NonlinearFit package.

In order to demonstrate the limitations of equation (18) for distinguishing the parameters $c$ and $\delta$, we observe that $V(t;c,\delta) = V(t;\delta,c)$. Therefore, if we tried to compute values for $c$ and $\delta$ we would not be able to distinguish between them.

# 7 Analysis of the Drug's Effectiveness ($\phi$) According to the L-Model

When the drug is 100% effective $\phi = 0$, and when the drug is completely ineffective $\phi = 1$. Therefore, as $\phi$ approaches 1 (i.e., as the drug loses its efficiency), the number of noninfectious virions approaches zero. This implies that at $\phi = 1$ the drug's effectiveness has ceased, thereby causing the patients to revert to their condition before treatment.

The drug's effectiveness eventually diminishes (i.e., $\phi \rightarrow 1$). With time the virus builds resistance and the drug's concentration in the blood stream vanishes. In order for the patients not to return to their condition before treatment, we must administer the drug periodically. Since the drug's effectiveness changes periodically with time, it must contain a periodic component accounting for the resistance it encounters, $\phi$.

After administering a protease inhibitor drug Ritonavir in two different strengths, the percentages of infectious virions ($V_1$), noninfectious virions ($V_{NI}$), $T$ cells ($T$), and infectious viron-producing $T$-cells ($T^*$) change. This variation is directly affected by the strength of the drug. Histograms allow us to approximate the percentages of virions and cells, and also explain Graph 1.

Analyzing the number of virions before treatment (Histogram 1), we observe that all of the virions produced before the drug's administration are infectious ($V_1$). In analyzing the number of infected and noninfected $T$ cells before the drug, we assume that 100% of the cells before treatment are producing only infectious virions. After the drug is administered, we divide our observations into two categories: the first one is when we have a drug that is 99% effective, and the second one is when the drug is 10% effective. When we use a 99% effective drug, we observe the percentage of healthy $T$-cells is greater. This is because the drug is stopping the production of infectious virions; therefore, there are not enough virions to infect $T$-cells.

In Histogram 2a, we use an extremely efficient drug (99% effective). A drug this efficient will transform cells from infectious virion-producing ($T^*$) to noninfectious viron-producing cells ($T$). The greater number of $T$ will show a large population of $V_{NI}$. On the other hand, in Histogram 2b, when the drug is only 10% effective, the percentage of infected virions will be higher than the noninfected ones (mainly because of the drug's inefficency in protecting cells from becoming $T^*$). By using a less effective drug, we have a tremendous production of infectious virions ($V_i$); these virions will infect a greater number of $T$-cells, consequenly converting them into infectious $T$-cells ($T^*$) at a fast rate.

**Results**

Figure 1 measures the predicted values for the number of free virions in the plasma over a 10-day period. If we use the P-Model, we expect to see an initial delay followed by a rapid then a slow decrease in the number of free virions. This initial delay is less than a day. The number of virions decreases to zero at the end of 10 days.

In Figures 2a-2c, the observed and predicted values are plotted for the three patients. The number of free virions does decrease over time. These results are consistent with our predicted values (refer to Figure 1 for the predicted values).

Figure 3 measures the predicted number of infected virions when the drug's efficiency is 10%, 50%, and 99%. The dashed curve represents the drug's efficiency when it is 99%, the middle curve when it is 50%, and the top curve when it is 10%. Q represents the number of successful attacks by $T$ cells when the $T$ cell count is 1%. When the drug's efficiency is 99%, the number of infected virions approaches zero after two days. The number of infected virions is significantly higher when the drug's efficiency is 10

Figure 4 measures the predicted number of noninfectious virions for drug efficiencies of 10%, 50%, and 99%. When the drug is 99% effective, the number of noninfectious virions reaches a peak of 15 virions 1.5 days after treatment. Then there is a slow decline in the number of noninfectious virions over the 10-day period. The peak only reaches eight noninfectious virions for a drug efficiency of 50%, and two noninfectious virions for a drug efficiency of 10%.

Figure 5 measures the predicted number of $T$ cells using the same drug. When the drug's efficiency is 99%, the $T$ cell count remains constant at a value of $1.3295 \times 10^4$ cells.

Figure 6 measures the predicted number of infected $T$ cells. When the drug is 99% efficient, the number of infected $T$ cells approaches zero. This occurs six days after drug treatment. When the drug is 50% effective, there is a gradual decrease in the number of infected $T$ cells. However, there are still 10 infected $T$ cells remaining after 10 days of drug treatment. The number of infected $T$ cells increases when the drug is 10% effective.

# 8 Conclusion

We look upon the work done here as only the beginning of an on-going learning process. Thus our work is not entirely conclusive. With this in mind, we offer to those individuals interested in expanding on our work some suggestions for improving the accuracy of our model. First, it is important to consider the long-term effects and treatment process for the antiviral drug. A long-term model would focus on the dynamics of HIV and include HIV's density, mutation rate, and drug resistance. Since HIV becomes resistant to Ritonavir, it is important to continue applying the drug. Reapplication can be modeled as a periodic funtion of time for the drug's effectiveness.

Graphically, we would expect to get a cyclic function which repeats itself every time the drug is applied. Over time, the total number of virions and infected $T$ cells declines, but as soon as HIV builds resistance, the number of virions will increase dramatically. Therefore, if we consider a long-term effect we will expect a cyclic funtion which initially decreases then increases rapidly.

To bring this model closer to reality, it is also essential to increase the sample size. Another suggestion for further research would be to administer more than one drug during the period of study. Although the list of ideas for further study is not exhaustive, we leave the generation of more interesting additions to our list up to the curious scientist in all of us.

**Acknowledgements**

The research in this manuscript has been partially supported by grants given by the National Science Foundation (NSF Grant DMS-9600027), the National Security Agency (NSA Grant MDA 904-96-1-0032) and Presidential Faculty Fellowship Award (NSF Grant DEB 925370) to Carlos Castillo-Chavez. Substantial financial and moral support was also provided by the Office of the Provost of Cornell University and by Cornell's College of Agricultural & Life Sciences (CALS) and the Biometrics Unit. The authors are solely responsible for the views and opinions expressed in this report. The research in this report does not necessarily reflect the views and/or opinions of the funding agenices and/or Cornell University.

**References**

Ad for Ritonavir in *The AIDS Magazine*, June 1996.

Altman, L.K., "A New AIDS Drug Yielding Optimism as Well as Caution," *The New York Times*, February 2, 1996.

HIV/AIDS Treatment Information Service, **Glossary of HIV/AIDS-Related Terms**, 1995.

Ho, D.D., Leonard, J.M., Markowitz, M., Neumann, A.U., and Perelson, A.S., *HIV-1 Dynamics In Vivo: Virion Clearance Rate, Infected Cell Lifespan and Viral Generation Time*, Santa Fe Institute, 1996.

Kalichman, S.C., "The HIV-AIDS Pandemic", Understanding AIDS, 12-18, 1995.

Schuphach, J., "Retroviral Replication Cycle", Classification, Structure, and Biology of Retroviruses, 5-11, 1990.

Wei, X. *et al.*, *Nature* **373**, p. 117, 1995.

# Figure 1

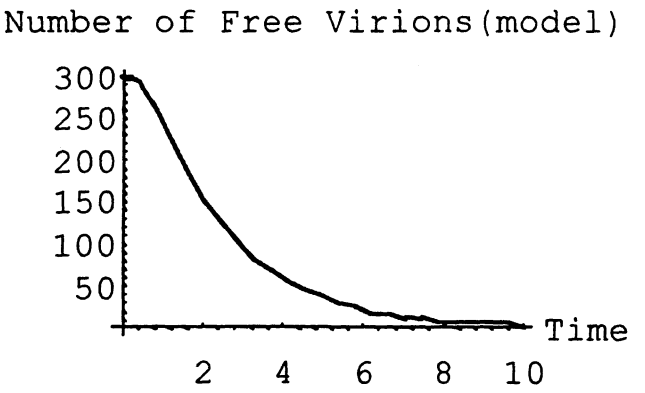
Number of Free Virions(model)
300
250
200
150
100
50
Time
2
4
6
8
10

# Figures 2a - 2c

***Number of free virions as a function of time for each of the three patients.***

**Figure 2a:**

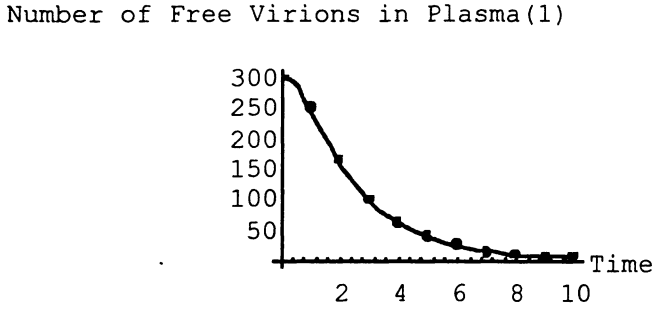


**Figure 2b**

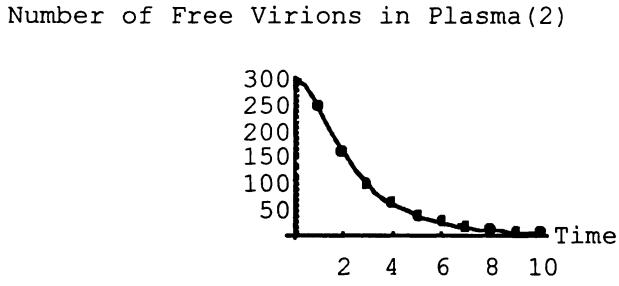


**Figure 2c:**

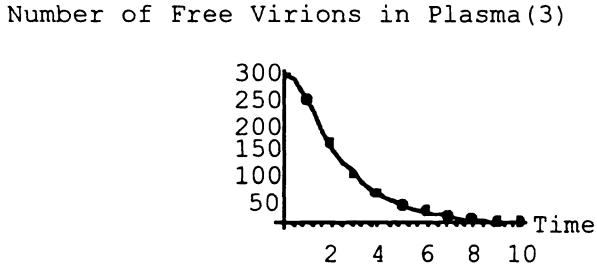

# Histograms

***Effect of the drug on Virions and on T-cells.***

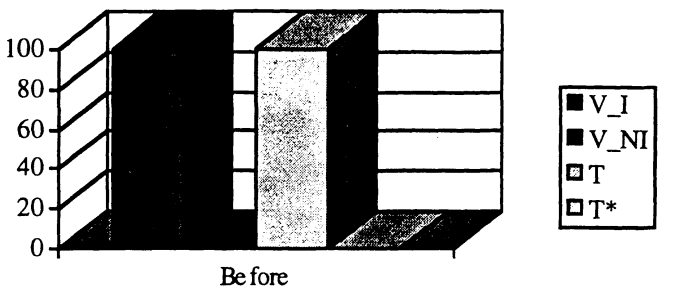


**Histogram 1**

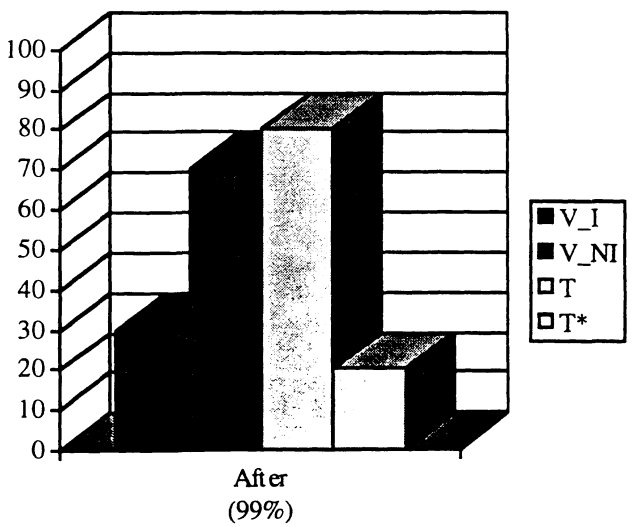


**Histogram 2a**

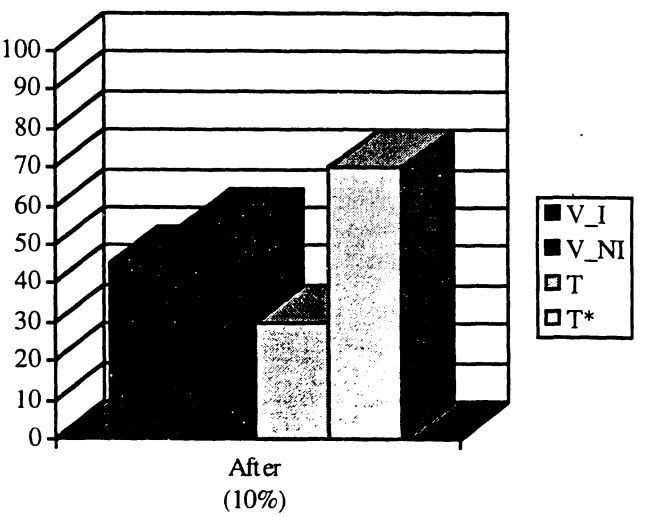


**Histogram 2b**

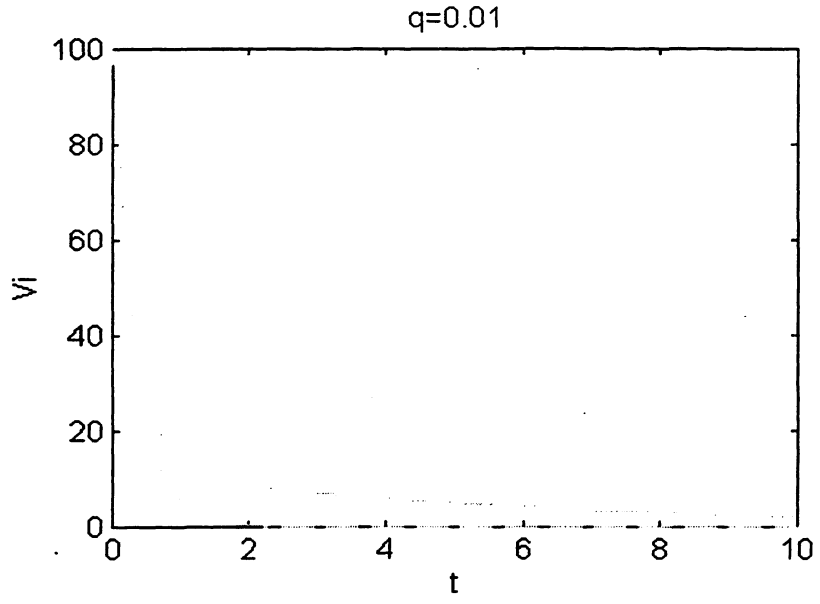


**Figure 3**

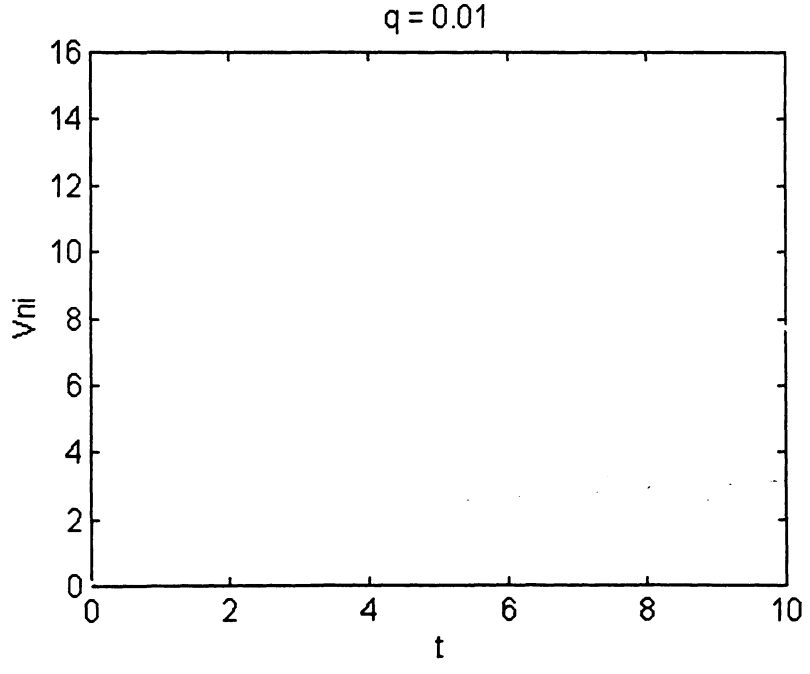


**Figure 4**

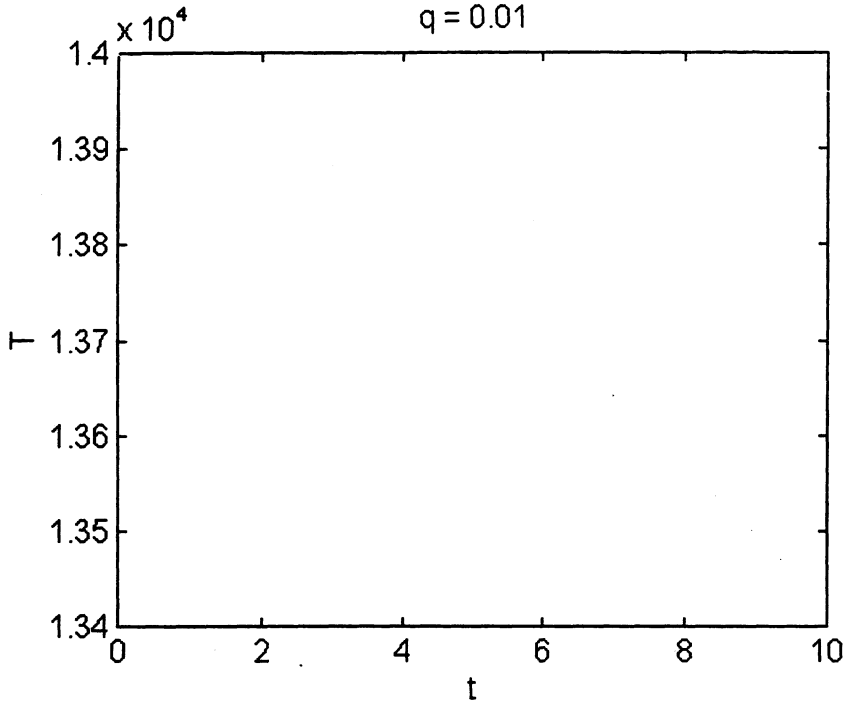


**Figure 5**

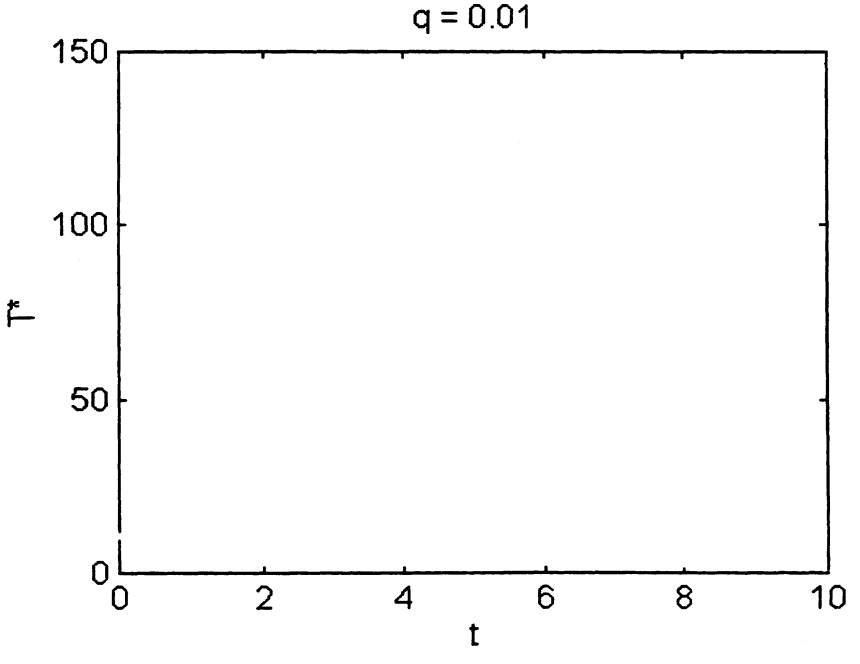


**Figure 6**

# The Effects of Vaccination in a Core Group

by

Marina Bobadilla
University of California
Santa Cruz, CA 95064

Sharon Ann Lozano
The University of Texas
Austin, TX 78705

Jessica Mendes Maia
Massachusetts Institute of Technology
Cambridge, MA 02139

Julio Cesar Villarreal
University of San Diego
San Diego, CA 92101

Novaline Dawn Wilson
University of New Mexico
Albuquerque, NM 87131

Roberta Winston
New Mexico State University
Las Cruces, NM 88003

## Abstract

This study examines a mathematical model in which a vaccine without complete effectiveness is applied to a core group. The prevalence of the disease within the core group determines the recruitment rate into the core group. The recruitment function in this model is set up for the case dependent on the proportion of infectious individuals. In particular, we study the possible oscillations of the disease over time caused by the vaccination rate and vaccine efficiency.

BU-1368-M

## Introduction

Induced immunity against infectious diseases has been a primary concern for centuries, from the inoculation of individuals in the Ming dynasty to Edward Jenner's small pox vaccination. In the late 1700's, during the widespread European epidemic of small pox, Jenner observed milkmaids' immunity to small pox. Further investigation revealed that the microbe species infecting cows with cow pox was closely related to small pox. Vaccination originated when Jenner inoculated susceptible individuals, persons capable of becoming infected, to induce small pox immunity with material taken from a pustular cow pox lesion. In 1760, Daniel Bernoulli introduced the first mathematical model to study the spread of infectious diseases and the benefits of vaccination.

A vaccine provides either permanent or temporary immunity. Successful implementation of a vaccination strategy will ultimately result in disease eradication. However, a vaccine can adopt any of the following properties: permanent immunity and complete effectiveness, temporary immunity and complete effectiveness; permanent immunity and partial effectiveness or temporary immunity and partial effectiveness.

Social relevance of vaccination models is significant. Vaccination models are used by health care officials to combat an infectious disease epidemic. Viruses do not recognize geographical or political borders. As a result, most successful disease eradication programs require cooperation of international, governmental, and local officials. Vaccination models are applied to improve the management of financial and human resources; vaccinating the core group requires less financial effort than vaccinating an entire population.

Our research examines the effects of a vaccination in a core group model. A core group is a subgroup of the population whose members are more prone to becoming infected and transmitting the disease. The concept of core group was first introduced by Hethcote and Yorke (1984), who studied effective treatment methods for gonorrhea in a prostitute core group. The results enabled limited financial resources to be used efficiently to control the epidemic.

Our research will incorporate vaccination into a similar model studied by Velasco-Hernandez, Brauer, and Castillo-Chavez (1996), in order to explore the behavior of a disease as the vaccination rate and the vaccine inefficiency

vary. This study is organized as follows: Section A defines and describes the equations used in this model; Section B describes computation and analysis of the basic reproductive number and the disease-free equilibrium; Section C proves the numerical existence of an endemic equilibrium; Section D includes graphical interpretations of the model; Section E considers death induced by disease; Section F concludes the paper and presents limitations to the model.

Section A: The Model

Let $S$, $I$ and $V$ represent the population size of susceptible, infected and vaccinated individuals respectively in the core group. The model equation is as follows:

$$\begin{aligned} \frac{dS}{dt} &= \Lambda e^{-(I/N)} - \mu S - \phi S - \beta S\frac{I}{N} \\ \frac{dI}{dt} &= \beta S\frac{I}{N} - \mu I + \sigma\beta V\frac{I}{N} \qquad (*) \\ \frac{dV}{dt} &= \phi S - \mu V - \sigma\beta\frac{I}{N}. \end{aligned}$$

Let the population of the core group be denoted by $N$, where $N = S + I + V$. The susceptible individuals become infected through contact with infected individuals at a rate $\beta$. Susceptible individuals are vaccinated at a rate $\phi$ individuals per unit time. Although the vaccination is permanent, it is not completely effective. As a result, there exists a group of vaccinated susceptibles. Vaccine inefficiency is measured by $\sigma$, where $0 < \sigma < 1$. If $\sigma = 0$ the vaccine is one hundred percent effective and if $\sigma = 1$, the vaccine is completely ineffective. The natural mortality rate is represented by $\mu$. $\Lambda$ is the recruitment rate of susceptible individuals into the core group from the general population. The fear or information factor affecting the recruitment of the non-core group into the core group is defined as $\alpha$.

The following compartmental diagram schematically illustrates the model.

$$S \rightarrow I \rightarrow V$$

The rate of change of the population of susceptible individuals is determined by the product of the constant recruitment rate ($\Lambda$) and the prevalence-dependent factor ($e^{-aI/N}$) less the sum of the natural mortality of susceptibles, the number of vaccinated susceptibles, and the number of susceptibles

becoming infected. The rate of change of the population of infected individuals consists of the sum of susceptibles becoming infected and the number of vaccinated individuals who became infected less the natural mortality of the infected individuals. The rate of change of the population of vaccinated individuals consists of vaccinated susceptibles less the individuals who die naturally and those who become infected. The inefficiency of a vaccine directly contributes to the sum of infected individuals, because the ineffective vaccine causes the susceptible individual to become infected through contact with infectious individuals.

In order to simplify the model several assumptions were made:

- Infectious individuals die at the same rate as susceptible and vaccinated individuals.
- Disease induced death was not taken into consideration.
- The number of infected individuals outside the core-group is negligible; there is no chance that an infected individual will join the core group.

Section B: Reproductive Number

The analysis of the model begins with the computation of the basic reproductive number $R_3$. The basic reproductive number expresses the average number of individuals that an infectious person infects when he/she is introduced into a population that is previously uninfected. Since $R_0$ assumes an initially uninfected population, we begin by computing the disease-free equilibrium $(S_0, I_0, V_0)$. Since $R$ assumes an initially uninfected population, we begin by computing the disease-free equilibrium, $(S_0, I_0, V_0)^{\mathrm{T}}$.

$$F(S,I,V) = \begin{pmatrix} \frac{\Lambda e^{-\beta SI/N}}{\mu+\phi} \\ \frac{\beta SI+\sigma\beta VI/N}{\mu} \\ \frac{\phi-\sigma\beta VI/N}{\mu} \end{pmatrix}.$$

Since $(S_0, I_0, V_0)^{\mathrm{T}}$ is the fixed point of $F$ for which $I_0 = 0$, it follows that

$$(S_0, I_0, V_0) = \begin{pmatrix} \frac{\Lambda}{\mu+\phi} \\ 0 \\ \frac{\phi\Lambda}{\mu(\mu+\phi)} \end{pmatrix} = \begin{pmatrix} \frac{\mu}{\mu+\phi}N \\ 0 \\ \frac{\phi}{\mu+\phi}N \end{pmatrix},$$

where $N = \frac{\Lambda}{\mu}(= S_0 + I_0 + V_0)$.

The dominant eigenvalue of the Jacobian matrix of $F$, $J$, evaluated at the disease-free equilibrium reveals the basic reproductive number.

$$J(S_0, I_0, V_0) = \begin{bmatrix} 0 & \frac{-\mu(\beta+\alpha\mu+\alpha\phi)}{(\mu+\phi)^2} & 0 \\ 0 & \frac{\beta(\mu+\sigma\phi)}{\mu(\mu+\phi)} & 0 \\ 0 & \frac{-\beta\phi\sigma}{\mu(\mu+\phi)} & 0 \end{bmatrix}.$$

The resulting dominant eigenvalue, which is also the basic reproductive number, $R$, is $\beta/\mu \quad (\mu + \sigma\phi)/(\mu + \phi)$. Since vaccination is considered in this model, $R$ is taken as a function of $\phi$, the vaccination rate, and $\sigma$, the inefficiency of the vaccination such that:

$$R(\phi, \sigma) = \left(\frac{\beta(\mu + \sigma\phi)}{\mu(\mu + \phi)}\right).$$

If $R(\phi, \sigma) < 1$ then the disease-free equilibrium, $(S_0, I_)), V_0)^{\mathrm{T}}$, is asymptotically stable. Considering $R(phi, \sigma)$ when there is no vaccination (i.e., $\phi = 0$) it is found:

$$R(0, \sigma) = \beta/\mu = R_0.$$

Consideration of a completely ineffective vaccination, $(\sigma = 1)$, results in:

$$R(\phi, 1) = \beta/\mu = R_0.$$

$R_0 = \beta/\mu$ is the basic reproductive number of the model without vaccination. Notice that if $\beta < \mu$, the disease dies out naturally and no vaccination is necessary.

Considering that

- $1/\mu$ is the mean duration of infectiousness,
- $1/\phi$ is the mean duration of susceptibility,
- $1/(\mu + \phi)$ is the average life of a susceptible, and
- $1/(\mu + \sigma\phi)$ is the average life of a vaccinated,

$R$ can be rewritten as

$$R(\phi,\sigma) = R_0 \cdot \frac{1/(\mu+\phi)}{1/(\mu+\sigma\phi)} = R_0 \cdot \frac{\text{average life as susceptible}}{\text{average life as vaccinated}}.$$

When $\sigma > 1$, the vaccine increases the chance of a susceptible becoming infected; consequently, $R)\phi,\sigma)$ increases. In contrast, when $\sigma < 1$, the vaccine decreases the chance of a susceptible becoming infected, and $R(\phi,\sigma)$ decreases. Infection caused by vaccination is not biologically feasible and is not considered relevant, thus we take $\sigma < 1$.

Section C: Endemic Equilbrium

In the previous section, the disease-free equilibrium was explicitly calculated. Finding the exact expression of a single endemic point is difficult so that only its existence will be discussed.

The endemic points $(S,I,V)^{\mathrm{T}}$ of the system are the fixed points of $F$ for which $I > 0$. Setting $\Lambda = I/N$, the equations $F\left((S,I,T)^{\mathrm{T}}\right) = 0$ can be written as:

$$\begin{aligned} S &= \frac{\Lambda e^{-\alpha\Gamma}}{\mu+\phi} - \frac{\beta S\Gamma}{\mu+\phi} \\ I &= \frac{\beta}{\mu}(S+\sigma V)\Gamma \qquad (*) \\ V &= \frac{\phi}{\mu}S - \frac{\sigma\beta V\Gamma}{\mu}. \end{aligned}$$

The next steps involve some manipulating of the equations in order to reach a single equation representing the entire system.

$$I + V = \frac{S(\beta\Gamma+\phi)}{\mu} = N - S$$

so

$$N = \left[1 + \frac{beta\Gamma - \phi}{\mu}\right] S$$

thus

$$S/N = \frac{\mu}{\mu+\phi+\beta\Gamma}.$$

From (*),

$$\begin{aligned} V/N &= \frac{\phi}{\mu}\frac{S}{N} - \sigma\Gamma\frac{\beta}{\mu}\frac{V}{N} \\ V/N &= \frac{S}{N}\left(\frac{\phi}{\mu+\sigma\beta\Gamma}\right). \end{aligned}$$

Since $N = S + I + V$, it follows that

$$\begin{aligned} \Lambda &= \frac{I}{N} = 1 - \left(\frac{S}{N} + \frac{V}{N}\right) \\ &= 1 - \frac{S}{N}\left(1 + \frac{\phi}{\mu+\sigma\beta\Gamma}\right) \\ &= \left(\frac{\mu}{\mu+\phi+\beta\Gamma}\right)\left(1 + \frac{\phi}{\mu+\sigma\beta\Gamma}\right) \\ &= \frac{(\phi\sigma\beta + \beta\mu + \beta^2\sigma\Gamma)\Gamma}{(\mu+\phi+\beta\Gamma)(\mu+\sigma+\beta\Gamma)}. \end{aligned}$$

For $\Gamma \neq 0$ (in particular we are interested in $\Gamma > 0$) this equation reduces to:

$$\Gamma^2 + a\Gamma + b = 0,$$

where

$$a = \frac{\sigma(\mu+\phi) + \mu - \beta\sigma}{\beta\sigma}$$

and

$$b = \frac{\mu(\mu+\phi) - \beta(\mu+\sigma\phi)}{\beta^2\sigma}.$$

When solving roots of $\Gamma$, the quadratic equation results in:

$$\Gamma = \frac{-a \pm \sqrt{(a2 - 4b)}}{2}.$$

Hence, to have $\Gamma > 0$, $b < 0$ is necessary:

$$\begin{aligned} b &< 0 \\ \frac{\mu(\mu+\phi)}{\beta^2\sigma} &< \frac{\beta(\mu+\sigma\phi)}{\beta^2\sigma} \\ 1 &< \frac{\beta}{\mu}\frac{\mu+\sigma\phi)}{(\mu+\phi)}. \end{aligned}$$

However, $R(\phi, \sigma) = \frac{\beta}{\mu}\frac{(\mu+\sigma\phi)}{(\mu+\phi)}$; therefore, it can be concluded that an endemic point exists if:

$$R(\phi, \sigma) > 1.$$

By introducing a vaccine into a core group, it is expected that the disease and the core population will coexist (note that this implies that stability of the endemic equilibria is expected). This coexistence will take place in either of two forms: one possibility is that the core population will reach a stable equilibrium, meaning that the population will reach a fixed proportion of susceptible, infected and vaccinated individuals; the second possibility is that the population of susceptibles, infected and vaccinated individuals will fluctuate. There will be a bound on how large and how small the population can reach. This fluctuation is what is the reoccurrence of epidemics. The introduction of the vaccine should attempt to stabilize the population, or if that is not possible, limit the fluctuation to a small range. It is crucial to note that the number of infectious, susceptible and vaccinated individuals is never zero.

Section D: Graphical Analysis

**Case 1**:

Figure 1 depicts a vaccination rate of 0.70 with a vaccine ineffectiveness of 0.05. The vaccinated population increases rapidly, implying that the recruitment rate and the susceptible population increase while the infected population decreases. A portion of the susceptible and the vaccinated populations becomes infected because the vaccine is not completely effective.

In this graph, the vaccinated population is larger than the susceptible population which in turn is larger than the infected population. Therefore, the infection within the core group is not eradicated, but contained by the vaccine.

Figure 2 graphically represents a vaccination rate of 0.70 and a vaccine inefficiency of 0.30. After the initial increase of the vaccinated population and the susceptible population, the infected population begins to increase. The spread of the infection slows the recruitment into the core group such that less people are susceptible and less people are vaccinated. At the minima of the vaccinated population, the infected population is the largest population.

This is due to the large vaccine inefficiency in combination with a large vaccination rate.

Figure 3 shows the effect of a high vaccination rate, 0.70, with a high vaccine inefficiency, 0.30, and a relatively low fear factor, 3. Initially, the populations of the vaccinated and the susceptible individuals increase. The population of infected individuals increases due to the high inefficiency of the vaccine. We note the recruitment rate will approach a constant value since $\alpha$, the fear factor, is relatively small. The vaccinated population remains greater than the infected population and the susceptible population.

**Case 2**:

Figure 4 above displays a vaccination rate $\phi$ of 0.137, a vaccine inefficiency $\sigma$ of 0.05, and a relatively high fear factor $\alpha$ of 6. As recruitment rate decreases, all populations decrease to constant values. The infected population is the largest of the three populations, because the vaccination rate is relatively low. The limit on the spread of infection is not affected by the vaccination of the susceptibles in the core group, and reflects an indirect quarantine.

Figure 5 above graphically represents a fear factor of 6, a vaccination rate of 0.137, and a vaccine inefficiency of 0.30. In this graph the populations of the infected, susceptible, and vaccinated approach constant values. The spread of infection is also limited in this graph. The recruitment rate decreases because the proportion of infected individuals is high.

Figure 6 above depicts a fear factor of 4, a vaccination rate of 0.137 and an inefficiency of 0.30. All populations approach constant values. However, the infected population is higher than the graph when the fear factor was 6. This behavior is attributed to the fact that the recruitment into the core group is less affected by the total infected population (I/N) ratio when the fear factor is relatively small. The recruitment into the core group approaches a higher constant.

Section E: Death Induced by Disease

One modification of the model considers death induced by infectious disease, $\delta I$. This would be the case in a disease such as HIV/AIDS (if there

were a vaccine for it). It is no longer assumed that infected individuals die at the same rate as susceptible or vaccinated individuals. Death from infectious disease surpasses natural mortality. It is reasonable to assume that $\delta > \mu$. Only one equation changes in (*), that is

$$\frac{dI}{dt} = \beta S\frac{I}{N} + \sigma\beta V\frac{I}{N} - (\mu + \delta)I$$

and

$$I = \frac{\beta S\frac{I}{N} + \sigma\beta V\frac{I}{N}}{\mu + \delta}.$$

The disease-free equilibrium is not affected by the introduction of $\delta$. The resulting equilibrium remains the same:

$$(S_0, I_0, V_0) = \begin{pmatrix} \frac{\mu}{\mu+\phi}N \\ 0 \\ \frac{\mu}{\mu+\phi}N \end{pmatrix}.$$

The Jacobian matrix evaluated at $(S_0, I_0, V_0)$ results in:

$$J(S_0, I_0, V_0) = \begin{bmatrix} 0 & \frac{-\mu(\beta_\alpha\mu+\alpha\phi)}{(\mu+\phi)^2} & 0 \\ 0 & \frac{\beta(\mu+\sigma\phi)}{(\delta+\mu)(\mu+\phi)} & 0 \\ 0 & \frac{-\beta\phi\sigma}{\mu^2+\mu\phi} & 0 \end{bmatrix}.$$

The only eigenvalue of $J[(S_0, I_0, V_0)^{\mathrm{T}}]$ is:

$$\frac{(\mu + \phi)}{(\delta + \mu)(\mu + \phi)}.$$

The only modification in $R(\phi, \sigma)\delta$ is that, instead of $R(0, \sigma) = R(\phi, 1) = \beta/\mu$, we get $R(\phi, \sigma)\delta = R_0(\phi, \sigma)\delta = \beta/(\delta + \mu)$. Note that $1/(\delta + \mu)$ is the average time an infectious individual lives before he/she dies from the disease. We find that with the introduction of death induced by disease, we no longer encounter oscillations for reasonable values of $\delta$. As $\delta$ approaches zero, $-\delta I$ becomes insignificant in dI/dt. In this case, we get our original model and conditions for oscillations to occur.

Section F: Conclusion

The recruitment rate, $\Lambda$, is influenced by the fear/information factor, $\alpha$, and by the proportion of infected individuals in the core group in the following manner: $\Lambda e^{-(\alpha I/N)}$. Previous studies have shown that the fear/information factor strongly influences oscillatory behavior of a system. Fluctuating values of the recruitment rate cause these reoccurring oscillations. However, the prevalence dependent factor, $e^{-(\alpha I/N)}$, has two other dynamic variables $I$ and $N$. A high percentage of infectious individuals, $I/N$, will cause the recruitment into the core group to decrease. In contrast, a lower value of $I/N$ will cause a higher recruitment. These values are directly affected by the rate of vaccination and the inefficiency of the vaccine. If the fear factor, $\alpha$, is relatively large, then the system oscillates at higher amplitudes with increased frequencies. A relatively smaller fear factor causes smaller oscillatory amplitudes with smaller frequency. If individuals belonging to the non-core group are educated about the actual number of infected individuals rather than a percentage of infected individuals (i.e., eliminating $N$ from the prevalence-dependent factor) then the recruitment rate will decrease and oscillation in the model will cease to exist.

This model can be utilized to control and eradicate a disease in a core group; however, it does not take into account the disease spread in the general population. This model is limited by the specific application to diseases for which a vaccine has been developed.

This model has some serious implications when attempting to control outbreaks of a disease. It is essential to consider the information people receive about the core population and the vaccination procedures within it. It can be useful to public health officials in focusing social resources to a core population.

REFERENCES

ANDERSON, R.M., CROMBIE, J.A. AND GRENFELL, B.T. (1987). "The Epidemiology of Mumps in the UK: a Preliminary Study of Virus Transmission, Herd Immunity and the Potential Impact of Immunization." *Epidem. Info.* (Great Britain) 99, 65-84.

ANDERSON, R.M. AND MAY, R.M. (1992). *Infectious Diseases of Humans.* Oxford University Press. item BRAUER, F., BLYTHE, S.P. AND CASTILLO-CHAVEZ,C. (1992). "Demographic Recruitment in Sexually Transmitted Disease Models." BU-1154-M, Biometrics Unit, Cornell University, Ithaca, NY.

BRAUER, F., CASTILLO-CHAVEZ, C. AND VELASCO-HERNANDEZ, J.X. (1996). "Recruitment Effects in Heterosexually Transmitted Disease Models." *Intl. Journal of Applied Sc. And Computations* 3, 78-90.

CASTILLO-CHAVEZ,C., HUANG, W. AND LI, J. (1996). "Competitive Exclusion in Gonorrhea Models and Other Sexually Transmitted Diseases." *Siam J. Appl. Math.* 56, 494-508.

CASTILLO-CHAVEZ, C. AND ZHILAN, F. (1996). "To Treat or Not to Treat: The Case of Tuberculosis." Bu-1288-M, Biometrics Unit, Cornell University, Ithaca, NY.

HADELER,K.P. AND CASTILLO-CHAVEZ,C. (1995). A Core Group Model for Disease Transmission." *Mathematical Biosciences* 128, 41-55.

HEIDERICH, K.R., HUANG W. AND CASTILLO-CHAVEZ, C. "Nonlocal Response in a Simple Epidemiological Model. (Manuscript).

HETHCOTE, H., "Three Basic Epidemiological Models," in *Appl. Mathematical Ecology*, ed. S. Levin, T. Hallow. Springer-Verlag, Berlin, pp. 119-144.

VELASCO-HERNANDEZ, J.X. , BRAUER, F. AND CASTILLO-CHAVEZ, C. (1994) "Effect of Treatment and Prevalence-Dependent Recruitment on the Dynamics of A Fatal Disease." BU-1247-M, Biometrics Unit, Cornell University, Ithaca, NY.

ACKNOWLEDGMENTS

The research in this manuscript has been partially supported by grants given by the National Science Foundation (NSF Grant DMS-9600027), the National Security Agency (NSA Grant MDA 904-96-1-0032) and Presidential Faculty Fellowship Award (NSF Grant DEB 925370) to Carlos Castillo-Chavez. Substantial financial and moral support was also provided by the Office of the Provost of Cornell University and by Cornell's College of Agricultural and Life Sciences (CALS) and its Biometrics Unit. The authors are solely responsible for the views and opinions expressed in this report. The research in this report does not necessarily reflect the views and/or opinions of the funding agencies and/or Cornell University. We would also like to thank the faculty and staff of the SACNAS Summer Math Institute who helped us throughout in the completion of this project. Special thanks to the following people without whom this would not have been possible: Carlos Castillo-Chavez, Bonnie Delgado, Mercedes Franco, Carlos Hernandez, Herbert Medina, Estelle Tarica, Steve Tennenbaum, Jorge Velasco-Hernandez and Steve Wirkus.

**Section D:** **Graphical Analysis**

**Case 1:**

**Figure 1**

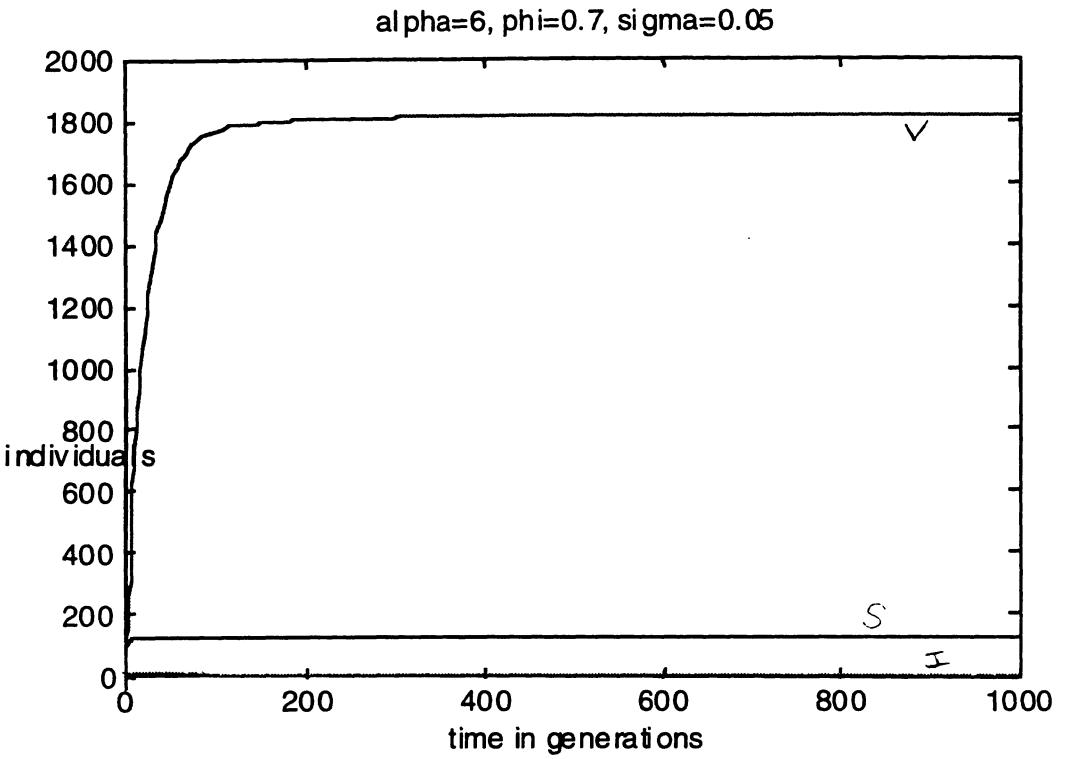


Figure 1 depicts a vaccination rate of 0.70 with a vaccine ineffectiveness of 0.05. The vaccinated population increases rapidly, implying that the recruitment rate and the susceptible population increase while the infected population decreases. A portion of the susceptible and the vaccinated populations becomes infected because the vaccine is not completely effective.

In this graph, the vaccinated population is larger than the susceptible population which in turn is larger than the infected population. Therefore, the infection within the core group is not eradicated, but contained by the vaccine.

**Figure 2**

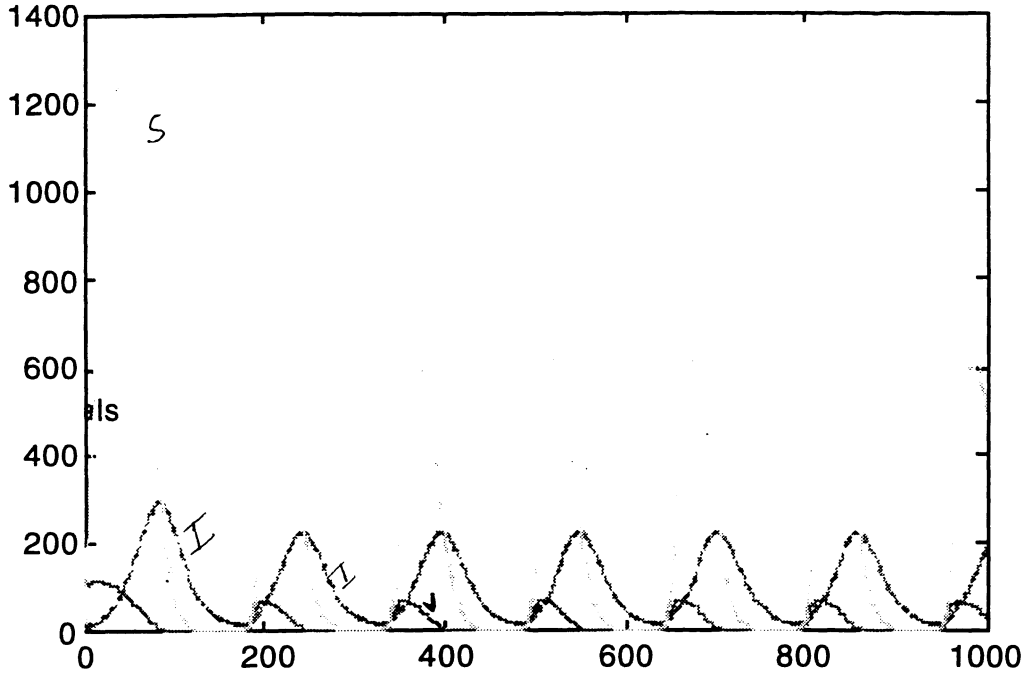


Figure 2 graphically represents a vaccination efficiency rate of 0.70 with and a vaccine inefficiency of 0.30. After the initial increase of the vaccinated population and the susceptible population, the infected population begins to increase. The spread of the infection slows the recruitment into the core group such that less people are susceptible and less people are vaccinated. When the vaccinated population reaches a minimum, the infected population becomes largest population.

**Figure 3**

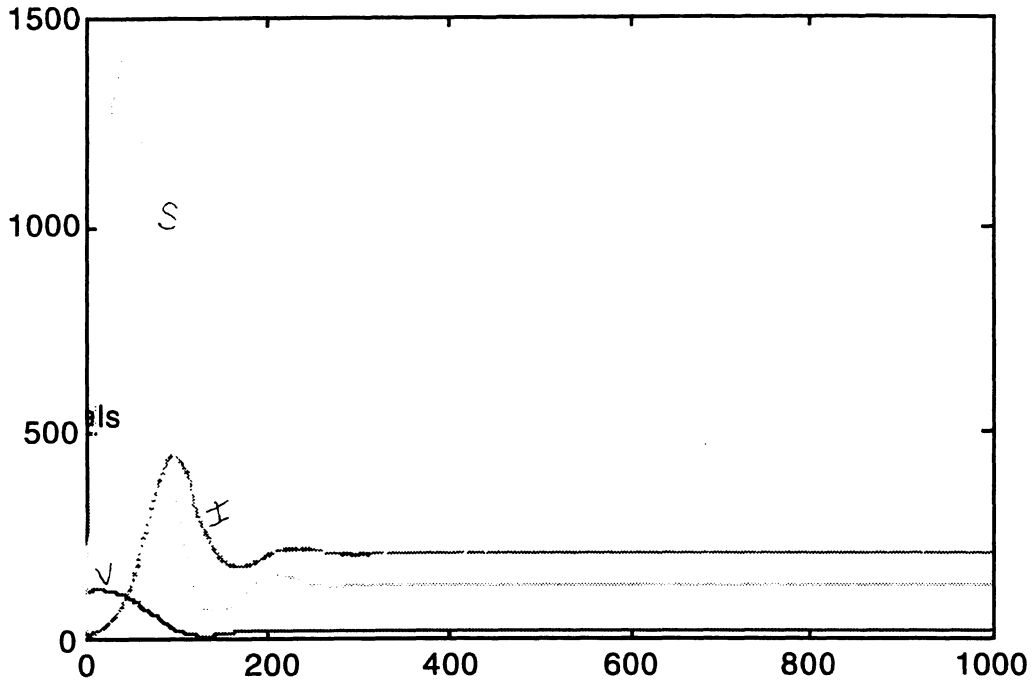


Figure 3 shows the effect of a high vaccination rate, 0.70, with a high vaccine inefficiency, 0.30, and a relatively low fear factor, 3. Initially, the populations of the vaccinated and the susceptible individuals increase. The population of infected individuals increases due to the high inefficiency of the vaccine. We note the recruitment rate will approach a constant value since $\alpha$, the fear factor, is relatively small. The vaccinated population remains greater than the infected population and the susceptible population.

**Case 2:**

**Figure 4**

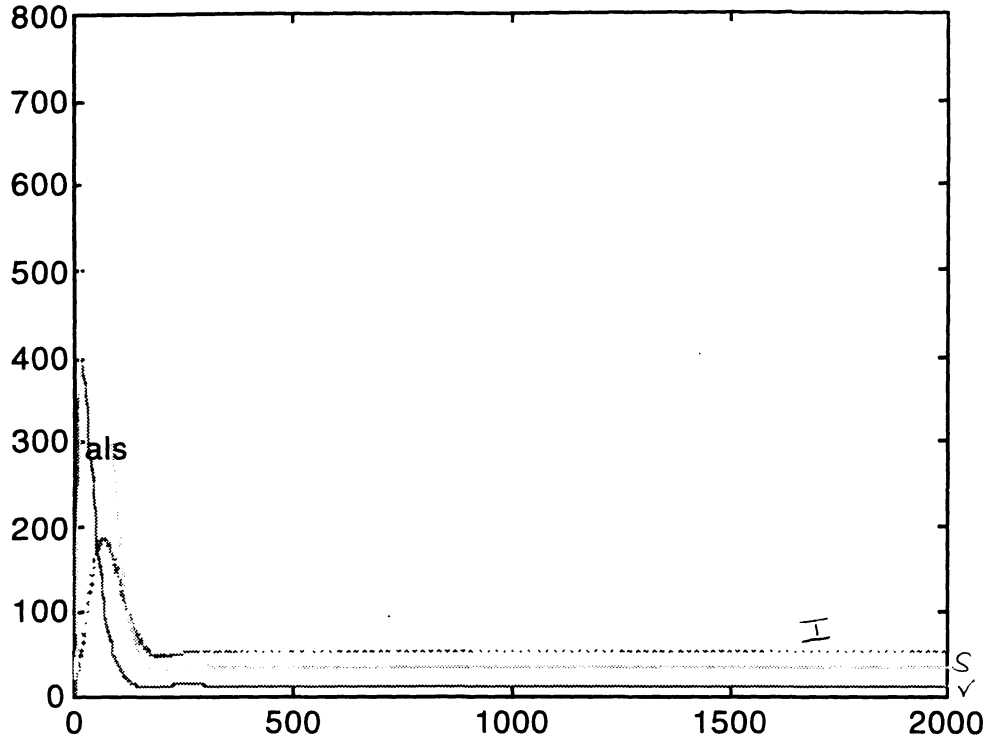


Figure 4 above displays a vaccination rate $\varphi$ of 0.137, a vaccine inefficiency $\sigma$ of 0.05, and a relatively high fear factor $\alpha$ of 6. As the recruitment rate decreases, all populations decrease to constant values. The infected population is the largest of the three populations, because the vaccination rate is relatively low. The spread of infection does not seem affected by the vaccination of the susceptibles in the core group.

**Figure 5**

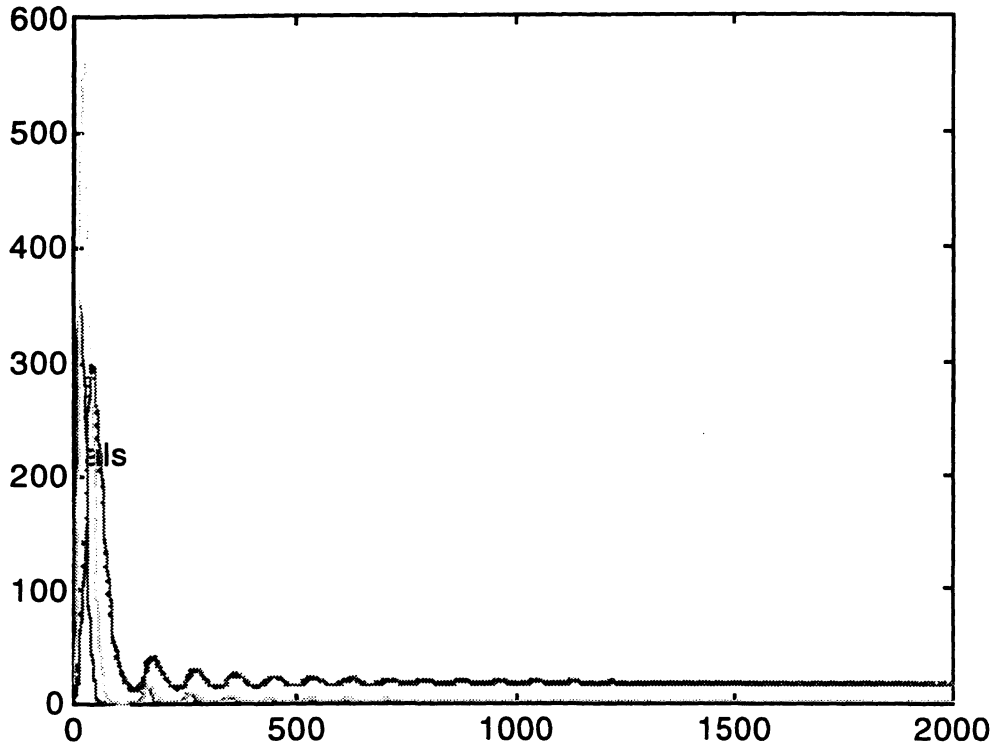


Figure 5 above graphically represents a fear factor of 6, a vaccination rate of 0.137, and a vaccine inefficiency of 0.30. In this graph the populations of the infected, susceptible, and vaccinated approach constant values. The spread of infection is also limited in this graph. The recruitment rate decreases because the proportion of infected individuals is high.

**Figure 6**

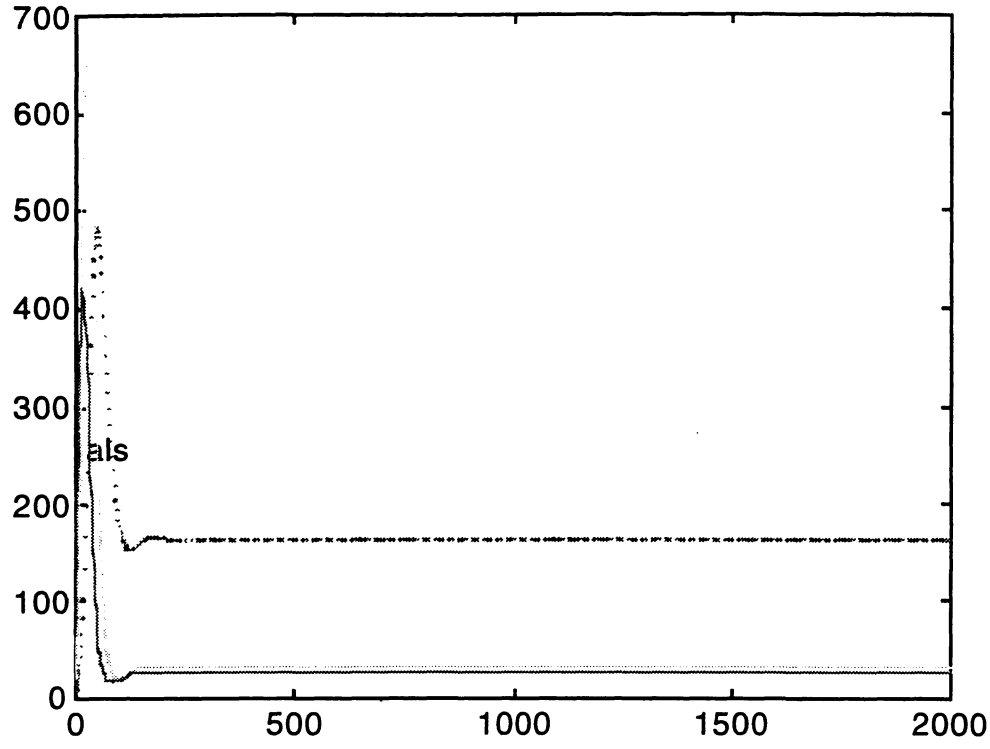


Figure 6 above depicts a fear factor of 4, a vaccination rate of 0.137 and an inefficiency of 0.30. All populations approach constant values. However, the infected population is higher than the graph when the fear factor was 6. This behavior is attributed to the fact that the recruitment into the core group is less affected by the total infected population (I/N) ratio when the fear factor is relatively small. The recruitment into the core group approaches a higher constant.

# A Mathematical Model of the Dynamics of *Rickettsia rickettsii* in Tick-Host Interactions

Mary E. Alderete
Arizona State University
jklizzy@IMAP2.asu.edu

Carlos W. Castillo-Garsow
Ithaca High School
cc96@cornell.edu

Guarionex Jordan Salivia
University of Puerto Rico, Rio Piedras
jordan@euler.uprr.pr

Carlos F. Lara-Moreno
Universidad Nacional Autonoma de Mexico
flara@servidor.dgsca.unam.mx

Gina F. Ramirez
California State University, Dominguez Hills
gramire2@bell.k12.ca.us

Monica F. Yichoy
Cornell University
mfy1@cornell.edu

BU-1369-M

## Abstract

This paper studies the dynamics of the tick population affected by *Rickettsia rickettsii* in order to understand how this disease affects other species. This project modifies the Busenberg-Cooke (BC) model to better account for biological aspects. Mathematical analysis assesses the effect of parameters on the dynamics of the model. One main result is obtained: the populations behavior is found to be chaotic in a region of parameter space that differs from that observed in the BC model. More importantly, the nature of the attractors seems qualitatively different.

# 1 Introduction

The disease *Rickettsia rickettsii* affects many species of animals, including humans. This is the most important rickettsial disease for humans in the U.S., since there are more than 1000 reported cases per year. The most important vector in the transmission of this disease is the American dog tick (*Dermacentor variabilis*) which is widespread in the Northeastern U.S. If not treated, this disease may be fatal. The original model (proposed by B & C in 1982) and our modified model focus on the population dynamics of ticks, the main vectors of this disease. In addition to RMSF, ticks carry diseases such as Lyme Disease and Heartwater. Organisms that serve as reservoirs of the disease and live in rural areas (generally small mammals such as rodents) are a constant source of infection to ticks, which in turn infect domestic animals like dogs and rats. Domestic animals bring the infected ticks into close contact with humans, who are the terminal hosts of ticks. Dogs, however, are not efficient reservoirs of the disease since they recover after three days.

The life history of the various species of ticks that carry *R. rickettsi* follows the same general pattern. However, there is a difference in the time required for each species to reach maturity. Some may live less than a year, while others have a life span of up to four years. They have three main life stages: larval, nymph, and adult. Larvae and nymphs feed on small mammals, whereas adults feed on large mammals, including humans.

Both models–the model proposed by Busenberg and Cooke (BC model) and our modified model–consider two types of transmission: horizontal and vertical. Horizontal transmission, which depends on the host, occurs between members of the same generation of ticks, whereas vertical transmission is passed from one generation to the next. Both horizontal and vertical transmission are described by their own set of equations: continuous and discrete, respectively. We choose different parameter values for these equations to determine if the population dynamics of ticks will tend to chaos. Our model is not intended to be a detailed description of the relationship between hosts and ticks, but rather an attempt to expand on what has already been modeled by Busenberg and Cooke [1993].

The following sections in this study describe the model equations and numerical results. The model equations section describes the modified model

and the method used to simulate the problem. The part on numerical results shows an analysis of the graphs acquired by implementing the model.

# 2 Model Equations

We start with six basic assumptions. First, the host groups demography is insignificant and its population size is constant. Second, the probability of transmission from tick to host is equal to that from host to tick, given contact. Third, there is a probability that immigrant ticks are infected or susceptible. The probability of susceptibility, $F$, is a relatively arbitrary value based loosely on the dynamics from simulations. Fourth, $\gamma$ includes all possible causes of death in ticks. Fifth, recovered hosts remain susceptible. Sixth, the immigration rate ($\Lambda$) is constant in this model.

To study the spread of *R. rickettsii*, it is necesary to understand the groups involved. First the ticks are separated into two classes, susceptible and infected. Second, the infection is spread through hosts, which are also divided into susceptible and infected classes: $dI_n/dt$, $dS_n/dt$, $dI_h/dt$, $dS_h/dt$ are the rates of change in the number of infected and susceptible ticks ($n$) and hosts ($h$), respectively, over time. With these criteria, we formulate a model that more accurately describes the relationship between the host and the tick than the one presented by Busenberg and Cooke.

$$\begin{aligned} I_h/dt &= LS_hIn - \Psi I_h \\ dS_h/dt &= -LS_hI_n + \Psi I_h \\ dI_n/dt &= (1-F)\Lambda + kS_nI_h - \gamma I_n \\ dS_n/dt &= F\Lambda - kS_nI_h - \gamma S_n \\ k &= pC_n/N_h \\ L &= pC_h/N_n. \end{aligned}$$

The susceptible ticks which get infected will move into the infected tick group at a rate of $KS_nI_h$, where $K$ is the horizontal transmission factor. $S_nI_n$ represents a susceptible tick coming into contact with an infected host. This horizontal factor represents the probability per contact per individual, that is, the probability that the infection will be spread from one tick to another tick of the same generation. The term $KS_nI_h$ is added into the same equation for the infected ticks because the newly infected ticks are entering

the group, while it is subtracted from the equation for the susceptible ticks because it represents the ticks which are leaving the group due to infection.

Ticks that die are also taken into account. The term $\gamma S_n$ is subtracted from the differential equation for susceptible ticks, and $\gamma I_n$ is subtracted from the differential equation for infected ticks.

The immigration of ticks into the tick community is represented by the symbol $\Lambda$. The probability that the incoming ticks will be infected is $(1-F)$, so $(1-F)$ is added to the equation for infected ticks. The probability that the incoming ticks are not infected is $F$, and $F$ is added to the equation for susceptible ticks.

Similarly, susceptible hosts are transferred into the infected host group at the rate of $LS_hI_n$, where $S_hI_h$ represents a susceptible host coming into contact with an infected tick, and $L$ is the horizontal transmission factor. The recovery rate for the host is $\Psi I_h$, which is added to the equation for susceptible hosts and subtracted from the equation for infected hosts. Since the host is immortal from the perspective of the tick, the number of hosts, $N_h = I_h + S_h$ , is a constant.

Vertical transmission is represented by the difference equations:

$$\begin{aligned} I_N(N) &= \frac{1-p}{M_2-M_1}\int_{M_1+N-1}^{M_2+N-1} b_1(t)I_{N-1}(t)\left[1-I_{N-1}(t)-S_{N-1}(t)\right]\,dt \\ S_N(N) &= \frac{1}{M_2-M_1}\int_{M_1+N-1}^{M_2+N-1} \left[b_s(t)S_{N-1}(t)+pb_I(t)I_{N-1}(t)\right] \\ &\quad \times\left[1-I_{N-1}(t)-S_{N-1}(t)\right]\,dt \\ \text{for } n &= 2,3,\cdots \text{and } I_1(1)=I_0, S_1(1)=S_0 \end{aligned}$$

Since the differential set of equations only deals with the horizontal transmission and not with the vertical transmission of the disease, the values of infected and susceptible ticks in a generation, $I_n(n)$ and $S_n(n)$, respectively, depend on the number of both groups from the previous generation. The life span of a tick is between 2 to 3 years. In the model we normalize this period to one unit of time, that is, each generation lives one unit of time. Ticks take a certain length of time to mature, after which they are able to lay eggs; $m_1$ and $m_2$ are the lower and upper boundaries, respectively, of the time interval in which a female tick can lay eggs. The interval $m_1 - m_2$ is called the maturation window. Vertical transmission occurs when the female

tick passes the infection to her offspring. Therefore, to measure the vertical transmission would mean to take the integral from $m_1$ to $m_2$. Thus, we have the integral taken from $m_1 + n - 1$ to $m_2 + n - 1$, where $n - 1$ is the end of the previous generation.

In the difference equation for the infected tick population $(1 - p)/(m_2 - m_1)$ represents the probability that the new generation is infected. The term $b_t(t)I_{n-1}(t)$ represents the number of infected born from previous infected generations. The second term, $[1 - I_{n-1}(t) - S_{n-1}(t)]$ is the logistic control on the oviposition, or the laying of the eggs.

In the difference equation for the susceptible ticks, the first term inside the integral, $[b_s(t)S_{n-1}(t)+pb_I(t)I_{n-1}(t)]$, represents the births for the susceptible ticks of the previous generation and the probability of susceptible births from the previous infected generation.

The second term inside the integral is the logistic control on the oviposition. The term outside the integral shows that there is no change in the spread of the infected from the previous generation during the maturation window.

In this model, the maturation window has been modified. It is assumed that all female adult ticks lay their eggs simultaneously, that is, $m_1 \rightarrow m_2 = m$. By applying the fundamental theorem of calculus to the difference equations, this new set of difference equations is obtained:

$$\begin{aligned} I_N(N) &= [(1-p)b_I(M+N-1)I_{N-1}(M+N-1] \\ &\quad [1 - I_{N-1}(M+N-1) - S_{N-1}(M+N-1)] \\ S_N(N) &= [b_s(M+N-1)S_{M+N-1} + pb_I(M+N-1)I_{N-1}(M+N-1)] \\ &\quad [1 - I_{N-1}(M+N-1) - S_{N-1}(M+N-1)]. \end{aligned}$$

Using the difference and differential sets of equations, two *Matlab* programs were developed and run on SunSparc4 and SunSparc5 for various values of $m$, $b_I$, and $b_S$. The first program, "driver" (see Appendix 1) depends on the second, "difchaos" (see Appendix 2). We assign arbitrary initial conditions to the four differential equations. Then we solve them for $I_h$, $I_n$, $S_h$, $S_n$. We graph these solutions over a time interval. At the end of this simulation, we obtain values for these variables, taking into consideration only $I_n$ and $S_n$ because they refer to the tick population. We ignore the variables $S_h$ and $I_h$ because they deal with the hosts, and relative to the lifespan of the ticks,

the hosts have a much longer life span and can be assumed to live forever. The ODEs are solved for the time interval $n$ and $n + m$, where $n + m$ will provide the population size at time $n + m$, when female ticks lay eggs. These are plugged into the difference equations to obtain the population sizes of $I_n$, $S_n$, $I_h$, $S_h$ at the beginning of the next generation. The ODEs are solved between $n$ and $n + 1$ and the values at n+1 are plotted. Then the process is repeated for the new initial values obtained from the difference equations.

# 3 Numerical Results

Using the computer simulations, we obtained several graphs which illustrate the chaotic behavior of our model. In Figures 1 and 2 we plot $I_n$ versus $S_n$ for $n = 101 : 1000$ (i.e., generation numbers $n$ ranging between 101 and 1000) with the constant parameter values $b_S = bS = 3.6$, $b_I = bI = 4.0$, $p = 0.01$, $L = 0.5$, $\Psi = \Psi = 0.5$, $\Lambda = \Lambda = 0.4$, $\gamma = G = 0.3$, $K = 0.4$, $F = 0.35$ and initial conditions: $I(1) = 0.3$, $S(1) = 0.6$. As $m$ was varied ($m = 0.02$ for Fig. 1, and $m = 0.5$ for Fig. 2), we observed that the shape of the attractor also changed. This result indicates that $m$ plays an important role in determining the dynamics of the systems.

In Figures 3 and 4, we tried to identify the transient and true attractors for $m = 0.05$, $bS = 4.0$, $bI = 3.6$ (all other constant parameter values were kept). In Figure 3 we plotted $I_n$ versus $S_n$ for $n = 101 : 1000$. As expected, we found points that more or less seemed evenly distributed. In Figure 4, we plotted $I_n$ versus $S_n$ for $n = 101 : 100,000$. We obtained a more or less evenly distributed region of points which intuitively indicated the existence of only one true attractor.

In Figures 5 and 6 we illustrated the dynamic behavior by plotting the last hundred points for infected and susceptible tick populations out of Fig. 3 and Fig. 4 versus time; at $m$ for each generation $n$, we obtain points with respect to time which describe the size of the infected and susceptible populations of the next generation. These points are connected so as to provide a better visual idea of the chaotic behavior of the system.

# 4 Conclusion

Based on the characteristics of chaos given by Kaplan and Glass (*Understanding Nonlinear Dynamics* 1995), we conclude by saying that our model seems to have chaotic behavior. It is important to note that our modified model has an attractor that seems to differ from that in the BC model. From a biological point of view because there is no pattern to follow in order to reach specific conclusions. More mathematical analysis is needed to see the biological implications of the systems behavior. Due to time constraints, this was not possible.

Suggestions for Future Study

In order to form a better model, revising the model is suggested so that a broader maturation window can be included in it. More simulations would enhance the hypothesis and help characterize chaos in a more precise way. Another way to describe the boundaries of chaos more clearly is to find the bifurcation diagram for this model. Unfortunately, the end of the summer also brought dissolution of our research group.

Acknowledgments

The research in this manuscript has been partially supported by grants given by the National Science Foundation (NSF Grant DMS-9600027), the National Security Agency (NSA Grant MDA 904-96-1-0032), and Presidential Faculty Fellowship Award (NSF Grant DEB-925370) to Carlos Castillo-Chavez. Substantial financial and moral support was also provided by the office of the Provost of Cornell University and by Cornells College of Agriculture and Life Science (CALS) and the Biometrics Unit. The authors are solely responsible for the views and opinions expressed in this report. The research in this report does no necessarily reflect the views and/or opinions of the funding agencies and/or Cornell University.

We would also like to thank the following people for their support and time: Carlos Castillo-Chavez, Herbert Medina, Jorge Velasco, Ricardo Oliva, Tamara Parker, Center for Applied Math (CAM) of Cornell University for the use of their computers, and most of all, Steve Wirkus who unselfishly dedicated his time and energy to help us in every way possible.

References

Busenberg, Stavros and Kenneth Cooke, "Vertically Transmitted Disease", *Biomathematics* **23**, Springer-Verlag, New York, 1993.

Fivaz, B. T. Petney, and I. Horak, *Tick Vector Biology: Medical and Veterinary Aspects*, Springer-Verlag, New York, 1992.

Kaplan, D. and Glass, L., *Understanding Nonlinear Dynamics*, Springer-Verlag, New York, 1995.

Figure 1

This is the graph for the infected ticks versus susceptible ticks for 1000 generations. The maturation window is 0.02, the birthrate of susceptible ticks is 3.6, and the infected birthrate is 4.0.

Figure 2

In this graph, all parameters were kep the same from the previous figure except that the maturation window is 0.5, which is of greater value. This graph also shows the simulation over 1000 generations.

Figure 3

In this figure, the value for the maturation window is 0.05, but the infected and susceptible birthrates have been switched. This graph also shows the simulation over 1000 generations.

Figure 4

This graph shows the simulation of infected versus susceptible ticks. The maturation window is 0.05, the infected birthrate is 3.6 and the susceptible birthrate is 4.0.

Figure 5

Last 100 generations of population of infected ticks with respect to the generations, graphing only every 15th generation of Fig. 3.

Figure 6

The last 100 generations of the population of susceptible ticks with respect to the generations, graphing only every 15th generation of Fig. 3.

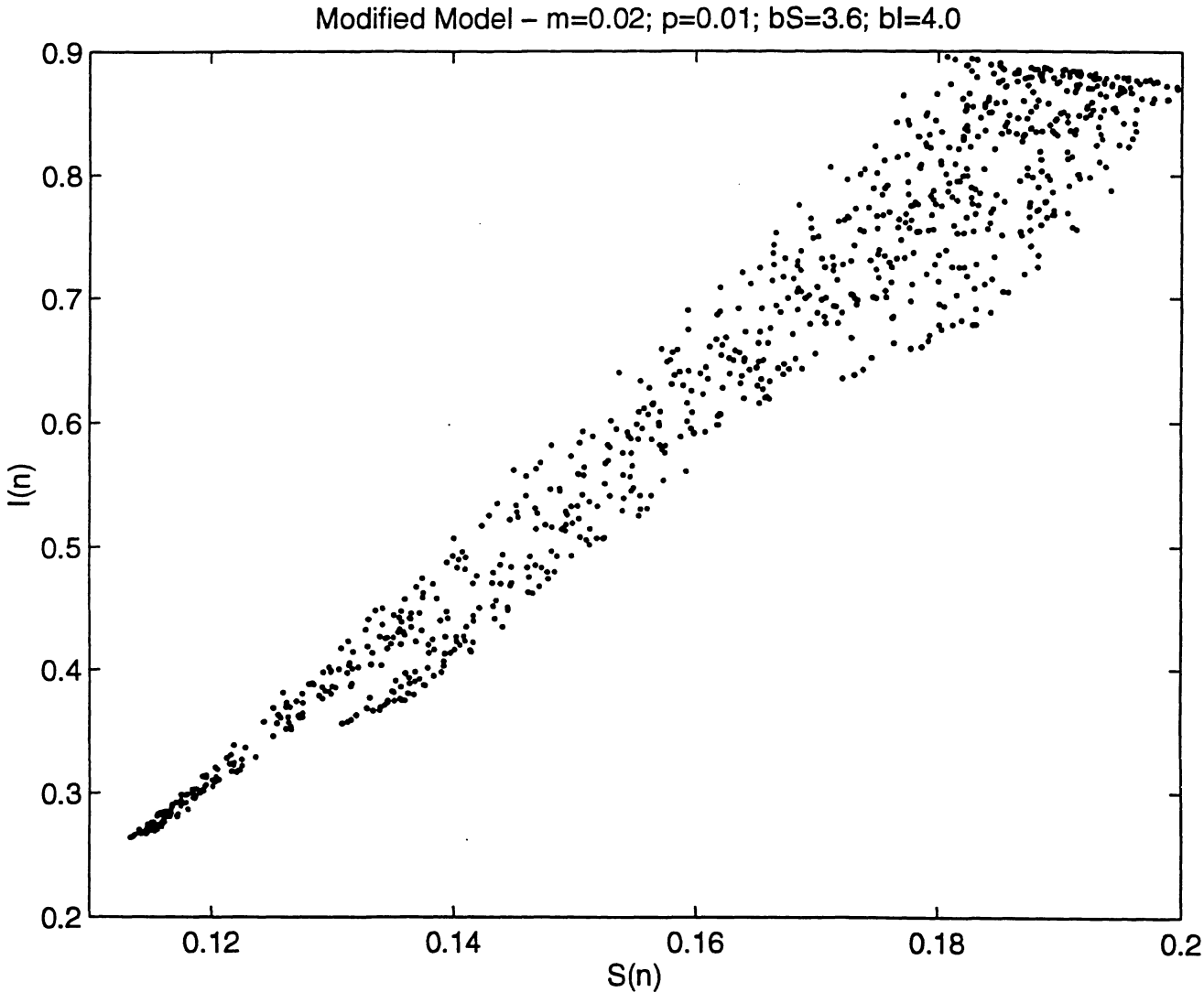
Modified Model – m=0.02; p=0.01; bS=3.6; bI=4.0
I(n)
S(n)
0.9
0.8
0.7
0.6
0.5
0.4
0.3
0.2
0.12
0.14
0.16
0.18
0.2

Figure 1

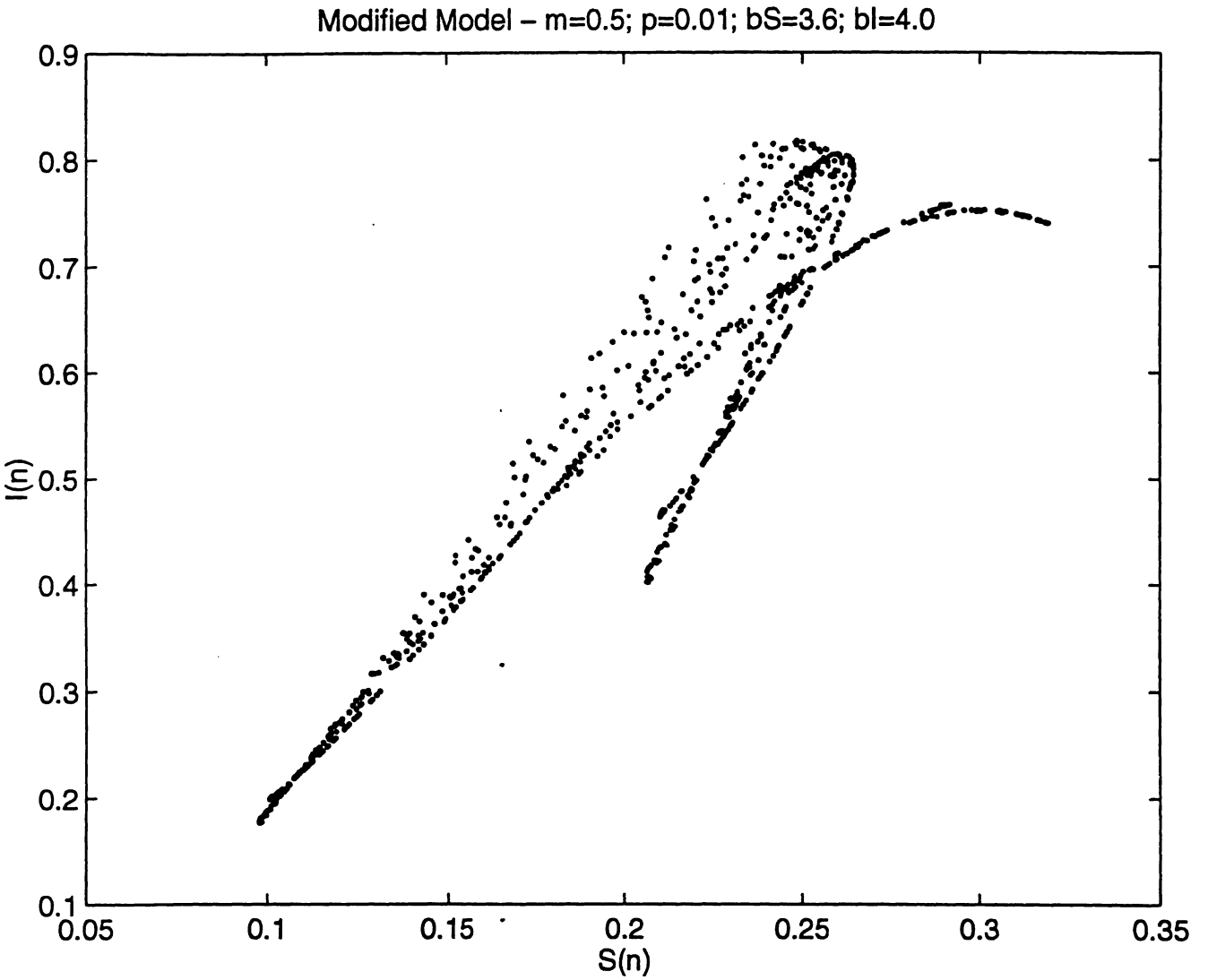
Modified Model – m=0.5; p=0.01; bS=3.6; bI=4.0
0.9
0.8
0.7
0.6
0.5
0.4
0.3
0.2
0.1
I(n)
0.05
0.1
0.15
0.2
0.25
0.3
0.35
S(n)

Figure 2

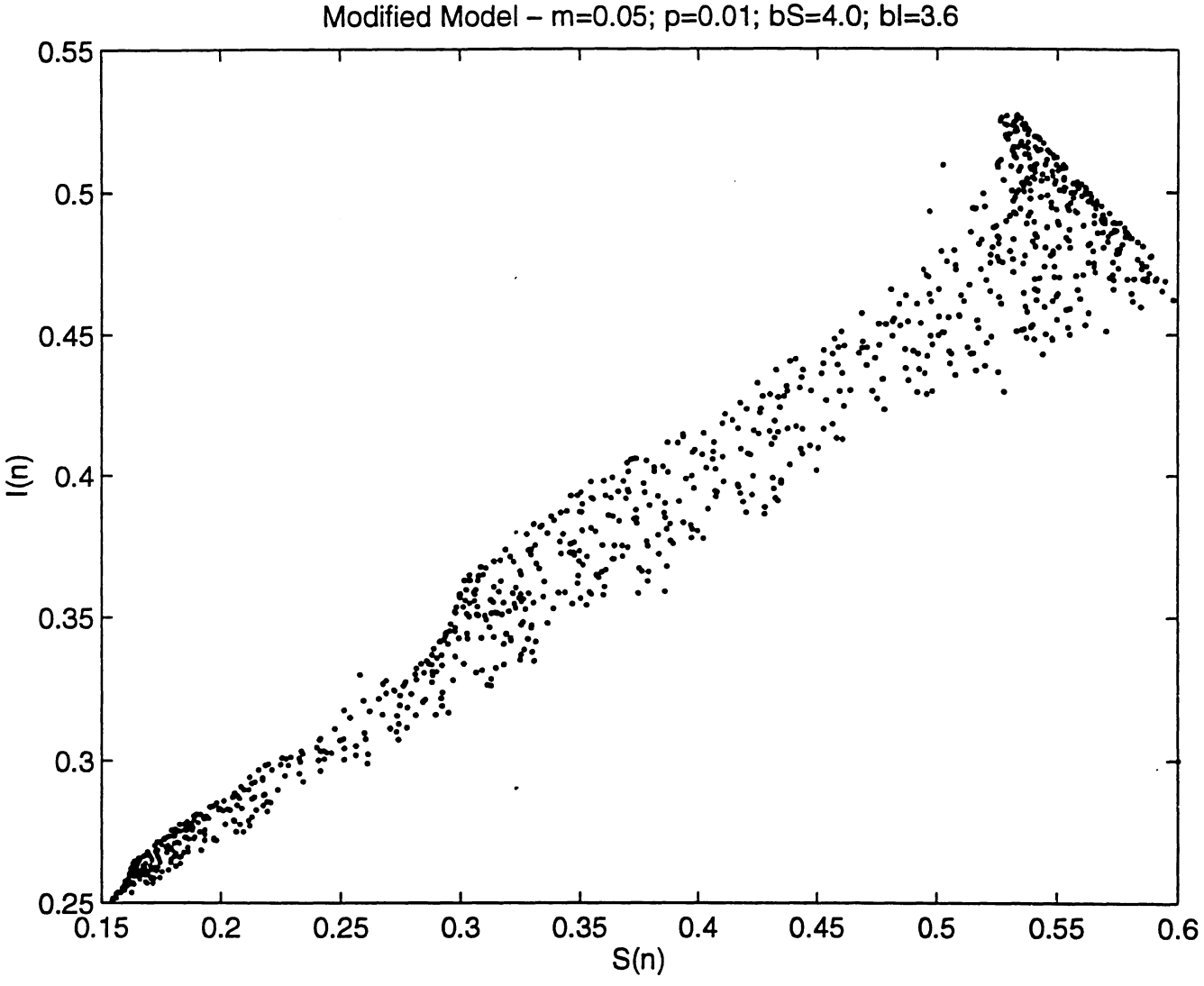
Modified Model – m=0.05; p=0.01; bS=4.0; bI=3.6
0.55
0.5
0.45
0.4
0.35
0.3
0.25
I(n)
0.15
0.2
0.25
0.3
0.35
0.4
0.45
0.5
0.55
0.6
S(n)

Figure 3

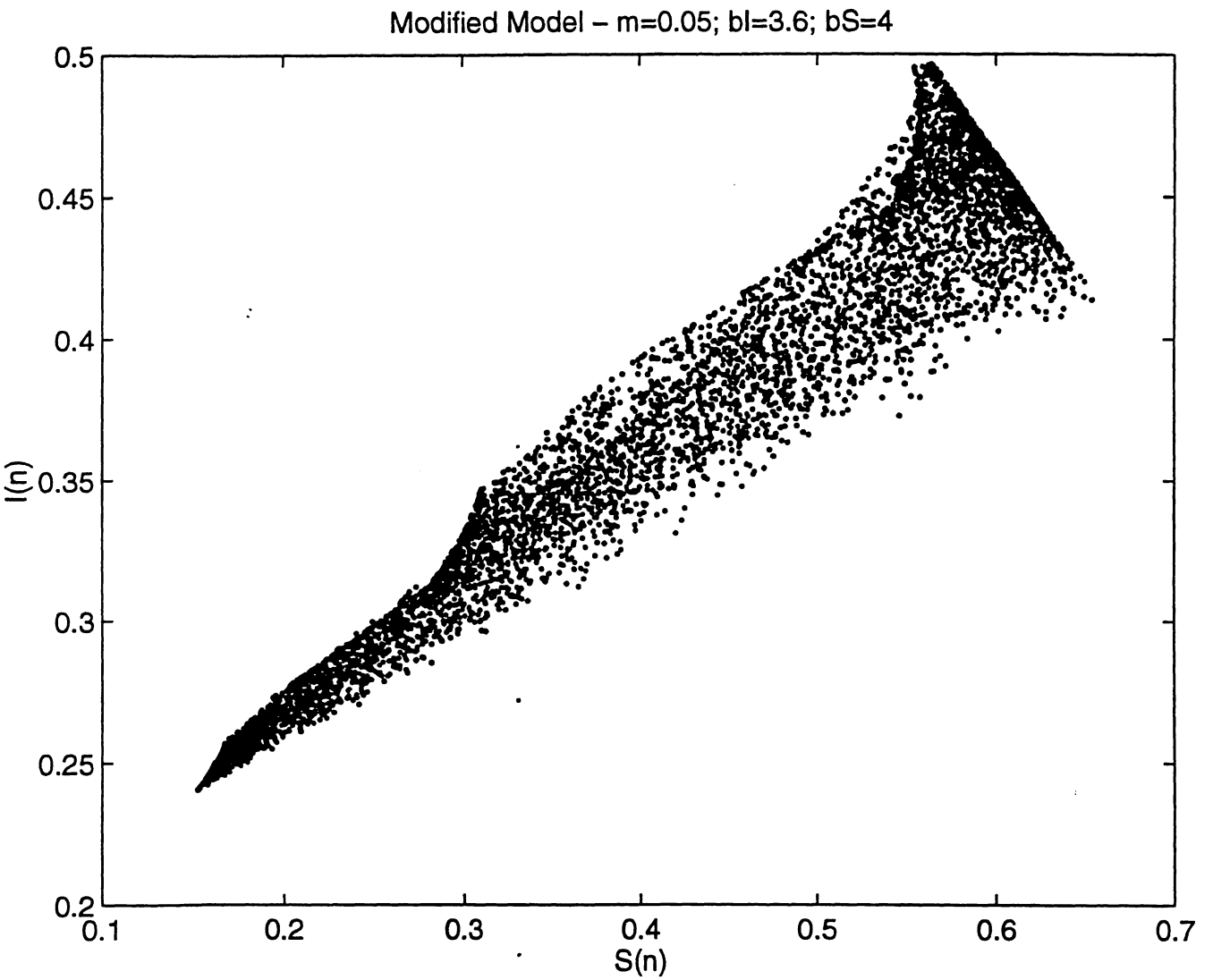
Modified Model – m=0.05; bI=3.6; bS=4
0.5
0.45
0.4
0.35
0.3
0.25
0.2
I(n)
0.1
0.2
0.3
0.4
0.5
0.6
0.7
S(n)

Figure 4

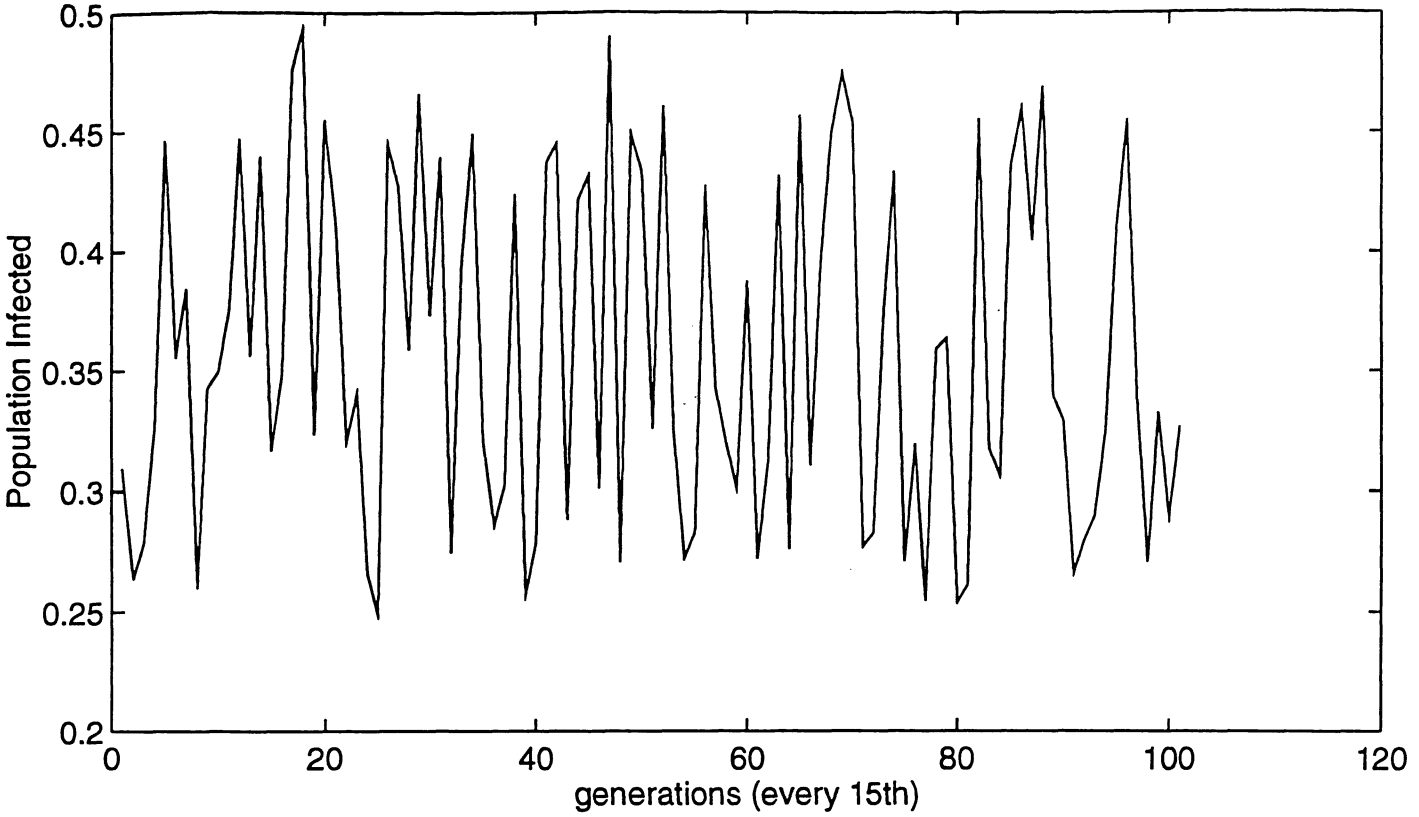


Figure 5

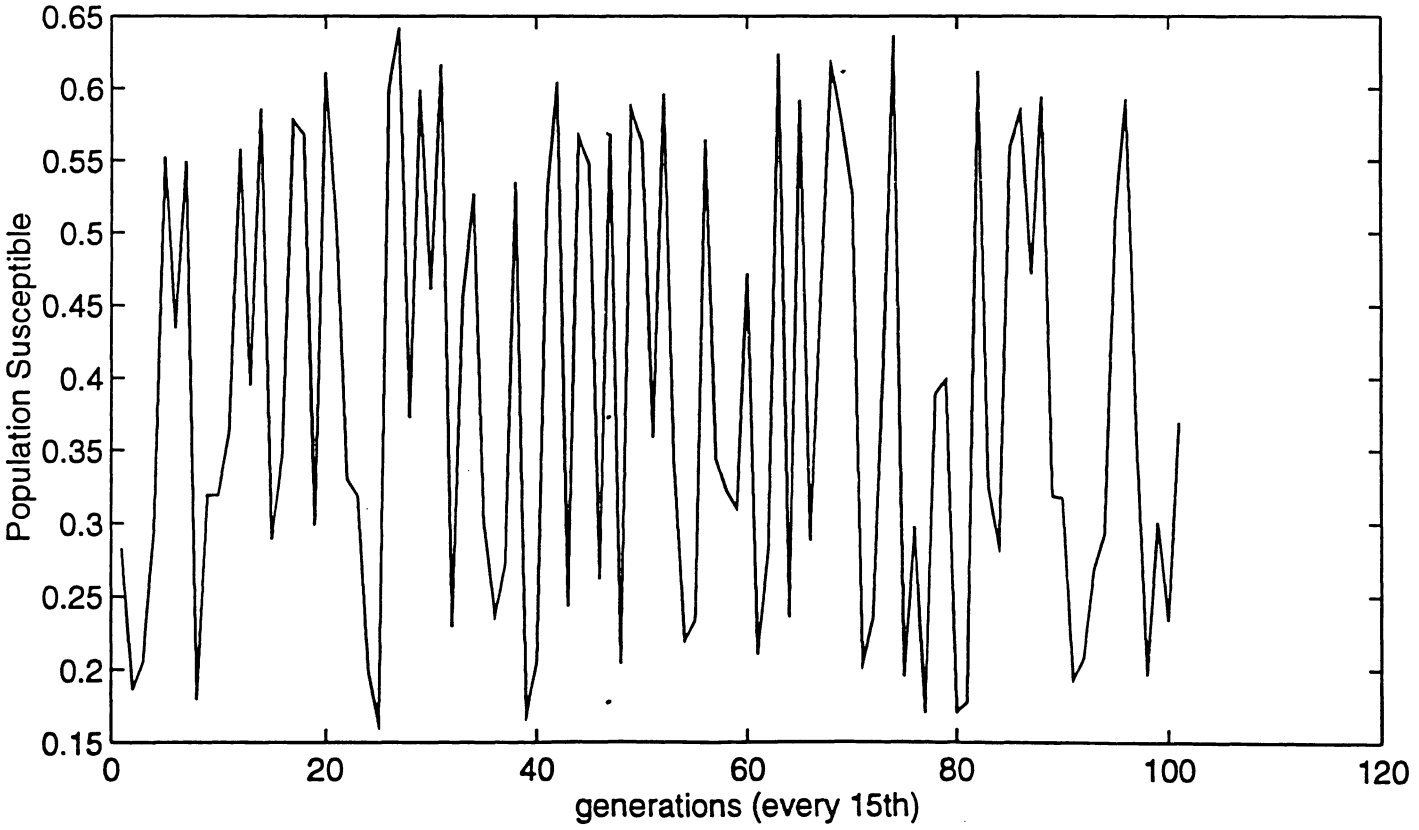


Figure 6

## Computer Programs

The following section contains the computer programs in *Matlab* used to generate the simulations.

```
function xdot = difchaos(t,x)

L=.5;
Psi=.5;
Lam=0.4;
G=0.3;
K=.4;
F=0.35;

% x(1)=Id(t), x(2)=Sd(t), x(3)=In(t), x(4)=Sn(t)


%system of ODE's
xdot(1) = L*x(2).*x(3) - Psi*x(1);
xdot(2) = -L*x(2).*x(3) + Psi*x(1);
xdot(3) = K*x(4).*x(1) - G*x(3) + (1-F)*Lam;
xdot(4) = -K*x(4).*x(1) - G*x(4) + F*Lam;
```

```
function y =driver(RR)

%parameter values will change at each simulation
bi=3.6; bs=4.0; p=0.01;

%initial time and number of ticks and dogs
i=1;
its=15;          %we save only every "its"th point
m=.5;            %maturation point,  time when ticks start laying eggs
x0=[.2 .8 .3 .6]';      %initial values Id, Sd, In, and Sn for generation 1

%initializes a matrix of zeroes where the solutions y will be saved
y=zeros(round((RR-100)/its),2);

%finds the solutions for every generation, from 1 to RR
for n=1:RR

%finds solutions to the ODE system from the beginning of the generation
%up to time n+m
[t2,x2]=ode45('difchaos',n,n+m,x0);

%finds the last component of the ODE solution x2
d2=length(x2(:,1));

x0=x2(d2,:)';

%finds solutions to the ODE system from the beginning of the generation
%up to time n+1
[t1,x1]=ode45('difchaos',n+m,n+1,x0);

%finds the last component of the ODE solution x1
d1=length(x1(:,1));


%x(3,d) = # infected ticks at end of the generation
%x(4,d) = # susceptible ticks at end of the generation

%set of difference equations
In=(1-p)*bi*x2(d2,3)*(1-x2(d2,3)-x2(d2,4));
Sn=(bs*x2(d2,4)+p*bi*x2(d2,3))*(1-x2(d2,3)-x2(d2,4));

%new initial points for the next generation
x0=[x1(d1,1) x1(d1,2) In Sn]';

%saves only every "its"th point
if ( (rem(n,its) == 0) & (n > 100) )

        y(i,1:2)=[x1(d1,4) x1(d1,3)];
        i=i+1;
end;

end;
```